INTERACTIONS BETWEEN BASE PAPER AND COATING COLOR IN METERED SIZE PRESS COATING

Ulla Forsström

Dissertation for the degree of Doctor of Science in Technology to be presented with due permission of the Department of Forest Products Technology, for public examination and debate in Auditorium K at Helsinki University of Technology (Espoo, Finland) on the 12th of December, at 12 noon.

Keywords: base paper, porosity, pore size, formation, hydrophobic sizing, coating, coating colour, film coating, coating coverage, coating structure, unevenness

ISSN 1457 – 6252
ISBN 952-99257-0-0

Oy Keskuslaboratorio
Ulla Forsström

Research Project M1702
KCL Communications 8

ABSTRACT

The purpose of the thesis was to gain a greater understanding of the interactions between the base paper and coating color in the metered size press (MSP) nip. The effect of base paper in precoating with an MSP was investigated using mill woodfree base papers, laboratory sheets, pilot base papers and non-porous materials. The coating color formulations consisted of commercial raw materials, in most cases latex-CMC colors with a pigment mixture of $CaCO_3$ and kaolin. Coating studies were carried out at 1000 m/min with a pilot-scale MSP coater.

The coating layer formation on woodfree base paper in MSP precoating depended mainly on the base paper surface openness. Lowering the base paper openness by raising the filler content, adding mechanical pulp or through more intensive refining of the chemical pulps resulted in lower coatweights, but better coating coverage. Base paper roughness, small-scale basis weight variation (beta formation) and surface chemical properties of the fibers (hydrophilic / hydrophobic) had no effect on precoating layer formation or coverage. Coating color liquid phase seemed to penetrate mainly into the voids between the fibers, because of the short contact time in the film transfer nip.

SEM-BSE and LIPS coverage measuring methods were found to give similar results for the precoated surfaces. The LIPS coverage results were lower than the SEM-BSE results at low coatweights. This indicated that the SEM-BSE method found thinner coating layers to be covered. Low base paper surface openness and high filler content on the surface of the sheet reduced coating color penetration into the base paper structure and the coating color stayed on the surface better. Dense base papers with high filler contents gave better small-scale uniformity than porous base papers. The coating coverage was sensitive to base paper shadow marking, which was clearly seen as large-scale coverage non-uniformity. With base papers with less filler on the surface, coverage could still be increased by increasing coating color viscosity. Using higher levels of kaolin in the coating formula improved coverage, especially at low coatweights. The machine speed and nip load did not affect coating coverage. The color solids content had only a minor impact on coating coverage.

Smaller differences in coverage two-sidedness were observed when both paper sides were coated simultaneously compared to the situation where only one side was coated. When the paper was coated using hard rolls, coating coverage depended largely on the pore size of the base paper. Coatweight was formed mainly through penetration, the result being a dense coating layer. With soft rolls coating layer formation occurred more by dewatering, in which case better coverage was obtained, albeit accompanied by a porous coating layer. The porous coating layer with good coverage was the result of filter cake formation in the film transfer nip. The main mechanism by which coating layer formation took place was pressure-induced penetration of bulk coating color or liquid phase into the voids between fibers in the transfer nip. Water sorption into the fibers was slower than capillary penetration, and the movement of coating color liquid phase by diffusion and possibly by capillary absorption took place mainly after the nip.

TABLE OF CONTENTS

PREFACE AND ACKNOWLEDGEMENTS

This experimental work concerning the interactions between base paper and coating color was carried out at KCL between 1998 and 2000. I would like to thank the management of KCL for the opportunity to do this work. The work has received financial support from the National Technology Agency (TEKES), the Finnish Cultural Foundation (Suomen Kultuurirahasto) and KAUTE (Kaupallisten ja teknisten tieteiden tukisäätiö), for which I am deeply grateful.

I would like to express my thanks to Professor Hannu Paulapuro, who supervised my thesis. My sincerest thanks go to the instructor of the thesis, Dr. Johan Grön, for quiding me into the deeper aspects of coating and showing me patiently the scientific way to finish the work. Very many colleagues at KCL were involved in the project. Without their help the project would not have been possible. Before anyone else I want to express my thanks to our visiting scientist Dr. Robert J. Dickson for his inspiring microscopic work and for encouraging me to do the thesis work. I would also like to thank the whole KCL project group, and especially Mr. Erkki Saharinen, Lic. Phil., and Ms. Kaarina Fagerholm, Lic. Phil., for their valuable work in preparing the experimental base paper materials for the study. I am also indebted to Ms. Tiina Pöhler, M.Sc., and Mr. Asko Sneck, M.Sc., for their skilful work in the area of developing and documenting our SEM-BSE coating coverage measuring method. The personnel of the pilot plants and laboratories at KCL and Metso Paper Inc, Rautpohja, did a wonderful job producing and testing all the base papers and coated papers in the study. All the samples for testing were kept by Ms. Tytti Aho, who did all this with great interest, care and well on schedule. Mr. Philip Mason is acknowleged for the linguistic revision of the manuscript.

Finally, I wish to express my thanks to my children, Lars, Kristina and Niklas, for all their patience over the years.

Espoo, May 2003

Ulla Forsström

LIST OF ABBREVIATIONS AND SYMBOLS

ABBREVIATIONS

MSP	Metered size press
1C2S	one MSP coater with two stations
2C1S	two MSP coaters with one station
MFC	Machine finished coated paper (low gloss)
LWC	Lightweight coated paper (high gloss)
TS	Base paper topside
BS	Base paper bottom or wire side
CMC	Carboxymethyl cellulose
P&J	Static hardness measurement unit
PU	Polyurethane
RUB	Rubber
FCC	First critical concentration
SCC	Second critical concentration
DIP	De-inked pulp
WC	Wood-containing, includes mechanical pulp
WF	Woodfree, only/mainly chemical pulp
CSF	Canadian standard freeness
AKD	Alkylketene dimer sizing agent
GW	Groundwood
PGW	Pressure groundwood
TMP	Thermomechanical pulp
SW	Softwood kraft
HW	Hardwood kraft
SEM	Scanning electron microscope
SEM-BSE	Scanning electron microscope with backscattered electron mode
PPS	Parker Print Surface measurement unit
KCL	Oy Keskuslaboratorio-Centrallaboratorium Ab
FIBRO	FIBRO 1100 DAT contact angle measurement unit
DPM	Dynamic Penetration Method
EMCO	Dynamic penetration measurement unit
LIPS	Laser-Induced Plasma Spectroscopy
DCC	Degree of Coating Coverage with LIPS
EDM	Euclidean Distance Map (image analysis method)
UV	Ultraviolet
ESCA	Electron spectroscopy for chemical analysis
MODDE	Multivariate program
Q^2	Predictive power of the model, underestimates the goodness of fit
R^2	Predictive power of the model, overestimates the goodness of fit

MATHEMATICAL SYMBOLS

y	amount of suspension transferred per unit area
L_{susp}	suspension film thickness originally on plate
$L_{accepted}$	thickness of immobilized or otherwise accepted suspension of the stock
f	constant fraction of non-immobilized suspension transferred to the stock
Q	flow rate
A	unit area, specimen area or filtration area
K	permeability constant
Δp	total pressure drop across a sample length or the differnce in pressure
L	sample length
K_v	permeability coefficient for viscous flow
η	fluid viscosity, kinematic viscosity
ϕ	porosity
d_{eff}	effective particle diameter
κ	Kozeny constant
p_c	capillary pressure
r	capillary radius
γ	surface tension
θ	contact angle between liquid and capillary wall
h	distance traveled
t	time
p_e	external pressure
p	pressure or total pressure
ε	void fraction
τ	tortuosity
D	diffusion coefficient
C	concentration of liquid
x	place
Q_{liquid}	amount of liquid removed through dewatering
b	flow coefficient
μ_f	pore coefficient
μ_l	path coefficient
$L_{filter\ cake}$	thickness of the filter cake layer
$C_{structure}$	structure coefficient
ρ_{liq}	density of the liquid phase
ρ_c	density of the coating color
Q_{immo}	amount of immobilized layer
ρ_{immo}	density of immobilized layer
B_{color}	color parameter

LIST OF PUBLICATIONS

I Forsström, U., Dickson, R. J., Grön, J., Strichdeckung und Struktur von holzfreien Papieren, die in der Filmpresse vorgestrichen wurden (in German). Wochenblatt für Papierfabrikation 128 (2000): 14/15, 985-992.

II Dickson, R.J., Forsström, U., Grön, J., Coating coverage of metered size press precoated paper. Nordic Pulp and Paper Research Journal 17 (2002): 4, 374-379.

III Forsström, U., Saharinen, E., Dickson, R. J., Fagerholm, K., Coating Layer Formation and Liquid Phase Penetration in Metered Size Press Coating. Journal of Pulp and Paper Science 29 (2003): 5, 159-166.

IV Forsström, U., Fagerholm, K., Saharinen, E., The role of base paper porosity in MSP coating. Accepted for publication in Paperi ja Puu - Paper and Timber (2003).

V Forsström, U, Grön, J., Interactions Between Base Paper and Coating Color with Double-Coated Paper, Wochenblatt für Papierfabrikation 130 (2002): 18, 1208-1214.

THE AUTHORS'S CONTRIBUTIONS

In the above publications I-V the author completed the following:

I All experimental work and analysis of the results and writing the article published originally in PTS Streicherei Symposium 1999

II Designing the experimental plan and writing the final article for NPPRJ

III Designing the experimental plan, all experimental work for the coating study, and writing the paper published first in TAPPI Coating Conference 2002 and the final article in JPPS

IV All experimental work for the coating study, analysis of the coating results and writing the article for Paperi ja Puu - Paper and Timber

V All experimental work for the study, analysis of the results, and writing the article published originally in PTS Streicherei Symposium 2001

1 INTRODUCTION

Metered size presses (MSP) were originally developed to overcome problems that limited the use of pond size presses at high machine speeds. One particular restriction in pond size presses at high speeds was splashing due to turbulence in the size pond. The gate roll size press had already been introduced in the 1960's for sizing purposes, and offered much greater speed potential than the pond size press. The gate roll press consists of six rolls of which two transfer rolls for each paper side are used to adjust the amounts of film and then applied to the nip rolls [1, 2]. Gate roll size presses have also been used for pigmentizing and coating for more than 30 years. The gate roll technique has been widely adopted in Japan for coating wood-containing printing paper grades to a maximum coatweight of typically 5 to 6 g/m²/side. In this case, misting between the transfer rolls and the nip roll limits the maximum operating speed to below 1200 m/min and coatweights to below 6 g/m²/ side [3].

The MSP technique is based on coating color premetering with a short-dwell type of application head onto a transfer roll, which applies the film onto the paper surface [1, 2] in the nip, where no stationary applicator device is in contact with the paper. The MSP coating method has many advantages and allows coatweights to be increased from 2- 6 g/m^2 to over 10 g/m^2 [3]. Base paper of lower strength can also be coated with this technique because the web is subjected to less mechanical stress than in blade coating [3]. For the same reason production efficiency is also greater because there are fewer web breaks than in blade coating, even at high operating speeds.

MSP coating has aroused a lot of interest because of its potential to improve production efficiency and is now a successful and more economic alternative to blade coating [3, 4, 5, 6, 7, 8]. Several mills today are producing wood-containing coated machine finished (MFC) [6, 7] or supercalendered lightweight coated paper (LWC) with an MSP [8]. The influence of base paper on coated paper quality has been investigated in numerous MSP coating studies with wood-containing base papers [4, 5, 9, 10, 11, 12, 13, 14, 15, 16, 17]. With MSP coating, high-quality coated paper can be produced, even with a high content of de-inked pulp, without scratches, streaking or other problems that are typical of blade coating [9]. MSP coating gives better fiber coverage thanks to the contour coating [10], and a lower degree of fiber roughening in heatset offset printing because it produces a more porous coating layer [9, 11]. MSP coating of wood-containing base paper is also reported to give better coverage at low coatweights (< 8 g/m² / side) than coating with a blade, but greater roughness [12].

The roughness of MSP-coated papers at high coatweights was much higher on the medium and large wavelength scales than that of blade-coated papers [16]. SEM cross-sectional images of MSP-coated and blade-coated papers at a coatweight of 10 g/m² [16] showed that the thickness of the coating layer varied considerably with both methods [17]. A quantitative analysis combined with a frequency analysis showed that MSP-coated paper has only a slightly better overall coating thickness uniformity than blade-coated paper, and that the difference in coating thickness variation between the MSP-coated and blade-coated papers was mainly on the large scale (> 500 μm) [17]. The conclusion from all earlier studies is that

the benefits of MSP coating over blade coating are significant mainly at low coatweights (< 8 g/m^2/ side). Due to the higher roughness of MSP-coated papers, the technique may be restricted to HSWO printing and is not yet suitable for commercial rotogravure printing [3, 9, 12].

Metered size presses are also widely used for precoating woodfree base paper to produce double-coated grades. Only a rather limited amount of information is available on the base paper requirements for MSP-coated woodfree papers. The most important properties of the base paper might differ from those suitable for blade coating. The present study focused on the interactions between woodfree base paper and coating color in precoating to low coatweights with an MSP in the production of offset grade papers.

2 OBJECTIVES AND APPROACH OF THE STUDY

2.1 Objectives

The main functions of the precoating are to fill, as far as possible, the large voids in the surface of the base paper, to cover the base paper, and to produce a suitable coating layer roughness and porosity for the top coating. The aim of this study was to investigate the effect of base paper properties on coating color transfer, its coverage potential and the porosity of the MSP precoated paper for woodfree paper grades. Several methods for analyzing coating coverage were tested and further developed.

The hypotheses set for the study as a whole were:

- The main mechanism for coating color transfer in MSP coating is initial bulk coating color penetration followed by penetration of liquid phase caused by pressure.
- The physical base paper properties determine coating layer formation in the MSP transfer nip.
- The surface chemical properties of the base paper influence coating color transfer in the nip only at long dwell times (e.g. low speed, soft rolls).
- The surface chemical properties of the base paper influence the movement of liquid phase after the roll nip exit, which may cause migration of the soluble binder through capillary absorption prior to the drying stage.

2.2 Approach

The study was carried out in the following sequence:

1. A review of the current knowledge of MSP coating, possible mechanisms in transport phenomena, and research methods related to coating coverage (chapter 3). Special attention was given to the methods used for characterizing the structure and surface properties of the base paper as well as the coverage and coating layer porosity of the precoated paper (chapter 4).

2. An investigation of the effect of base paper in MSP precoating using mill base papers, other base papers and non-porous materials. The other base papers were produced on either the laboratory or the pilot scale. Both base paper surface openness and surface chemical properties were varied simultaneously over a wide range (chapters 5, 7 and 9). The effect of base paper porosity and average pore size were then studied alone in more detail (chapter 8). The non-porous materials were coated in order to investigate the movement of coating color liquid phase into the base structure (chapter 7).

3. An investigation of the effect of the MSP coating process and coating color variables on precoated paper quality (chapter 6). Most of this work was done by coating just one side, but the effect of the pressure pulse in the transfer nip was investigated by coating both sides simultaneously (chapter 9).

4. Finally the effect of precoated paper properties on the formation of the top-coating layer and top-coated paper quality was assessed (chapter 10).

The thesis is partly based on five publications, which are included as Appendices I to V. The thesis also includes some new and unpublished results.

2 LITERATURE REVIEW

The present state of knowledge was reviewed from three different perspectives: knowledge of the metered size press coating process, the theoretical background to the transport phenomena, and the research methods used for characterizing coating coverage.

3.1 The metered size press coating process

The MSP coating process involves two stages: premetering the coating color onto the roll, and transferring the film in a roll nip onto the base paper (Figure 1). The coater can handle both sides at the same time (1C2S) or else each side can have its own coating station (2C1S) [12]. These process stages can affect coating color transfer and coating layer uniformity in three ways:

1. Coating color film application onto the roll surface can cause large-scale non-uniformities [18, 19], which in turn affect the large-scale uniformity of the coating layer.
2. Coating color penetration into, and filter cake formation on, the base paper in the film transfer nip [20, 21], which includes the uniformity of the coating layer on both the micro and macro scales.
3. Film splitting at the transfer nip exit followed by leveling of the coating layer [20, 21, 22, 23], which affects uniformity on the micro scale.

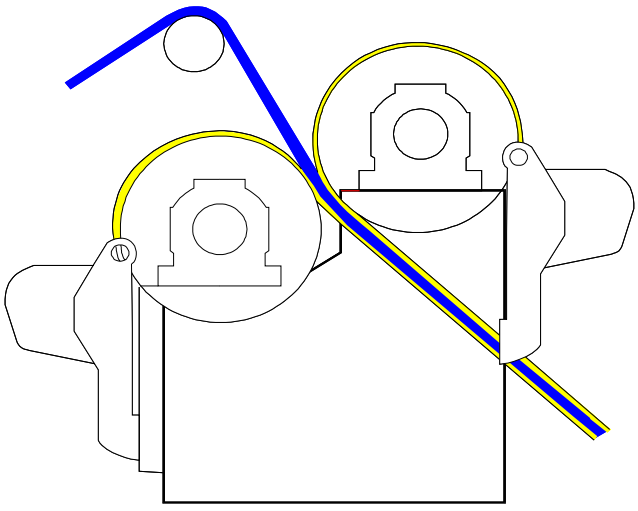

Figure 1. Schematic illustration of a 1C2S MSP coating unit, in which both paper sides are coated simultaneously.

3.1.1 Coating color application onto the transfer roll

Coating color premetering can be carried out with bent blades [2, 24], with grooved rods [1, 3, 4, 5, 24, 25] or with smooth large-diameter rods [2, 3, 5, 24, 25]. The essential advantage of the bent blade over the grooved metering rod is its flexible coatweight and coatweight cross profiling with profiling screws. The drawback of the bent blade is the risk of scratches and streaks in the film at high speeds. The grooved rod, with which the film thickness is adjusted volumetrically, is very commonly used for sizing and pigmentizing paper at low coating color solids contents. Although the metering is done volumetrically, a high rod pressure in combination with a soft roll cover reduces the groove volume. Rapid wear of the grooved rods is a drawback at high coating color solids contents as it causes variations in the amount of film [20]. The smooth, large-diameter rod was developed to improve rod lifetimes and film profile stability [3]. For these rods, diameters ranging from 10 to 35 mm are normally used [20].

Smooth, large-diameter rods are mainly used for coating at high coatweights or low speeds. Premetering with a large-diameter rod is governed by hydrodynamics, the machine speed and the coating color viscosity controlling the force in the nip between the rod and the roll [5, 25]. The pressure in the converging metering nip creates a hydrodynamic force and an impulse force acting against the dynamic element, and these forces dominate the metering process [20]. The amount of premetered coating film can be adjusted by changing the rod diameter, rod pressure, coating color properties, transfer roll cover material and machine speed [5, 20, 25].

3.1.1.1 Effect of the rod

Increasing the rod diameter by 5 mm normally gives about 1 g/m² more coating color on the roll [20]. The contact area increases as the rod diameter is increased, the result being a smaller hydrodynamic force per unit contact area and a greater amount of film on the roll. During normal operation the amount of film is adjusted by means of the rod pressure. Increasing the rod pressure from 50 to 250 kPa reduced the coatweight by about 2 g/m² [20]. Because of the limited coatweight controllability with rod application, coatweight is normally adjusted by changing the coating color solids content.

The maximum pressure and its distribution in the nip between the rod and roll have been studied with different measurement methods [18, 19, 26, 27, 28, 29, 30, 31]. Reglat and Tanguy [18, 19, 26] used a piezotransducer mounted on the surface of a large-diameter metallic metering rod. The diameter of the metering rod was initially 80 mm, which is quite large compared to the rods used in the MSP coating process [18, 19]. Later, they reduced the diameter of the rod to 40 mm [26]. The diameter of the transducer was 2 mm, which was about the same magnitude as the width of the nip between the rod and roll. The spatial resolution of the measurement could not have been very precise. According to their results, the maximum pressure increased almost linearly, whereas the width of the nip increased only slightly as the speed of the transfer roll was increased [18]. In the nip exit region, where the

pressure is subatmospheric, a greater reduction in pressure appeared when the speed of the transfer roll was increased or the speed of the rod or the viscosity of the fluid was decreased [18]. The same workers examined how process parameters such as the speed of the transfer roll, the rotation speed of the metering rod, and coating color properties influenced the measured pressure distribution and the coating film uniformity on the roll [18, 19]. Complete verification of the experimental results was not possible because the gap between the roll surfaces was not measured [31].

Poranen *et al.* [27, 28, 30, 31] presented two different techniques to measure the pressure profile on the surface of the metering rod. The first studies were conducted with a small drilled hole on the rod surface to allow actual pressures to be collected throughout the nip [27, 28, 31]. The shape of the measured pressure profiles has three regions, the entering region, the middle region and the exit region. A small subatmospheric pressure was detected in the exit region [27, 28, 31]. Later, the pressure and strain distributions were measured in both metering nip and film transfer nip using pressure sensors placed at different depths in the roll cover material [30, 31].

According to the measurements [27, 31], the maximum pressure and the area under the measured pressure profile increased as the loading pressure of the rod was increased. The hydrodynamic force was defined as the area under the pressure profile, which was calculated by integrating the measured pressure profile over the position. The higher hydrodynamic force with high loading pressure resulted in a smaller opening between the rod and the roll, which gave a smaller wet film on the roll. The rotational speed of the metering rod did not affect the maximum pressure or the total area under the pressure curve [27, 31]. This was stated to demonstrate that the measuring system was fast enough to measure this type of pressure pulse [27, 31].

Most important in coating color application is to deliver a uniform film onto the roll without ribbing or spitting at the outlet of the metering nip [18, 19, 20, 32, 33, 34]. Ribbing is a series of waves on the film surface (Figure 2, left side). An increase in either metering rod velocity or fluid viscosity, which reduces the minimum pressure in the rod nip exit, also seemed to stabilize the ribbing pattern [18]. The rib width increased with particle and/or polymer concentration and decreased as the nip gap was narrowed [19, 32]. The expulsion of small droplets from the metering nip - spitting (Figure 2, right side) - usually started at the roll edges and then propagated toward the center of the nip [32]. This coating color spitting occurred with high coating color solids contents and rod loads when a low coatweight was targeted [20, 32, 33, 34]. Delaminated kaolin as a pigment combined with a low fluid phase viscosity caused more spitting than standard kaolin [33]. Spitting can be eliminated by changing the process conditions (e.g. increasing the rod rotation speed) or by optimizing the coating color properties (e.g. reducing the solids content) [20, 33, 34].

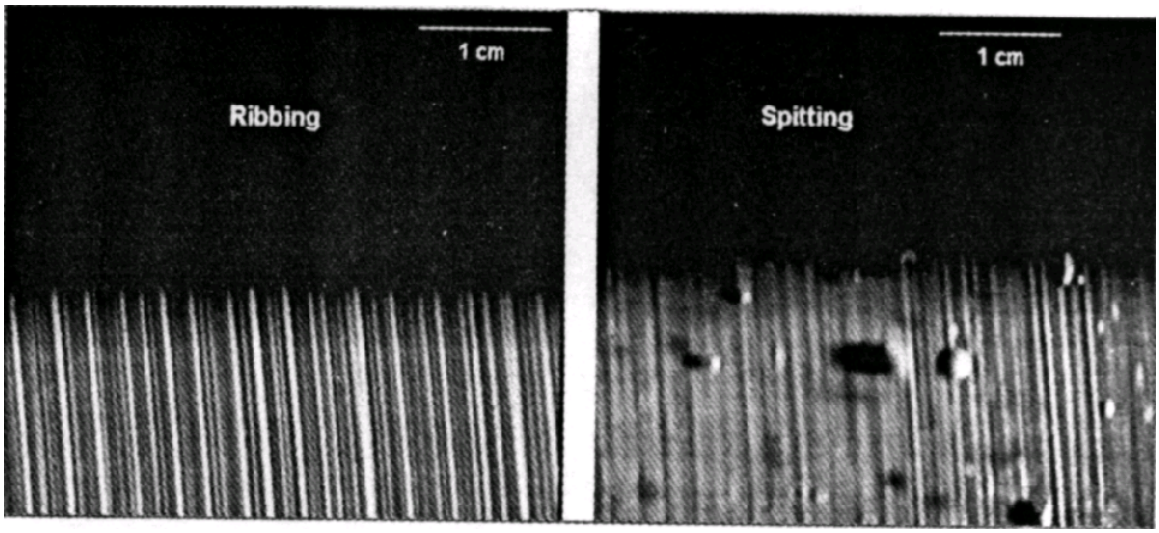

Figure 2. Ribbing patterns on the roll surface (left) and spitting of coating color droplets on the roll surface (right) at the premetering [32].

3.1.1.2 Effect of the coating color

Coating color properties such as color composition, dry solids content and high shear viscosity influence the hydrodynamic pressure in the nip. When the solids content is increased, the rod pressure is also increased to maintain a constant amount of film, the result being an increase in the hydrodynamic force [28, 31]. These observations agree with simple lubrication theory [28, 31]. When the gap between the rolls was kept constant, the roll separating force increased as the viscosity of the fluid increased [28, 31]. A kaolin-based coating color needed almost twice the rod loading compared to $CaCO_3$ to achieve the same film thickness at the same solids content and under the same process conditions [28, 31]. To achieve comparable behavior for both coating colors during the application, the solids content of the kaolin coating color had to be about 4% lower than that containing $CaCO_3$. The results of the high shear viscosity measurements were very similar to those of the pressure profile measurements: the measured high shear viscosity was about twice as high for kaolin as for $CaCO_3$ at equal solids contents [28, 31].

Coating color binder content also affected the hydrodynamic forces. The hydrodynamic force decreased as the latex content of the coating color was increased [28, 31]. This was explained as being due to less pigment particle-particle interaction and to greater lubrication of the pigment particles. When CMC was replaced with starch in the coating colors, the suspension viscosity increased [28, 31]. The measured hydrodynamic force was about 50% higher with starch-latex than with CMC-latex under the same process conditions [28, 31].

When the CMC content of the coating color was increased at constant speed and film thickness, the hydrodynamic force also increased [28, 31]. This means that with a higher CMC content, a higher rod load was needed to keep the amount of film constant. The effect of CMC addition on the hydrodynamic force was greater with $CaCO_3$ than with kaolin. Similar results were obtained from high shear viscosity measurements [28, 31]. This was

explained as being due to CMC adsorption onto the kaolin pigment, which meant that the flow behavior of the coating color did not change as much as with commercial $CaCO_3$ slurries [28, 31, 35] in which the CMC remained mainly in the liquid phase.

An experimental correlation was determined for the amount of metered film on the transfer roll as a function of relevant process parameters using dimensional analysis and the results of pressure profile measurements [29, 31]. The correlation formula included four unknown parameters that depended on the composition of the coating color or on process conditions. The values of the linear fit constants in the correlation model depended on the coating color properties [29, 31]. The pressure profile measurements at the surface of the metering rod were compared with the results of numerical simulations. A good correlation was found between the simulation results and experimental measurements for the coating colors containing $CaCO_3$ and latex, but not for the coating colors also containing CMC. This was explained as indicating that the rheological model used did not adequately describe fluid flow with more non-Newtonian coating colors [31].

3.1.1.3 Effect of the transfer roll

Raising the machine speed increased both the hydrodynamic force in the rod-roll nip and the amount of film at a given rod pressure [5]. The pressure measurements made at the surface of the metering rod by Poranen *et al.* [27, 31] showed that, for a constant film thickness on the roll, both maximum pressure and hydrodynamic force increased as the speed of the transfer roll was increased. The total width of the pressure profile measured in the metering nip did not depend on the speed of the transfer roll [27, 31]. The results [30, 31] from the pressure and strain distribution measurements in the cover material showed that the shapes of the measured pressure strain profiles were very symmetric relative to the position of the maximum pressure.

The hardness of the roll cover material is also important in premetering, softer roll materials giving higher film amounts [20, 25, 36] than harder roll cover materials. Softer roll cover materials increased the contact area and therefore reduced the hydrodynamic force per unit contact area. The roll cover material affected roll hardness under dynamic conditions when polyurethane and rubber covered rolls were compared [31]. The P&J hardness for polyurethane rolls was 28 P&J (PU28) and for rubber rolls 65 P& J (RUB65). The film thickness measured was about the same at a low speed of 800 m/min, but when the speed was increased to 1600 m/min, the film thickness increased more rapidly with PU28 than with RUB65 [31]. This was stated to indicate that RUB65 behaved as a harder material under dynamic nip conditions than PU28 due to the more viscous nature of the rubber cover material.

3.1.2 Coating color transfer in the roll nip

Coating color transfer in MSP coating is a very fast phenomenon. The base paper is in contact with the coating color in the transfer nip only for 1-4 ms. The contact time depends on the coater running speed, roll diameter, and roll cover material and its thickness. The coating color transfer is similar to ink transfer in printing, where a constant film is premetered and film splitting is involved [37]. In both cases, the substance transferred exhibits non-Newtonian behavior and the properties of the coating color or ink change as the coating color liquid phase or the ink solvent is absorbed into the paper [37]. In printing, the total amount of the ink transferred is generally assumed to be the sum of the immobilized ink and a constant fraction of non-immobilized ink [38]. The split of the non-immobilized ink in printing with a high film thickness has usually been assumed to be 50%, but it has seldom been that high [38].

The coating color in MSP coating is pressed against the base paper in a nip between two rolls. Coating color dewatering and immobilization in the transfer nip was originally modeled by assuming that it is a filtration process with constant specific pressure for a very short time [4, 5]. Film splitting was assumed to happen in the fluid layer (in the non-immobilized coating layer). Coatweight was later reported to be affected also by bulk coating color penetration into the largest pores in the paper [33, 39, 40, 41]. The latest results (Figure 3) showed that coatweight was affected by bulk coating color penetration and dewatering in the nip and by the film splitting in the middle of the non-immobilized layer at the nip exit (between the filter cake and the roll surface) [20, 33, 40, 41].

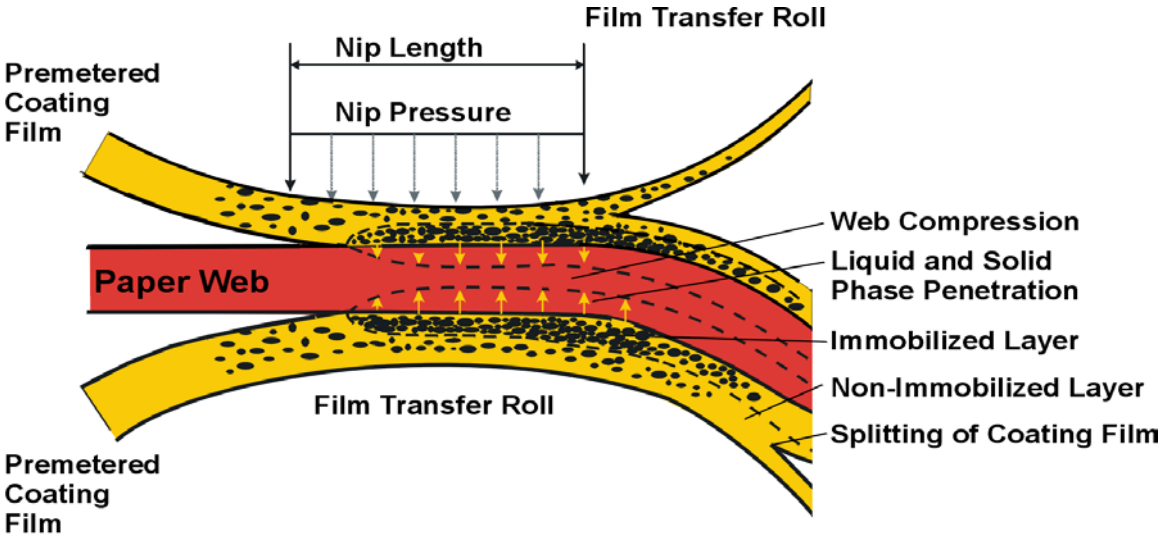

Figure 3. Coating layer formation in the MSP transfer nip [41].

The main variable affecting film transfer is the amount of film on the roll. As mentioned above, this is controlled by means of the film premetering variables and the coating color properties, especially coating color viscosity at high shear rates. The other factors that are assumed to affect coating layer formation on the base paper are:

1. coating color composition (due to bulk penetration: coating color viscosity at low shear rates and due to liquid phase penetration: coating color dewatering, filter cake formation and the properties of the coating color liquid phase),
2. base paper properties (permeability, pore size, surface openness, absorption potential of the base paper, surface chemical properties of the fibers), and
3. the pressure pulse in the transfer roll nip (the maximum pressure and the width of the pressure pulse are affected by roll diameter, roll cover material and thickness, and linear load in the nip) and nip dwell-time (the width of the pressure pulse and the machine speed).

3.1.2.1 Effect of coating color composition in the transfer nip

Coating color composition has a pronounced effect on initial color penetration followed by dewatering and filter cake formation in the nip. Initially, there is a possibility for the coating color to flow into the large voids of the sheet without any liquid phase separation from the bulk suspension. It is speculated that penetration of the suspension is governed by low shear viscosity and the size of the external nip pressure.

Many different theories for the principle of coating color dewatering have been proposed over the years. Windle *et al.* [42] have introduced a “filtration mechanism”, in which an immobilized layer consisting of coating pigments and all non-soluble components is formed at the base paper surface due to filtration dewatering. This immobilized layer, which grows with dewatering, builds up a structure that is denser than the bulk structure. According to this principle, the coating layer is composed of two distinct layers: the one with the application solids content is called the bulk layer, and the one with higher solids content is called the immobilized layer. Pure filtration implies a sharp transition from lower solids content to a higher solids content without the presence of a transition zone [43].

The immobilization point of coating color was defined by Watanabe and Lepoutre [44] to be at the first critical concentration (FCC) at which particle motion was greatly restricted. As long as the surface of the wet coating had a continuous water film, the specular reflection remained high [44]. A sudden drop in gloss was assumed to indicate that the water film was no longer continuous and menisci formed in the coating structure. At the FCC, the particles of the coating color formed a three-dimensional network and could not move freely [44]. After the FCC, when more water leaved, the capillary forces grew and compacted the pigment-latex network [44]. Latex deformation started after the FCC and was probably finished at the second critical concentration (SCC). The SCC was defined by Watanabe and Lepoutre [44] as the concentration at which the network was fixed and air entered the rigid coating structure.

At the SCC the reflectance rose sharply, indicating that the light scattering process was considerably enhanced [44]. The change was assumed to be due to the fact that the largest of the liquid filled spaces became filled with air. At the SCC, overall latex coalescence and flow appeared to be complete with no further structural changes [44].

The other suggested dewatering principle is a “thickening mechanism”, suggested by Böhmer [45]. For the thickening mechanism, a solids content gradient is assumed to be formed in the coating layer during the dewatering process while water transport is assumed to be based on a diffusion mechanism. The main difference between the two mechanisms is the lack of a transition zone in the non-immobilized layer for the filtration mechanism [43]. The experimental work carried out on the pilot scale under dynamic conditions [43] suggested that both mechanisms are present. More resent model experiments and analysis using static conditions have demonstrated that there is a concentration gradient of particles in the filter cake formed, which is not accounted for in the traditional filtration theory [46].

When the filter cake is thin at the initial phase of contact with the coating, paper surface openness is the most important factor. But once the filter cake becomes established, the rate of dewatering is controlled entirely by the properties of the filter cake. Based on the dewatering principle, dewatering has been modeled as liquid transport through a porous material of growing thickness. The coating color dewatering model was first introduced for blade coating [47, 48, 49], but similar calculations have since been made for MSP coating [4, 5, 50].

The filtration volume is proportional to the square root of both time and dewatering pressure. A pressure drop is therefore needed to start and maintain the dewatering of the coating color into the base paper. The pressure drop is equal to the sum of the external pressure and capillary pressure [51]. The most important coating color variables affecting the extent of dewatering and filter cake thickness by filtration dewatering are the viscosity of the liquid phase, the type of particles in the color (e.g. size, shape and distribution), and the packing structure of particles in the immobilized layer (porosity and packing of the filter cake)[47, 49]. Coarse pigments with a rather steep size distribution gave a fairly open structure due to their low degree of packing, which results in fast dewatering [4, 5, 45, 47, 48, 52, 53, 54]. Coating structures based on plate-like particles with a high shape factor and a broad size distribution exhibited pronounced tortuosity, which reduced the dewatering rate [47, 49, 53].

The amount of water removed is not a function of the application solids content but a function of the difference between initial application and immobilization solids contents [47, 49, 54]. This is why $CaCO_3$ coating colors with a higher immobilization solids content can be applied at a higher solids content than pure kaolin coating colors [53]. If the immobilization solids content is high, a densely packed matrix forms at the coating/base paper interface, preventing the wet film from further dewatering. The higher the immobilization solids content the lower the pore volume of the coating structure [54]. The porosity of the immobilized layer alone does not determine the rate of dewatering, which is also affected by the way in which the particles are packed at a certain porosity [47, 49]. The liquid phase viscosity affecting dewatering is dependent on both the amount and the type of thickener used and on the prevailing temperature, with an increase in temperature leading to lower viscosity [47, 49].

3.1.2.2 Effect of base paper properties in the transfer nip

The structure and surface properties of the base paper are affected by the dewatering conditions in the paper machine forming and wet pressing sections. The forming section determines the main structure of the paper, which can be characterized as a filler or fines distribution. The construction of the forming section (fourdrinier, hybrid or gap former) and the variables on the forming roll and blade section in a gap former determine the distribution of fillers and fines in the paper structure [55, 56, 57]. By layering the different fiber fractions or different chemicals in the headbox, it is possible to control the fines and filler distributions without changing other paper characteristics [57, 58].

The final density distribution of the paper was significantly changed during wet pressing, but the fines and filler distributions in the paper web were not affected by laboratory wet pressing [59, 60, 61]. The density increase was always greatest on the felt side, which was the direction of water transport, and smallest on the solid roll side [60, 62]. When water was removed slowly without any significant hydraulic pressure being formed in the sheet, no z-direction density gradient was observed [60, 61]. Changes in the absorption capacity of the paper closely followed the changes in surface density [60, 61, 62]. The press section has a major influence on the two-sidedness of oil absorption (density distribution) and roughness (felt marking). When wood-containing mill base papers were coated with an MSP, the base paper side with the higher oil absorption resulted in lower paper gloss than the denser base paper side [4, 5]. The lower gloss was suggested to be the result of deeper penetration of the coating color [4, 5].

Base paper porosity and absorption properties are affected not just by forming and press section dewatering but also by the furnish composition. A paper surface of low “openness” can be defined as a surface with small, shallow pores. The openness of wood-containing base paper was lowered by increasing the amount of DIP pulp in the furnish [6]. This reduced the permeability of the base paper, increased the MSP-coated paper gloss and gave the most even printed image in heatset offset printing [9]. Paper surfaces of low openness were achieved by pre-calendering the base paper or by increasing the filler or fines content of the base paper furnish [10, 13, 14]. A paper surface of low openness obtained by calendering resulted in a slight decrease in coating color penetration as determined from the cross-sections [10] and gave improved printing results [11]. A higher filler content has been suggested to reduce bulk coating color penetration and to increase water penetration into the base paper and thereby increase coating color dewatering [10, 14]. Mechanical pulps with high fines contents (GW) gave dense base paper structures [14]. The closed surface obtained by using short-fibred mechanical pulp, a high filler content or pre-calendering of the wood-containing base paper improved both coating coverage [13, 14] and coatweight uniformity [14]. Coatweight variations can be defined to indicate the coat mass uniformity at the surface.

The use of TMP or CTMP with a low fines content and a high long fiber content makes it difficult to achieve high coating coverage and coatweight uniformity in MSP coating [17]. Coating color flow throughout porous base paper is critical when one side of the base paper is coated with an MSP, especially with low basis weights and porous base sheet structures [20].

Coating color “strikethrough” has been seen even at the mill, and this has caused coating color buildup on the roll [20, 63]. This is thought to be especially critical for woodfree base papers with a high average pore size.

Base paper formation has been found to influence MSP-coated paper gloss evenness and printed paper quality in the case of wood-containing base papers [21]. In other studies base paper formation has not been found to influence MSP-coated paper or printed paper quality [15, 22]. This is quite different from blade coating where, in the same study, improved formation was found to yield slight improvements in coated paper gloss and print quality [15].

Coating transfer ratios and non-immobilized coating color amounts with two base papers with different absorption potentials (wood-containing, marked here WC and woodfree, WF base paper) were measured using slow and fast dewatering coating colors at two different speeds (500 and 1000 m/min) [64]. The amount of film applied was kept constant by using grooved rods [64]. According to the results, transfer ratios were higher with fast dewatering colors on a base paper with higher absorption potential and with a longer dwell time in coating [64]. The absorption potential was measured using the dynamic penetration method (DPM, known as the EMCO measurement). The result is water penetration without separating the effect of the structure’s openness from the surface chemical properties of the base paper. The absorption potential of the WC paper was higher than that of the WF paper [64]. The faster dewatering might be due to the differences in the number of pores and in the average pore size, or from the hydrophobic sizing of the WF base paper. In general, wood-containing base papers have smaller pores, but the number of pores is higher due to the shorter fibers used in the furnish than those in WF base papers.

The effect of hydrophobic sizing has not been studied for MSP coating. According to the results from a laboratory blade coating study, in which the absorbency of the base sheets was modified by hydrophobic sizing, the sizing did not determine coating coverage or coating layer holdout and uniformity [65]. In that study, the coating holdout was defined as the degree to which the coating contributed to surface brightness [65]. The study was based on handsheets prepared in the laboratory using different refining, wet pressing and sizing conditions, and covered a wide range of pore sizes, pore volumes and surface chemical properties. Laboratory blade coatings carried out with these base sheets showed that coating holdout and coating mass distribution uniformity were significantly lower with all porous sheets than with dense sheets [65]. On dense, smooth sheets, hydrophobic sizing led to lower coating pickup [66]. Microscopic examination of the surfaces showed that the coating beaded up into islands and left uncovered areas [66]. This was attributed to a reduced filter cake buildup under the capillary pressure from the base sheet pores prior to metering by the blade, and was explained by a negative capillary pressure due to the hydrophobic sizing agent. In a study by Salminen [51], the main water transport mechanism with hydrophilic base papers was suggested to be capillary absorption but with hydrophobic base papers diffusion [51]. Diffusion is relatively slow [51, 67] and a thinner filter cake was therefore formed than in the case of dewatering by capillary absorption [66].

With woodfree paper grades, chemical pulp refining has a major impact on the base paper structure. The refining of chemical pulp loosens the structure and surface of the fiber wall. It

also breaks fragments from the fiber wall, thereby increasing the fines content. Internal fibrillation corresponds to a partial delamination of the fiber wall. The delamination increases the degree of swelling, flexibility and conformability of the wet fiber wall. Fibrils that spread out from fiber surfaces are a clear indication of external fibrillation. Both internal and external fibrillation make the base paper structure denser and reduce the average pore size of the base paper. Refining also affects the average size and fractional free volume of the fibers. The average pore size in the fiber wall decreased [68] but fractional free volume (pore volume) increased when chemical softwood fibers were refined to lower CSF [68, 69]. A work by Stone and Scallan [70] has shown that in the dry state fiber walls are essentially non-porous. In the wet state, the walls are swollen above their dry volume by an amount equal to the volume of water [71]. The wall structure of wood fibers, the change in the structure during pulping [71, 72], and the changes induced by drying and refining of the chemical pulp [72] affected the pore size distribution in the fiber wall. Pores smaller than 25 Å are called micro-pores and pores up to 300 Å are called macro-pores [73].

Fiber wall swelling was studied with a high-speed camera [74]. In this study, the swelling of individual fibers was observed as a function of time when a large amount of water was applied to the fibers. The increase in fiber wall width was measured and the time when about half of the total swelling had occurred was recorded. The time was 70 ms for chemical pulp fibers from pine and 100-140 ms for mechanical pulp fibers [74]. In the wet pressing and drying of paper, the macro-pores are first dewatered and closed [75]. The work by Weise [76] and Maloney [75] on porosity of the fiber wall has shown that part of the pore collapse in wet pressing and drying is non-reversible and will therefore in later process stages decrease water transport into the fiber wall and thus fiber swelling.

3.1.2.3 Effect of the pressure pulse in the transfer nip

Coating layer formation in MSP coating is a very fast phenomenon. As mentioned earlier, the base paper is in contact with the coating color in the transfer nip only for 1-4 ms. This contact time depends on the coater speed and on the width of the pressure pulse in the MSP transfer nip. The transfer roll diameter, the roll cover material and its thickness, and the nip linear load affect the width of the pressure pulse. Poranen *et al.* [30, 31] measured the width of the transfer nip to be about 60 mm with polyurethane roll giving a dwell time of 3.6 ms at 1000 m/min and 1.8 ms at 2000 m/min. Metered size press coating applications generally operate with wider nip widths (lower nip pressures) than surface sizing applications [77]. The length of the pressure pulse and the dewatering time with soft rolls are longer but the maximum pulse pressure is lower than with hard rolls. When thinner cover material is used, a higher load is needed to produce the same contact length [31]. An increase in the roughness of the roll surface gave a greater wet film thickness under the same process conditions than a smoother roll of the same material [78].

Letzelter and Eklund [50] modeled dewatering of the coating color in an MSP transfer nip using an assumed pressure distribution. In order for dewatering to take place, a pressure potential is required. In the case of MSP coating, the pressure potential was the sum of the capillary pressure and the external pressure pulse in the nip acting on the coating color [50,

51]. The roll diameter, cover material and the linear load determined the shape and area of the external pressure pulse in the model. The time during which the color was subjected to this pressure pulse was determined by the machine speed [50]. The calculations of the pressure pulse were based on the Hertz theory. Both the maximum pressure pulse and the nip length in a roll nip have been calculated according to this theory [50]. The shape of the pressure pulse was assumed to be elliptical. The shape of the pressure pulse in the proposed model had no influence on the final calculated amount of water removed. In fact, it was found to be the total area of the pressure pulse that determinated the amount of water removed in the model [50].

According to the calculations by Letzelter and Eklund [50], the width of the pressure pulse increased with increasing linear load. The effect of linear load has been shown to be very small in practical MSP coating. Poranen *et al.* [30, 31] measured the pressure distribution in both the metering nip and the transfer nip using pressure sensors placed in the roll cover. According to their results, the total width of the pressure distribution was not changed, but the maximum pressure and the area both increased as the linear load between the rolls was increased. The width of the pressure pulse was of the order of 60 mm for all linear loads. The measured pressure distributions were symmetric and the pressure pulse resembled normally distributed curves [30, 31] more than elliptical forms. Raising the speed increased the maximum pulse pressure and lowered the dwell time in the nip. When the coater speed was increased from 500 to 1500 m/min [30, 31], the pressure pulse maximum and area both increased at a constant pressure profile (Figure 4), but the total width of the pressure profile was almost the same.

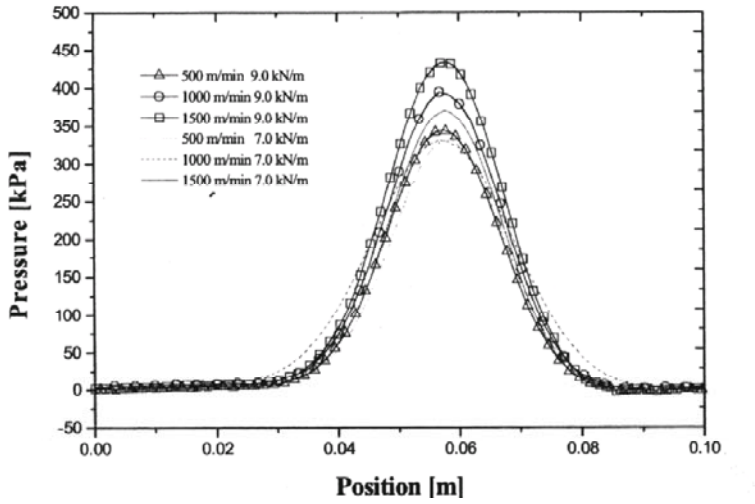

Figure 4. Pressure pulse in the MSP transfer nip at different speeds (500, 1000 and 1500 m/min) and linear loads (7.0 and 9.0 kN/m) [30, 31].

The pressure pulse measured in the transfer nip was positive throughout [30, 31]. This might be due to the limitations of the measuring technique or to the high nip pressure. The pressure profile measured from the premetering nip had a small subatmospheric pressure at the exit of the nip [18, 19, 28, 29]. Similar results have been reported in a study where a printing press tack meter was built by fitting a pressure sensor into the printing cylinder of a laboratory printing press [79]. A subatmospheric pressure was seen at the nip exit and greater reduction in pressure was measured with an increasing amount of ink in the nip [79]. Relatively non-

porous substrates such as coated papers produced subatmospheric pressure further from the nip exit than porous substrates such as newsprint [80]. This pressure is below the vapor pressure of water. Therefore it is possible that the liquid layer will cavitate at the exit: vapor bubbles will form and a non-uniform flow of coating (filament formation) will take place [81].

The dewatering models presented by Trefz [5] and Letzelter and Eklund [47, 48, 49, 50] are based on a constant or assumed symmetric pressure distribution in the metering nip. These models capture the fundamentals of dewatering in coating processes, but do not take into account the dependence of the pressure profile on the loss of fluid and on the buildup of a filter cake. Ninnes *et al.* [82] modeled the pressure distribution and the absorption of coating into the web in the nip. Fluid mechanics equations were coupled with absorption rate equations to predict coating color transfer and the buildup of a filter cake. The result of the calculations was a non-symmetrical pressure pulse with a small but finite subatmospheric pressure peak at the exit from the nip. According to these calculations, the extent of coating color liquid phase penetration was found to influence the pressure distribution in the nip [82] and the model predictions compared well to the transfer ratio reported by Grön *et al.* [33].

3.1.3 Film splitting and leveling after the roll nip

In the early 90' s, the MSP coater was believed to cause runnability problems such as color misting, film splitting patterns and orange peel patterns. Most of the previous research has concentrated on optimizing coating color formulations and machine parameters to prevent or reduce the occurrence of these problems [20, 21, 22, 33, 34, 63, 83, 84, 85, 86, 87, 88, 89]. Later 1C2S MSP installations with both sides coated simultaneously introduced the problems of uncontrolled web release and web stealing [20, 40, 41, 63, 90].

Salminen *et al.* [83] presented a hypothetical model taken from print nip studies and applied it to the film splitting process (Figure 5). The film splitting process was divided into three regions. In the first region, the dewatering region [83], an immobilized coating layer starts to form at the interface between the base paper and the applied coating color by the dewatering mechanism [4, 5, 50]. The kinematical picture in this region is one of shear and the movement of the suspension is predominantly laminar [91]. The actual origin of droplet formation (misting) is from the second region, the film splitting region [83]. Surface tension forces and rheological properties determine events in this region. This region consists of both cavitation and filamentation regions [91]. The normal pressure profile for any forward rolling nip geometry has a pressure peak and a pressure minimum. If the pressure drops below the vapor pressure of the fluid, cavitations occurs in the nip exit. The vapor bubbles cause regions of less liquid and as the nip opens up filaments are formed [91]. The third region, the relaxation region, affects the leveling-off of the unevenness of the coating surface (orange peel formation) [83].

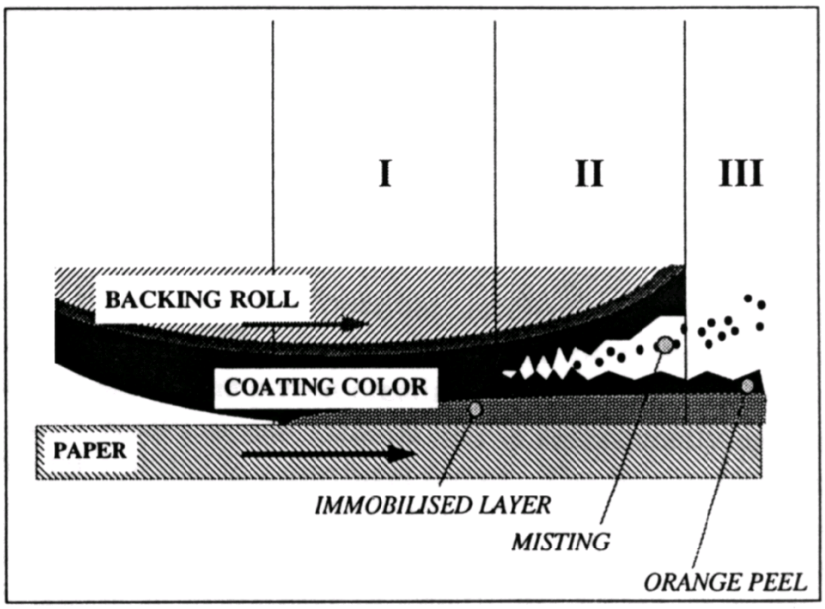

Figure 5. Schematic model of the film splitting process [83].

Two possible mechanisms to describe misting have been presented by Roper III *et al.* [21, 86]:

1. a filament breaks at two or more locations within a short time period creating an air-borne drop, or
2. a filament breaks at one location and is subsequently ejected from the roll due to centrifugal forces.

The coating color is believed to accelerate misting and orange peel formation because of the easier filament break-up into small droplets due to the surface tension forces as well as the centrifugal forces ejecting large droplets into the air [21]. Experimental work with different coating colors has suggested that a low misting tendency could be achieved by increasing the solids content [33, 34, 40, 84, 85], or by including in the color formulation low-viscosity sole-binder latexes [83]. The use of thickeners and additives giving water retention without forming strong elastic interactions in the coating color has been suggested to reduce misting [87]. Another study [88] suggested that the viscoelastic properties of the coating color are not relevant in MSP coating. It has been stated that the optimal transfer ratio is dependent on coatweight range: at 9-10 g/m^2 the ratio is 70-80% and at 6-8 g/m^2 75-90% [33, 40]. In both cases a thin bulk coating color layer exists where the film split will appear [33, 40]. When the solids content was increased, the thickness of the non-immobilized layer decreased and the transfer ratio increased. The trend towards increased solids contents also imposes a challenge in terms of coating drying on the roll surface at high transfer ratios [20, 63].

Patterns in the coated surface can be divided into two different groups. At low coatweights (below 8-9 g/m²) coating color penetration into the paper surface voids and the lack of coating coverage dominate. Film splitting patterns (i.e. “orange peel”) arise at high

coatweights and low solids contents [20, 21, 22, 63]. These patterns in the coating layer, or with uneven coating mass distributions in MSP-coated papers [21], appeared to be associated with print non-uniformities [89]. At high coatweights these patterns had a significant machine orientation, probably governed by the base paper structure rather than by film splitting [21]. The significant MD orientation implies that the coating filling in the surface pores will also be oriented in the MD because the shapes of the pore entrances of the base paper have an MD orientation as well [92]. Increasing the application solids content has clear benefits: increased coating coverage [20] and reduced drying demand. Coating color strikethrough is the flow of coating color through porous base paper, when only one side of the base paper is coated in MSP coating (2C1S). This strikethrough might also create a pattern due to pronounced coating penetration on the side of the base paper coated in the first pass [20].

Web release is especially critical when both sides are coated simultaneously. An uncontrolled web release, or web stealing, occurs as web flutter between the rolls. When the process conditions were similar on both sides of the paper, the web did not know which roll surface to follow [20, 63, 89, 90]. Sheet openness and smoothness were the main base paper properties affecting web release at coatweight below 10 g/m² [20, 41, 62, 90]. In the case of paper two-sidedness, the more closed surface dominated when the difference was large enough. In that case, the web was released from the more closed web surface. With no significant absorption two-sidedness, web release was dominated by base paper smoothness [20, 40, 41, 62, 90]. The best way of controlling web release was to induce a difference in coating color composition, coatweight or solids content between the top and bottom coating films [20, 41, 62, 90]. Web release can also be controlled to some degree by arranging a difference in hardness between the rolls and also through a certain speed difference between the rolls [20, 41, 62, 90].

3.2 Theoretical background to the transport phenomenon

Coating color transfer in MSP coating is similar to ink transfer in printing, where a constant film is premetered and film splitting is involved [38]. The total amount of ink transferred has been assumed to be the sum of the immobilized or otherwise accepted ink and a constant fraction of the non-immobilized ink [38]. Film splitting can be expressed mathematically as follows [38]:

$$y = L_{accepted} + f(L_{susp} - L_{accepted}) \quad (1)$$

where y is the amount of suspension transferred per unit area,
L_{susp} is the suspension film thickness originally on the plate,
$L_{accepted}$ is the thickness of the immobilized or otherwise accepted suspension of the stock, and
f is constant fraction of non-immobilized suspension transferred to the stock.

Nordström and Grön [93] have shown that thin-film transfer in printing and coating can be described using the Fetsko-Walker equation. However, the practical range of interest is narrower than that described by the Fetsko-Walker equation. MSP coating involves the use of a thick film, and it is advantageous to keep the non-immobilized coating layer thickness low in order to avoid misting [20, 33]. The variables that affect coating color penetration and immobilization are therefore the ones that can be used to adjust coating layer formation in practice.

3.2.1 Bulk coating color penetration

The amount of premetered coating film is the main factor determining the maximum amount of coating that can be transferred to the paper. The flow rate of bulk coating color into the base paper structure is proportional to the pressure gradient. Bulk coating color penetration under pressure into the paper can be described according to the experimental rule found by Darcy [94]. In the simplest case, Darcy' s law gives the flow rate per unit area, Q/A, of laminar flow as:

$$\frac{Q}{A} = \frac{-K \cdot \Delta p}{L} \quad (2)$$

where Δp is the total pressure drop across the sample length, L, and
K (m^3s/kg) is the volume permeability coefficient or permeability constant, which depends on the porous medium and the fluid viscosity.

If the fluid viscosity, η, is separated from K, the flow rate is defined [94] by:

$$\frac{Q}{A} = \frac{-K_v \cdot \Delta p}{\eta \cdot L} \quad (3)$$

where the constant K_v (m²) is the permeability coefficient for viscous flow (the coefficient depends only on the structure of the porous medium), and η is the fluid viscosity (in this case coating color viscosity).

The Krozeny-Carman equation gives a relationship between permeability and porosity. The model assumes a uniform bed of packed particles with an effective particle diameter, d_{eff}. Classically, investigators have used the following equation for paper to relate permeability to porosity [95]:

$$K_v = \frac{\phi^3 \cdot d_{eff}^2}{36 \cdot (1-\phi)^2 \cdot \kappa} \quad (4)$$

where ϕ is porosity,
d_{eff} is the effective particle diameter, and
κ is the Kozeny constant.

Experimental studies of the relationship between the permeability and porosity of fibrous filters and compressed fiber substrates have given results showing that, with reasonable accuracy, porosity alone determines the specific permeability in dimensionless form, K_v/d_{eff}^2 [95]. The permeability of paper may differ from that of ideal fiber network because the effects of external fibrillation, fines and fillers have not been studied [96]. The porous fiber network in paper is anisotropic, which means that the flow resistance in different directions is different. According to Lindsay [97], the MD permeability $K_{v,x}$ was greater than the CD permeability, $K_{v,y}$, and the z-direction permeability was the smallest.

3.2.2 Coating color liquid phase penetration

The penetration of the liquid phase of the coating color into paper is believed to be more important for coating color transfer than the bulk flow into the paper structure. All models assume that the void structure is a bundle of cylindrical capillaries. Liquid penetration takes place through capillary flow into the capillaries. The Lucas-Washburn equation can to some degree be used to analyze liquid penetration into paper. Assuming that the flow is driven solely by surface tension, capillary pressure p_c is [96]:

$$p_c = \frac{2 \cdot \gamma \cdot \cos\theta}{r} \quad (5)$$

where γ is the surface tension,
θ is the contact angle between the liquid and the capillary wall, and
r is capillary radius.

The Lucas-Washburn equation [96] is usually presented in the following form:

$$h^2 = \frac{r \cdot \gamma \cdot \cos\theta}{2 \cdot \eta} \cdot t \quad (6)$$

where h is the distance traveled,
η is fluid viscosity, and
t is time.

Salminen [51] studied liquid transport using a measurement system based on a liquid applicator with a slit opening using different web velocities to adjust the contact time. He demonstrated experimentally without the use of external pressure that water transport by capillary absorption was strongly affected by the surface tension of the liquid phase but not as clearly by the viscosity of the liquid phase as shown by the Lucas-Washburn equation (6). If there is also an external pressure difference, p_e, in addition to the capillary pressure, we have the following form [96]:

$$h^2 = \frac{r^2 \cdot t \cdot (2 \cdot \gamma \cdot \cos\theta / r + p_e)}{4 \cdot \eta} \quad (7)$$

The high nip pressure employed in the MSP coating process forces the liquid to penetrate into the paper. The pressure pulse may thus be very high compared to the capillary driving pressure difference. According to the experimental work by Salminen [51] the liquid transport with high external pressure was strongly influenced by the viscosity of the liquid phase.

In this case another equation can be derived by combining Darcy's law with Kozeny-Carman's equation [98]:

$$h^2 = \frac{2 \cdot r^2 \cdot t \cdot p}{\kappa \cdot \eta} \quad (8)$$

where κ is the Kozeny constant (approximately 6 for paper) [98], taking into account the irregular and tortuous pores, and
p is the liquid pressure in the nip.

These models assume that the void structure is a bundle of cylindrical capillaries with radius r. But real porous systems are tortuous and the equations should be modified by adding terms describing the pore volume, void fraction ε, and the tortuosity of the paper structure, τ [98] instead of using only the Kozeny constant.

According to Equations 6-8, the penetration depth of liquid is proportional to the square root of the penetration time. At sufficiently high pressures, liquid penetration into paper has been found to be approximately proportional to the square root of time, though at low pressure it was not [51]. A dependence on the square root of time is quite often found in experiments, where the Lucas-Washburn equation can be used to evaluate the data. However, the square root of time dependence of penetration can also arise from diffusion processes [96]. Bulk diffusion into the fiber wall and surface diffusion along fiber surfaces may be more important than capillary absorption, especially with long contact times [51, 67].

3.2.3 Dewatering by diffusion (thickening mechanism)

Water transport in paper by diffusion has been proposed to consist of diffusion transport of vapor in the pores, surface diffusion in the pores, and water transport through the fiber walls [51]. Fick's first law can describe diffusion, in which the important factors are the diffusion coefficient of the material and the concentration [100]. If water vapor behaved like an inert gas its flow rate should be almost constant. The real flow rate is much higher except at the lowest vapor pressures [101]. At sub-saturation vapor pressures, the water transport mechanism may also be surface diffusion [101]. As long as the pore is larger than the water molecules its size has no effect on the rate of their movement. Water transport is driven by the gradient in the surface concentration, not by the gradient in the volume concentration of water vapor in the inter-fiber pores [96].

The transport of water through fiber walls causes swelling of fibers and affects liquid penetration. This also applies to other polar liquids. Sorption into the fiber wall and diffusion within the fiber wall material causes the fibers, and hence the paper, to swell. Water sorption into the fibers increases paper volume by the volume of water absorbed. In contrast, pore

penetration does not increase paper volume. The diffusion process can be described by Flick's second law, which is obtained by combining Flick's first law with the equation of continuity. This gives the relationship between the rate of concentration change, dc/dt, and the concentration gradient [44, 51]:

$$\frac{dc}{dt} = \frac{D \cdot d^2c}{dx^2} \qquad (9)$$

where D is the diffusion coefficient, assumed to be independent of concentration,
c is the concentration, and
x is the flow direction.

Assuming that the diffusion coefficient is constant, the amount of liquid absorbed at the early stage of the diffusion process is proportional to the square root of time [51]. Regenerated cellulose films are non-porous but absorb water by a diffusion mechanism. The dynamic liquid absorption was measured at atmospheric pressure and at elevated external pressures and liquid temperatures [51]. The measured amount of liquid transferred to the cellophane followed the square root of time dependence, and the transport was found to be relatively slow, 1-2 s [51]. The external pressure used in the experiments did not influence the water transport rate [51].

With cellulose fibers, the diffusion along the fiber axis was assumed to be faster than in the perpendicular direction because of the extension of channels along the microfibrils. Because the diffusion coefficient was measured [102] as an average over all fiber orientations in the sheet plane, anisotropic diffusion led to a distribution of the diffusion coefficient. Diffusion is a dynamic process: as water diffuses into the walls, chain mobility increases, which accelerates the process. The diffusion coefficient of water absorbed into cellulose was found to have a fairly broad distribution of values, and the average diffusion coefficient increased with increasing moisture content [102]. In systems containing several diffusing components, i.e. several components initially present on only one side of the boundary, an average apparent diffusion coefficient is used, which depends on concentration [100]. Water transport into the fiber wall and swelling of the fiber wall were found to be relatively slow (70-140 ms) according to the experimental work carried out by Kartovaara [74] under dynamic conditions.

3.2.4 Dewatering by filtration (filtration mechanism)

If the immobilized layer is formed at the interface between the paper and the coating color, the properties of the coating color determine the amount of liquid phase lost through dewatering. All liquid transport through a porous material of constant thickness can be described with the following expression, which was modified from the Kozeny-Carman equation [47, 49]:

$$\dot{Q}_{liquid} = \frac{A \cdot b \cdot \Delta P}{\mu_f \cdot \mu_l \cdot L_{filter-cake}} \quad (10)$$

where Q_{liquid} is the amount of liquid phase removed through dewatering,
A is the filtration area,
b is the flow coefficient,
ΔP is the difference in pressure,
μ_f is the pore coefficient,
μ_l is the path coefficient, and
$L_{filter\ cake}$ is the thickness of the filter cake layer.

The flow coefficient, b, for a purely laminar flow during the dewatering of a coating color is a function of pore diameter and kinematic viscosity [47, 49]. For pigments in coating colors with a known particle size and aspect ratio, the equivalent diameter (d) can be estimated using porosity, particle diameter, and form factor [47, 49]. For the technical pigments used in coating colors, it is difficult to define an accurate particle diameter and aspect ratio. Therefore, the average mass flow equation 10 was simplified by introducing a structure coefficient, $C_{structure}$, which could be determined experimentally [47, 49]:

$$\dot{Q}_{liquid} = \frac{A \cdot C_{structure} \cdot dP}{dL} \quad (11)$$

The thickness of the immobilized layer ($L_{filter\ cake}$) can be determined as follows [47, 49]:

$$L_{filter\cdot\cdot cake} = \frac{Q_{immo}}{\rho_{immo}} \cdot \frac{1}{A} \quad (12)$$

where Q_{immo} is the amount of the immobilized layer, and
ρ_{immo} is the density of the immobilized layer.

The density of the immobilized layer, ρ_{immo}, can be determined when the density of the coating color, the density of the coating color liquid phase, and the solids content of the immobilized layer are known [47, 49].

$$\rho_c = \frac{(Q_{immo} + Q_{liquid})}{(\frac{Q_{immo}}{\rho_{immo}} + \frac{Q_{liquid}}{\rho_{liq}})} \quad (13)$$

where ρ_c is the density of the coating color,
Q_{liquid} is the amount of liquid removed through dewatering, and
ρ_{liq} is the density of the liquid phase.

By assuming that the pressure is time independent and constant, and by introducing a color parameter, B_{color}, which can be determined experimentally, the amount of liquid phase dewatered can be determined as a function of time as follows [47, 49]:

$$\frac{Q_{liquid}}{A} = \sqrt{C_{structure} \cdot B_{color} \cdot \Delta P \cdot t} \quad (14)$$

where $C_{structure}$ is the structure parameter (a function of the liquid phase viscosity, particle shape, the void fraction in the filter cake, and tortuosity),
B_{color} is the color parameter (a function of the application and immobilization solids contents),
ΔP is the prevailing pressure, and
t is time.

3.2.5 Summary

In MSP coating, all these mechanisms might be present simultaneously: bulk coating color penetration, liquid phase penetration by pressure pulse and by capillary absorption, and dewatering by diffusion. On the other hand, the amount of liquid removed by dewatering can be limited by the filtration resistance of the immobilized layer formed by either filtration or thickening. The main mechanism depends on the process conditions, especially pressure and time. The transport mechanism also affects the coating layer formed in the process.

3.3 Coating coverage measuring methods

The coating result is usually evaluated by measuring how well the coating color covers the base paper or by measuring the coatweight variation. Substantial research has been carried out on the subject of coverage and the variables affecting it. An interesting review of different methods to determine coverage has been presented by Engström [103]. One technique not included in Engström's review is SEM in the Back-Scattered Electron mode (SEM-BSE). This technique is widely used in different coating studies at KCL [104, 105]. Coating coverage was defined by Engström as, "The extent to which the coating is characterized by a uniform mass (thickness) and a surface free from any pattern or texture originating from the base paper" [103]. The methods available to characterize coating coverage are based on several different principles, including the following:

1. Scanning electron microscopy has been used to measure the uncovered area of coated surface samples at low coatweights [104, 105] or the coating thickness variation from cross-sections of the coated paper at high coatweights [106, 107, 108, 109, 110].
2. Radiography has been used with β-radiation [105] or x-rays [111] for measurement of the coating mass distribution based on a statistical difference and electron beam [112] for a point-to-point correlation between the local grammages of the coated paper and the base paper. For precise coating variation measurement, radiograms should be exposed on the same sheet before and after coating, but this technique is not applicable to papers coated on a pilot-scale without special arrangements.
3. The burnout test can evaluate coatweight variations subjectively [113] or quantitatively when image analysis is used [114, 115] in order to achieve a value for the coatweight distribution. In the case of image analysis of the burned sample, it has been assumed that both the porosity of the coating layer and the blackness of the base paper beneath the coating layer were uniform. These conditions are not fulfilled when a wide range of base papers is studied.
4. Laser-Induced Plasma Spectroscopy (LIPS) has been used to measure coating coverage. With this technique, a laser is used to ablate a portion of the sample, producing plasma that is then analyzed [116, 117].

3 EXPERIMENTAL

The experimental part of this work consisted of five pre-coating studies with an MSP (Table 1) and one top coating and calendering study, all of which were carried out on the pilot scale. The aim was to investigate the effect of base paper properties on coating color transfer, its coverage potential, and the porosity of the MSP precoated paper for woodfree paper grades. In the first two studies the main factors affecting coating layer formation and paper quality were screened using mill base papers. The effects of the different base paper properties were then studied further with base materials produced either in the laboratory or on the pilot scale. Finally the results were confirmed with mill base papers and the effect of precoated paper properties on final double-coated paper quality was evaluated.

Three of the MSP coating studies were carried out with woodfree base papers supplied by different mills. In these studies, coatweights were measured on-line and controlled using metering rod diameter and rod pressure. The laboratory base sheets and other materials (plastic and cellophane) were coated with a help of a supporting paper web. Coating was carried out at constant rod pressure in the application, which means a constant amount of coating color film on the roll. With this approach coating color transfer was determined by the interaction between base paper and coating color. The pilot base papers were coated with four amounts of coating color film on the roll by changing the coating color solids content (56 and 60%) and the rod pressure (1.3 and 2.2 bar).

Table 1. Experimental plan with the main variables used in the different parts.

Coating study	**1**	**2**	**3**	**4**	**5**
Base paper					
Mill base papers	X	X			X
Other base materials			X	X	
Variables					
Physical structure	X	X	X	X	X
Surface chemistry	X	X	X		X
Coating color composition			constant	constant	
Variables					
Co-binder	X				X
Pigment		X			
Amount of film on the roll			constant		
Variables					
Rod pressure	X	X		X	X
Rod diameter		X			X
Solids content		X		X	
MSP transfer nip	constant		constant	constant	
Configuration					
Coating one side only (2C1S)	X	X	X		
Coating both sides (1C2S)				X	X
Variables					
Linear load		X			
Speed		X			
Roll cover material					X
Hardness		X			X

4.1 Materials

4.1.1 Precoating colors

The coating color materials used in the precoating studies consisted of commercial coating color raw materials. The pigments used were ground $CaCO_3$ (HC 90, Omya, Lappeenranta, Finland) and kaolin (SPS, Imerys, Cornwall, England). The ground $CaCO_3$ pigment had a particle size distribution with 90% of the particles smaller than 2.0 μm. The English kaolin pigment had a particle size distribution with 80% of the particles smaller than 2.0 μm. Most of the coating colors were latex-CMC colors. The binder used was SB-latex (DL930 or DL 931, Dow Suomi Oy, Hamina, Finland) with CMC as water-soluble thickener (Finnfix 5, 10, 30 and 150, Noviant CMC Oy, Äänekoski, Finland). The SB-latex polymer was a dispersion of a copolymerate with a specific glass transition temperature of 5°C and an average particle size of 150 nm. The amount of coating color dewatering was lowered by increasing the viscosity of the CMC (with higher average molecular weight). A coating color with starch (Raisamyl 302 E, Raisio Chemicals, Raisio, Finland) and latex as binders was used as reference.

4.1.2 Top-coating colors

In the top coating study, the pigments used were ground $CaCO_3$ (HC 90, Omya, Lappeenranta, Finland), fine kaolin (Hydro Gloss 90, J. M. Huber Corporation, Macon GA, USA) and plastic pigment (HP 1055, Rohm and Haas Nordiska AB, Landskrona, Sweden). The American kaolin pigment had a particle size distribution with 90% of the particles smaller than 2.0 μm. The plastic pigment was hollow with an average particle size of 0.5 μm. The binder used was SB-latex (DL940, Dow Suomi Oy, Hamina, Finland) with CMC (Finnfix 10, Noviant CMC Oy, Äänekoski, Finland) and PVA (Celvol 305, Celanese Chemicals, USA) as soluble thickeners. The SB-latex polymer was a dispersion of a copolymerate with a specific glass transition temperature of 23°C and an average particle size of 140 nm.

4.2 Methods

4.2.1 Base paper characterization

The base paper surface composition was defined in terms of the filler content at the paper surface obtained from filler distribution results and from SEM-BSE images of the surface. Permeability, average pore size, roughness, formation and oil absorption rate with short contact times were used for physical testing. The surface chemical properties were characterized by measuring the contact angle and absorption rate with coating color liquid phase using short contact times.

4.2.1.1 Structure and surface composition

The filler distribution in the z-direction of the base sheet structure was determined. The base paper was divided into four different layers using the Beloit Sheet splitting method according to the TAPPI UM 576 standard, or into ten different layers using Metso Paper's tape splitting method [118]. The z-direction filler distribution of the sheet layers is measured as the ash content at a temperature of 575°C according to the SCAN-P 5:63 standard.

4.2.1.2 Physical testing

Air permeability was measured according to the ISO 5636-3 standard. The average pore size of the base paper structure was measured using KCL's internal method using a commercial Coulter porometer [119]. In this method, the base paper is immersed in oil that has a low surface tension. The wetted paper is then placed in a suitable holder that allows a controlled pressure air supply to be applied to one side. A flow measurement device is incorporated into the circuit. The air pressure is then increased and the rate of air passing through the pores of the wetted sample is measured. When the surface tension of the oil is low there is a linear relationship between air pressure and pore size, which is calculated using the Young-Laplace equation. Pore size distribution and average pore size are calculated from the pressure needed to remove the oil.

Bendtsen roughness was measured according to ISO 8791-2:1990 and Parker Print Surface (PPS - s10) roughness according to ISO 8791-4:1992. Formation measurement based on beta radiation was used to characterize basis weight variation. The standard deviation of basis weight is used as a formation index. A lower numerical value indicates better formation [120, 121]. Specific formation is the normalized standard deviation obtained by dividing the standard deviation by the square root of the average basis weight of the sample. Again, a lower numerical value indicates better formation [120, 121].

Oil absorbency at short contact times (0.02 – 1.2 m/s) was measured with the KCL nozzle applicator, which is a modified Bristow Wheel [122]. The KCL nozzle applicator moves horizontally and measures the amount of liquid absorbed for a given area, not the length of the track left by the liquid. The amount of mineral oil absorbed ($ml/m^2s^{1/2}$) characterizes the porosity of the structure, while the chemistry between the oil and the substrate having a negligible role.

4.2.1.3 Testing surface chemical properties

The characteristics of the base paper's surface chemistry were determined by contact angle measurement using a FIBRO 1100 DAT instrument and coating color liquid phase. Base paper samples were laboratory calendered before measurement (23°C, 600 kPa, 4 nips, 20 m/min). High surface openness and roughness have been found to affect the contact angle measurements [123]. The base papers were therefore calendered to make the contact angle measurement results more reliable [123]. The conditions were chosen so that the chemical character of the surfaces would not be affected (low temperature). The contact angles between the liquid and smooth base paper samples were measured for a short contact time (0.1 s).

The absorption properties of the base papers with coating color liquid phase were measured with the KCL nozzle applicator using short contact times in order to demonstrate the effect of surface chemistry on liquid movement without applied pressure.

4.2.2 Coated paper characterization

In most cases the coated papers were characterized using methods that determine coverage: how well the coating color covered the base paper, coating color bulk or liquid phase penetration into the base paper, and the porosity of the coated paper surface.

4.2.2.1 Coatweight

The coatweight was calculated as the difference in ash content between the base paper and the precoated base paper. Ash contents were measured according to the SCAN-P 5:63 standard.

4.2.2.2 Coating coverage

The main technique chosen to measure coating coverage for the coated paper samples in this study was the SEM-BSE method [104]. However, two other methods were also used: the LIPS method [117] and the burnout method [113], but for subjective evaluation only.

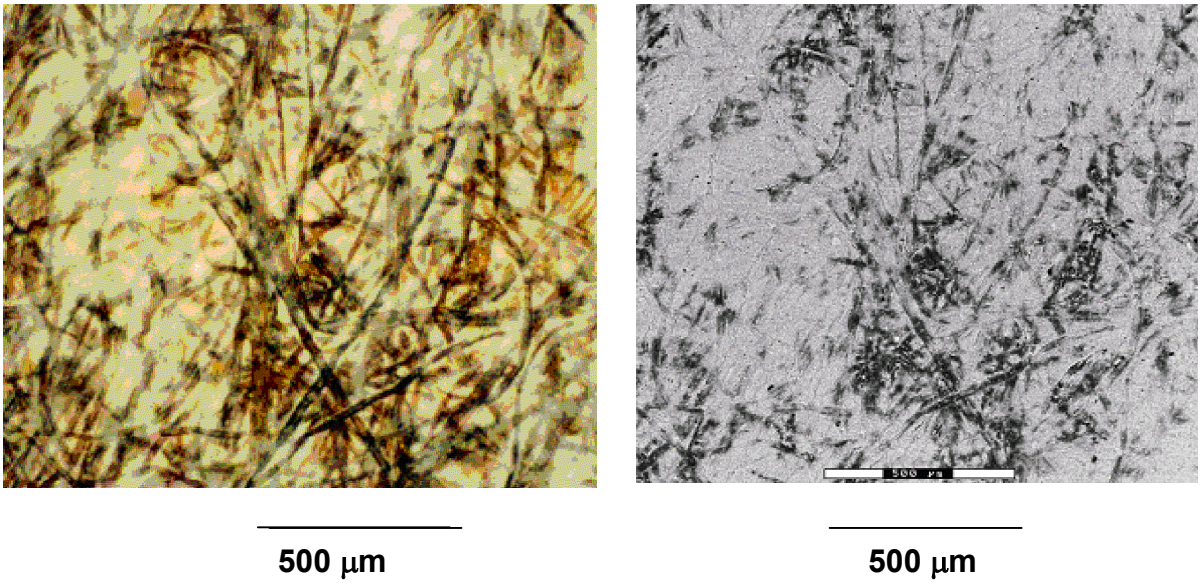

Figure 6. A sample that has undergone the burnout test (left) and the same area imaged using the SEM-BSE method using an acceleration voltage of 20 keV (right).

The SEM-BSE method was used in preference to the burnout method because burnout measurements depend on the structure of both the coating layer and the base paper with fillers. Figure 6 (left) shows an area that has undergone burnout treatment, where most of the surface is uncovered. When the same area was imaged with the SEM-BSE method (Figure 6, right), the surface appeared to be covered. The burnout test is less reliable for measuring coverage at coatweights of 5-8 g/m^2. It is recognized that the SEM-BSE method also has its

limitations, such as its dependence on the microscope conditions. For example, increasing the accelerating voltage reduces the apparent coverage. Nevertheless, the SEM-BSE is considered to be a good method for measuring surface coverage at coatweights of 5-8 g/m^2.

SEM-BSE coverage was characterized by analyzing scanning electron microscope images in the backscatter mode. The contrast in the BSE mode is based on elements present in the sample, a higher atomic weight gives a brighter gray value for this element in the image. Coating coverage is expressed as the pigment-covered area as a percentage of the whole image area. Samples were cut into two7x35 mm pieces. The sample plate was sputter coated with a mixture of gold and palladium to create a conductive layer on the sample surfaces.

The SEM was set at an acceleration voltage of 20 keV, a working distance of 15 mm and 50x magnification. Image analysis requires minimum noise and an even background to produce reliable results. The acceleration voltage affects the quality of the images. In the case of KCL's SEM, the quality of the BSE images with a high keV is better than with a low acceleration voltage. A certain constant acceleration for the measurement has to be chosen so that the results are comparable from one time to another. If the specimens measured normally have a very low coatweight, a low acceleration voltage is recommended. If the coatweights of the samples vary a lot, a high acceleration voltage is preferred, as this gives large differences in coverage between the samples and good measuring accuracy. In order to get good quality images and because the coatweights of the samples in this study varied a lot, we chose a high acceleration voltage of 20 keV. A working distance of 15 mm has been found to optimum with KCL's equipment with this acceleration voltage and was also used in this study.

The SEM-BSE coating coverage was measured by collecting the SEM-BSE-image using Link-ISIS software (Autobeam). The image size is 256x256 pixels from an area of 1.8 x 1.8 mm (50x magnification). 40 frames are collected with Kalman averaging. The auto contrast of the BSE detector controls was used to keep the brightness and the contrast constant. The threshold gray value was set manually to a constant level. The image analysis results were also evaluated visually by comparing the gray value image with the binary image. The result was given as the average of five measurements. One image of one measured area was used for visual examination and later on to characterize the size of the uncovered area with a numerical parameter (EDM number). This parameter characterizing the size of the uncovered areas was calculated for some precoated papers using Euclidean Distance Mapping (EDM). The bigger the uncovered areas, the higher the value of the parameter.

Laser-Induced Plasma Spectroscopy (LIPS) was used to measure coating coverage. A laser is used to ablate a portion of the sample, producing a plasma that is subjected to elemental analysis. From the results of this analysis, the composition of the sample can be determined, and the formulation and coverage subsequently determined. For each measurement a line length of 50 mm at 250 points with a step size of 0.2 mm was used. The laser spot size was 0.25 x 0.1 mm. The pulse energy was approximately 1.0 mJ. The degree of coating coverage (DCC) was evaluated by allowing a uniform 4 g/m^2 thick layer to give 100% coverage. Since the spot that is ablated could contain several fibers as well as coating, the DCC will be an average value for that spot. The depth and area of each ablation depends on coating layer porosity, density, pigment size and type, etc. The resulting crater size and depth were not determined.

The burnout method used at KCL is based on the following procedure: the coated paper sample is saturated with a solution consisting of 25 g/l of ammonium chloride in a mixture of equal parts of water and propanol. The samples are allowed to dry completely at room temperature. The dried samples are then transferred to a ventilated oven at a temperature of 210ºC for 15 minutes. This method was used to indicate visually large-scale non-uniformity caused by shadow marking originating from the dynamic sheet farmer's drum holes (laboratory sheets) and from the wire section suction roll (pilot papers).

4.2.2.3 Gloss and openness of the coated paper

The Hunter gloss of the coated papers was measured according to the TAPPI T480, om-92, standard. The openness of the coated paper was measured in terms of its air permeability according to the ISO 5636-3 standard and in terms of its oil absorbency at short contact times (0.02-1.2 m/s) with the KCL nozzle applicator, which is a modified Bristow Wheel [122]. The openness of the structure was the result of the amount of mineral oil absorbed ($ml/m^2s^{1/2}$), in which the chemistry between the oil and the substrate plays a negligible role.

4.2.2.4 Z-directional analysis

Coating color penetration was determined visually from cross-sectional images of the coated paper. The cross-sections were cut with a microtome and stained with toluidine blue. In light microscopy dyed fibers appear gray and coating color black.

The dry cut-offs were also studied in UV light. Coating color liquid phase penetration into the base paper was determined visually as the penetration depth of the water-soluble optical brightener into the base paper. In light microscopy with UV light, optical brightener appears as a bright layer in otherwise dark surroundings.

4.3 Pilot equipment used in the coating studies

The five precoating studies were carried out with a metered size press (OptiSizer, Metso Paper) either at KCL's pilot plant in Espoo, Finland (Figure 7) or at Metso Paper's pilot plant in Jyväskylä, Finland (Figure 8). The coating trials were carried out mainly at a speed of 1000 m/min. The drying configuration of the pilot coaters consisted of IR-driers and air-driers. The conditions in different trials are described in more detail in the following chapter.

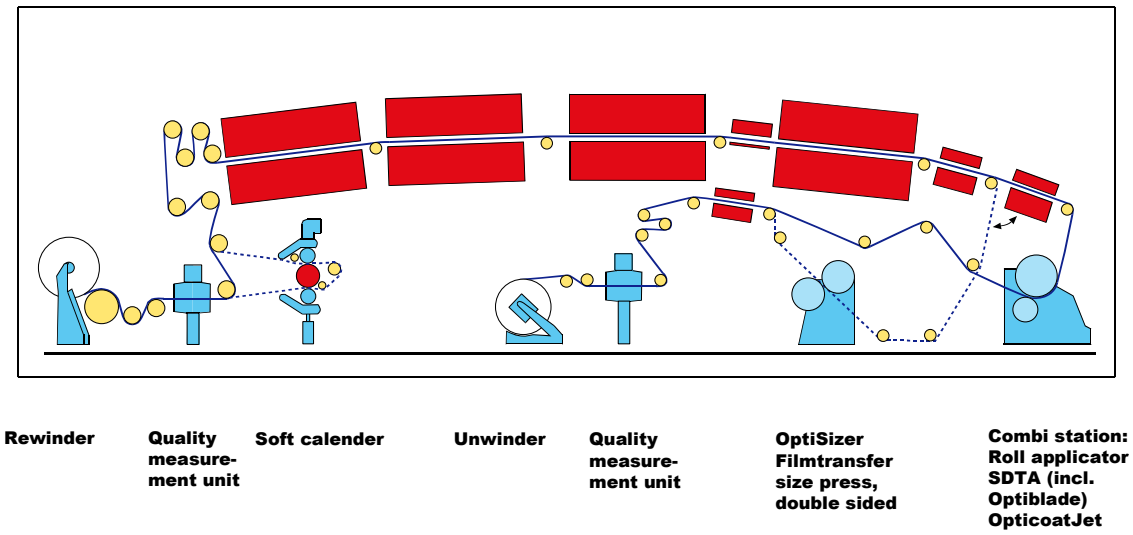

Figure 7. Illustration of the pilot coater at KCL (Espoo, Finland).

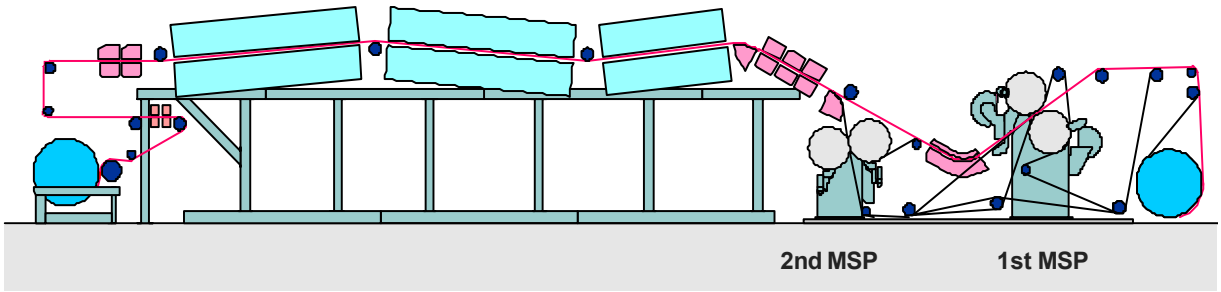

Figure 8. Illustration of the pilot coater at Metso Technology Center (Jyväskylä, Finland).

The precoated papers from the fifth precoating study were top coated with a jet application coating head (OptiJet, Metso Paper) at KCL (Figure 7). During this operation the coatweight was kept constant by changing the blade pressure according to the measured on-line coatweight. The top-coated papers were calendered at a speed of 1200 m/min using a modern multinip calender (OptiLoad, Metso paper) at KCL' s pilot plant (Figure 9). Calendering was performed using full dead load relief, which meant that the linear load was the same in each nip. The roll cover of the soft roll was DuraStar supplied by Metso Paper. The hardness of the rolls was 92 ShD.

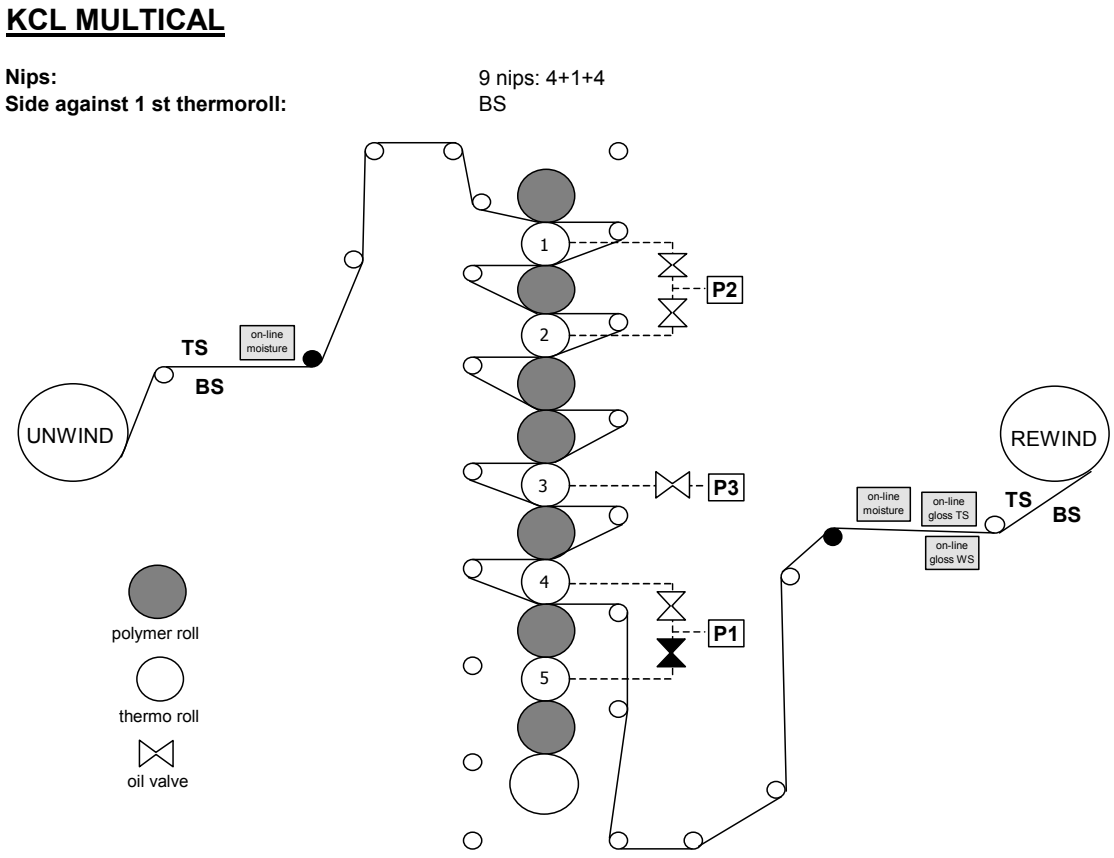

Figure 9. Illustration of the pilot calender (OptiLoad, Metso Paper) at KCL (Espoo, Finland).

4.4 Coating studies

4.4.1 First precoating study with mill base papers

The aim of the first study was to determine the most important base paper properties affecting coating layer formation and coverage in MSP coating. Mill base papers were used, two of them were porous and hydrophobic with a difference in formation and filler distribution (e.g. – and /- formed, produced on a gap former and a fourdrinier). The third base paper was produced on a fourdrinier with a /-shaped filler distribution. The surface of this base paper was hydrophilic and denser than that of the other two base papers.

The coating colors were based on a mixture of $CaCO_3$ and kaolin (70 : 30) with SB-latex as binder and CMC as water-soluble thickener. Two different molecular weights of the CMC were chosen as thickeners for the coating trial. The immobilization solids content of the coating color and the surface tension of the liquid phase were not affected. Coating was carried out at 1000 m/min with an MSP coating unit. The roll cover material was polyurethane with a hardness of 29 P&J. The amount of coating film on the roll was adjusted using the rod pressure. The roll nip pressure was kept constant.

A more detailed description of the base paper properties, coating colors, MSP process conditions and the coated sheet properties is given in Appendix I.

4.4.2 Second precoating study with mill base papers

In the second coating study, the effect of coating process and coating color variables on coating coverage was studied to determine the sensitivity of the results in these variables. The study was designed using the MODDE multivariate design and analysis program [124]. The study included factors such as roll cover hardness, machine speed, nip load, coating color pigment ratio ($CaCO_3$: kaolin), color solids content, coatweight and base paper (type and surface filler content, Table 2). The coating colors were based on different $CaCO_3$: kaolin ratios with SB-latex and CMC as water-soluble thickener. The MODDE program takes the input factors and finds the best combination for a best-fit model. To check for linearity, a center point was used.

To ensure that the model was accurate, the experimental design matrix was corrected using measured coatweight values. The output responses of the MODDE analyses were coating coverage with both the SEM-BSE and LIPS methods. Each response was initially evaluated using the full model, including all input responses. Variables that had little or no effect were removed to improve the Q^2 value. Q^2 is a measure of the model's ability to predict responses for new experimental conditions. A large Q^2 indicates that the model has sufficient predictive ability with small prediction errors. R^2 is the fit of the measured data, the percent variation of the response explained by the model. The input variables were combined to detect any interactions, e.g. solids * coatweight. If an interaction term existed, it meant that if the

interacting variable changed, the other variable changed in response. Each of the variables in an interaction term must be included in the model, even though it may not be significant by itself, as the MODDE program maintains the hierarchy.

Table 2. MODDE input factors

Variable	Symbol	Values
Roll cover hardness	Ro	26, 42 P&J
Pigment ratio	Pr	30-70% ($CaCO_3$)
Surface filler content (i.e. Top or Bottom side of the paper)	Bp	10, 30% Filler
Solids content of the color	S	56-60%
Coat weight	Cw	5-8 g/m^2
Machine speed	Sp	800-1200 m/min
Nip load	Nl	20-30 kN/m
Base sheet type	Ba	Base 1 and Base 2

A more detailed description of the base papers and coating formulations, coating process and coated papers is given in Appendix II.

4.4.3 Third precoating study with laboratory sheets

The aim of the third coating study was to confirm the results of the effect of base paper properties on coating coverage obtained with mill base papers in the first coating study. This third coating study was carried out with laboratory base sheets, which covered a wider quality range than the mill base papers. The laboratory woodfree base sheets were produced on a dynamic sheet former [125].

4.4.3.1 Woodfree base sheets

Sheets differing in air permeability were produced using variables such as the type of hardwood species (birch or aspen), softwood pulp refining, and the hardwood content of the furnish (Table 3). The differences in sheet properties between the hardwood species were only minor and not statistically significant. The hardwood pulp was refined to constant CSF (400 ml). The amount of softwood pulp refining gave the greatest differences in base paper permeability. The slightly refined chemical softwood pulp (CSF 540 ml) gave the most porous structures, with air permeability in the range 800-1500 ml/min. The chemical softwood pulps refined to low CSF gave the densest base paper structure, with air permeability in the range 115-480 ml/min.

Table 3. Experimental design for statistical analysis of laboratory base sheets.

Experi-mental point	Hardwood Species	Softwood pulp CSF ml	AKD amount added %	HW content added %	Ash content (measured) %	Starch (measured) %
1	Birch	200	0	30	11.6	0.6
2	Birch	540	1	70	11.3	0.9
3	Birch	200	1	43.3	12.8	0.7
4	Birch	200	0.67	70	10.5	0.6
5	Birch	540	0	43.3	12.0	0.9
6	Birch	540	0.67	30	12.7	0.6
7	Birch	345	0	70	12.7	0.9
8	Birch	440	0	70	11.8	0.8
9	Birch	345	1	30	11.7	0.7
10	Aspen	200	0	30	11.0	0.8
11	Aspen	540	0	30	12.8	0.8
12	Aspen	200	1	30	11.7	0.7
13	Aspen	540	1	30	12.1	0.7
14	Aspen	200	0	70	11.0	0.7
15	Aspen	540	0	70	12.0	1.0
16	Aspen	200	1	70	11.0	0.8
17	Aspen	540	1	56.7	12.2	0.7
18	Aspen	540	0.33	70	11.3	0.8
19	Aspen	430	1	70	11.6	0.8
20	Aspen	370	0.5	50	11.2	0.7
21	Aspen	370	0.5	50	12.2	0.7
22	Aspen	370	0.5	50	11.8	0.6
23	Aspen	370	0.5	50	12.0	0.8

The filler content (20%), the z-directional filler distribution, and the starch content (1%) were constant in all base sheets. Some of the sheets were AKD sized in order to change the chemical character of the base surface from hydrophilic to hydrophobic. The chosen AKD addition levels were 0, 0.33, 0.5, 0.67 and 1%, but all sheets with AKD were totally hydrophobic. The results are therefore discussed only by comparing un-sized and sized sheets, or hydrophilic and hydrophobic sheets as they are called later. The base sheet topsides (TS) were chosen for coating, because they were more uniform and had higher filler contents at the surface than the bottom sides (Figure 10).

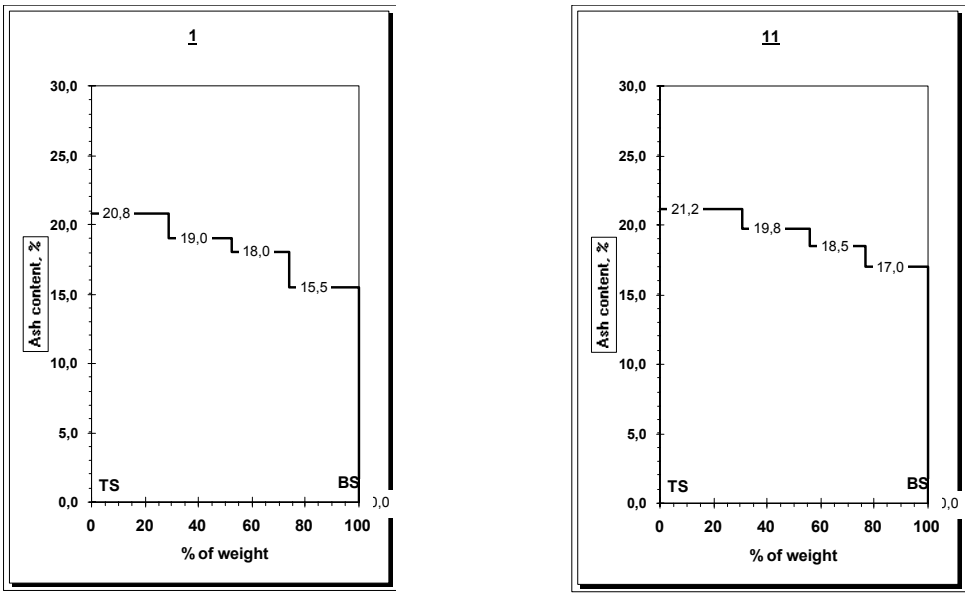

Figure 10. Examples of the filler distributions measured from sample 1 (dense, left) and sample 11 (porous, right).

The movement of the coating color liquid phase was studied using model substrates: absorbent cellophane and non-absorbent plastic. Regenerated cellulose films are non-porous, but absorb water by a diffusion mechanism [48]. The measured amount of liquid transferred to the cellophane followed a square root of time dependence, and the transport was found to be relatively slow, 1 to 2 s [48]. Although water is not a solvent for cellulose, it is a powerful swelling agent; it was found that 1.0 g of cellophane absorbed up to 1.65 g water in the fully swollen state [126]. The relative absorbance was slow. When measured with a method for measuring diffusion using a simple ATR device, absorbance increased after tens of seconds up to hundreds of seconds [126].

The laboratory base sheets and other materials (plastic and cellophane) were coated with an MSP. The sheets were taped onto the surface of the supporting mill paper. Coating was carried out at constant rod pressure in the application, which means a constant amount of coating color film on the application roll. The coating colors were based on a mixture of $CaCO_3$ and kaolin (70 : 30) with SB-latex as binder and CMC as water-soluble thickener. Optical brightener was added to the coating color. The optical brightener used had a moderate fiber affinity. The coating color solids content was 60%. The precoating was carried out at 1000 m/min with an MSP coating unit. The roll cover material was polyurethane with a hardness of 29 P&J. The amount of coating color was kept constant with a constant rod pressure. The roll nip pressure was also kept constant.

A more detailed description of the base paper properties, coating formulations, coating process conditions and coated paper properties is given in Appendix III.

4.4.3.2 Woodfree base sheets with mechanical pulp addition

In addition to the laboratory sheet study presented in the third coating study, the effect of the addition of short fibred pulps was also evaluated. Some of the hardwood in the woodfree paper furnish was replaced by PGW, TMP, DIP or chemical pulp from eucalyptus. The laboratory sheets were coated with a constant amount of coating color film on the roll.

The properties of the coating color and the coating process conditions were the same as those presented in Appendix III. The detailed furnish compositions of the laboratory sheets are presented in Table 4.

Table 4. The pulp composition of the laboratory sheets.

Experimental Points	Hardwood species	Softwood pulp CSF, ml	Extra pulp/ CSF, ml	Extra pulp amount %	Birch %	Softwood %
8	Birch	430		-	70	30
24	Birch	440	PGW/ 40	35	35	30
25	Birch	440	TMP/ 90	35	35	30
26	Birch	440	DIP/ 110	35	35	30
27	Birch	440	Eucalyptus/400	35	35	30

4.4.4 Fourth precoating study with pilot base papers

The aim of this paper machine study was to produce woodfree base papers for MSP precoating. The base paper permeability was varied over a wide range by varying the degree of refining. Base papers were produced at KCL on the pilot-scale using a slow fourdrinier paper machine. A wide range of different papers was produced by changing the degree of softwood and hardwood chemical pulp refining and the proportions of these pulps in the furnish (Table 5). The basis weight was 80 g/m². Dewatering conditions in the slow fourdrinier were not changed during the trial.

The total filler content and z-directional filler distribution of the base sheets were constant (20% $CaCO_3$). The filler was coarse $CaCO_3$ (Hydrocarb 60, 20%). Cationic starch (Raisio 135) was added (1%). The base papers were machine calendered on-line so that constant base paper Bendtsen roughness (300 ml/min) was achieved (measured during the trial).

Table 5. Experimental plan and results from refined chemical pulps and machine calender linear loads.

Sample	Softwood target CSF/ measured CSF	Hardwood target CSF/ measured CSF	Softwood amount, target/ analyzed, %	Linear pressure machine calender kN/m
1	200 / 190	200 / 215	70 / 72	19
2	200 / 190	200 / 215	30 / 41	19
3	500 / 515	200 / 215	70 / 68	30
4	500 / 515	200 / 215	30 / 46	30
5	200 / 190	500 / 485	70 / 66	25
6	200 / 190	500 / 485	30 / 39	19
7	500 / 515	500 / 485	70 / 70	30
8	500 / 515	500 / 485	30 / 43	25
9	350 / 350	350 / 340	50 / 54	20

A coating study was performed in which both sides of the pilot base paper were coated simultaneously on an MSP. The coating colors were based on a mixture of $CaCO_3$ and kaolin (70 : 30) with SB-latex as binder and CMC as water-soluble thickener. Optical brightener was added to the coating color. The optical brightener used had a moderate fiber affinity. The coating color solids content was 56 and 60%.

Both sides were coated simultaneously. Precoating was carried out at 1000 m/min on the MSP coating unit. The roll cover material was polyurethane with a hardness of 43 P&J on both top and bottom rolls. The amount of coating color applied was kept constant with a smooth rod. Two different rod pressures and two solids contents were used in the trial. The roll nip pressure was kept constant.

A more detailed description of the base paper properties, coating color, coating process conditions and coated paper properties is given in Appendix IV.

4.4.5 Fifth precoating study with mill base papers

The aim of the fifth coating study was to find out the effect of the roll cover material and the base paper properties on coated paper properties. Four different woodfree base papers produced on fourdrinier paper machines were used in the studies, and both sides of the base paper were coated simultaneously.

The coating colors were based on a mixture of $CaCO_3$ and kaolin (70 : 30) with SB-latex as binder and CMC as water-soluble thickener. Two different molecular weights of CMC were chosen as thickeners for the coating trial. The immobilization solids content of the coating color and the surface tension of the liquid phase were not affected. The coating color with starch and latex as binders was used as reference.

Both sides of the mill base paper were coated at the same time on the MSP coating unit at 1000 m/min. The main roll cover material used in the studies was polyurethane (X-Mate X,

Metso Paper, Finland), with a hardness of 44 P&J on the top roll and 42 P&J on the bottom roll (later called **hard rolls**). Some runs were performed using supported rubber rolls with a hardness of 88 P&J on the top roll and 84 P&J on the bottom roll (**soft rolls**). Pre-coatweight and its uniformity in the cross-direction were examined for every study point by El sensor measurement. The amount of coating color was adjusted with the diameter of the smooth rod or with the rod pressure. Roll nip pressure was kept constant.

A more detailed description of the base paper properties and coating colors, coating process conditions and coated paper properties is given in Appendix V.

4.4.6 Top coating and calendering studies

In studying the top coating layer the aim was to determine the effect of precoated paper properties on the final double-coated paper quality. The precoated papers were top-coated with a jet application coating head (OptiJet). The speed used in the coating study was 1200 m/min. The jet angle was 34°, the jet gap was 0.8 mm and the distance from the backing roll was 5.0 mm. The blade used was 0.457 mm thick and the blade angle was 45º. Precoated papers were top-coated to a constant coatweight. The target coatweight of 11 g/m² was achieved by controlling the blade pressure according to the on-line coatweight measurement.

The top coating was a mixture of fine $CaCO_3$, fine kaolin and plastic pigment. The binder used was SB-latex with CMC and PVA as soluble thickeners. The topside of the precoated paper was coated first and then the bottom side. Coating color solids content (64%) was kept constant.

The top-coated papers were calendered at a speed of 1200 m/min using a modern multinip calender (OptiLoad 10). The rough bottom side of the double-coated paper was taken against the first steel roll. The double finisher was situated in the roll stack in position 5/6. The surface temperatures were 110-130°C. Slightly higher temperatures were used in the lower part of the stack to minimize gloss two-sidedness. The calender was loaded with a constant linear load of 300 kN/m.

A more detailed description of the precoated papers and coating formulation, coating process and top-coated papers is given in Appendix V.

5 EFFECT OF BASE PAPER IN COATING LAYER FORMATION

The effect of the base paper in MSP coating has been intensively studied with wood-containing base papers, whereas the properties of woodfree base papers have been studied to a lesser extent. Compared to wood-containing base papers, woodfree base papers from slightly refined chemical fibers result in a more porous structure that is hydrophilic and therefore water absorbent. The contact time in the MSP transfer nip is very short (1-4 ms). Due to the high pressure pulse in the nip, coating layer formation is assumed to be based on pressure penetration causing bulk coating color penetration [33, 39] and coating color dewatering through filter cake formation [4, 5, 33, 39, 50]. With hydrophilic papers water is absorbed by capillary absorption, a process that has been claimed to be very fast [51]. When the surface chemical properties of the hydrophilic chemical fibers were modified with a hydrophobic agent, the water transport mechanism was assumed to proceed through diffusion [51]. Water transport through diffusion is reported to be slower than that through capillary absorption [51, 67].

The aim of this coating study was to determine the most important base paper properties affecting coating layer formation and coverage in MSP coating. In first part of the study, the effect of base paper in MSP coating was examined using commercial base paper supplied by different mills producing woodfree base paper for coating.

5.1 Base paper properties

The base paper properties measured are shown in Table 6. Two of the base papers were porous and hydrophobic. These two base papers differed in relation to formation and structure in the z-direction (filler distributions, base papers produced on a fourdrinier and a gap former). The third base paper was produced on a fourdrinier. Its surface was hydrophilic and its structure denser than the other base papers. Both base papers produced on the fourdrinier (P1 and P3) had a low ash/filler content on the bottom side and a high ash/filler content on the topside. The base paper produced with a gap former (P2) had a uniform ash/filler content in the z-direction and a relatively high amount of ash/filler at the surface.

Table 6. Properties of the base papers.

Base paper No.	side	Structure Filler surface, %	Roughness Bendtsen,	PPS 10	Absorption Nozzle application oil	liq.phase	Surface chemistry FIBRO contact angle
		%	ml/min	μm	ml/m²/s½	ml/m²/s½	°
1	**top**	**30**	**300**	**5.7**	**145**	**0.4**	**90.1**
1	**bottom**	**10**	**600**	**8.2**	**155**	**2.1**	**91.3**
2	**top**	**20**	**480**	**8.1**	**130**	**5.9**	**79.0**
2	**bottom**	**20**	**280**	**5.9**	**165**	**0**	**85.0**
3	**top**	**30**	**245**	**5.9**	**95**	**12.4**	**61.8**
3	**bottom**	**10**	**290**	**6.5**	**95**	**26.7**	**43.9**

Base paper surfaces were scanned with a Back Scattered Electron (BSE) detector using a Scanning Electron Microscope (SEM). Fibers at the base paper surface appear black in the images and pigments appear white (Figures 11-12).

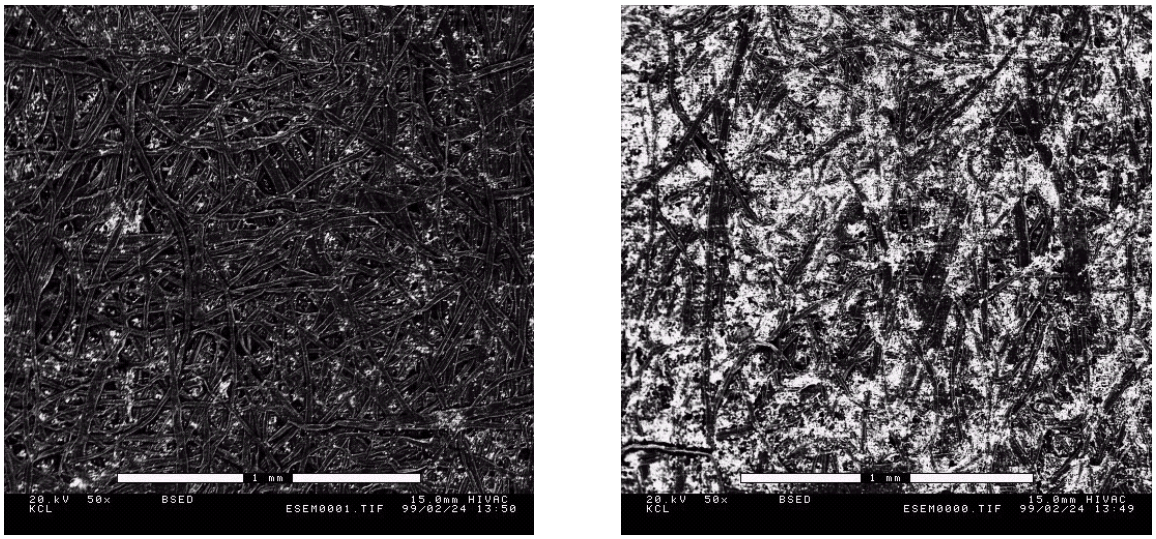

Figure 11. Base paper surface filler content measured by SEM-BSE for a fourdrinier base paper. Base paper bottom side (left) and topside (right).

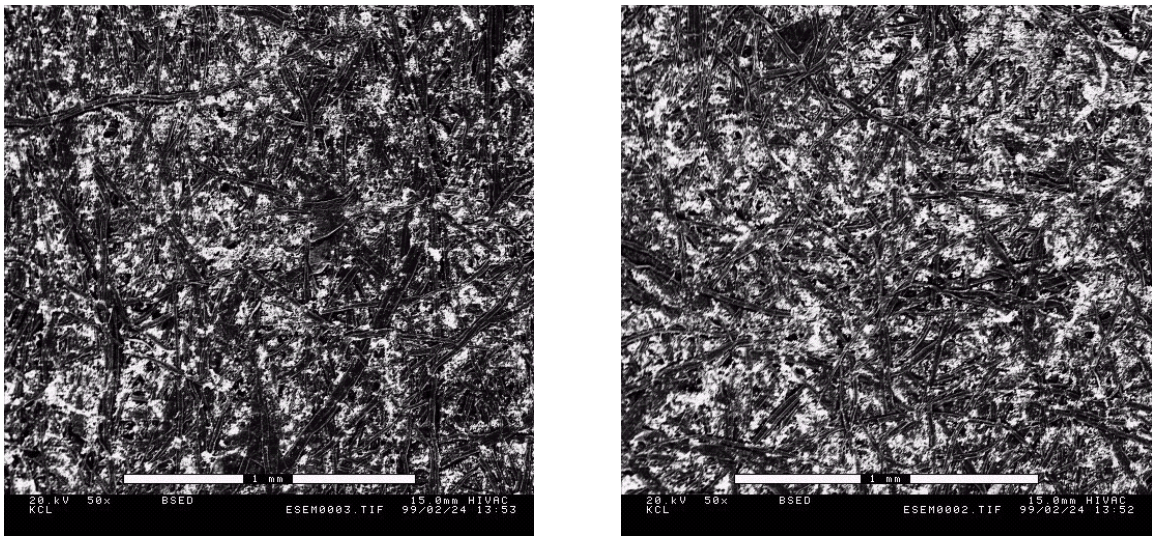

Figure 12. Base paper surface filler content measured by SEM-BSE for a gap former base paper. Base paper bottom side (left) and topside (right).

5.2 Coating layer formation

Coating color transfer was controlled by means of the amount of coating color film applied to the roll, which increased as rod pressure was reduced. The surface openness indicated by oil absorption rate seemed to be the single most important paper property governing coating layer formation. Neither roughness nor surface chemical properties had any major influence on coating layer formation. The coating colors were based on a mixture of $CaCO_3$ and kaolin (70 : 30) with SB-latex as binder and two different CMC as water-soluble thickener. The lowest coatweights were obtained on the hydrophilic and dense base paper (Figure 17, left oil absorption rate 95 ml/m²/s½) and the highest coatweights on the smooth but porous base paper (oil absorption rate 165 ml/m²/s½) in the study with CMC 5 coating color. With CMC-30 coating color the film transfer ratios were very high and the base paper had no significant effect on coating color transfer (Figure 17, right).

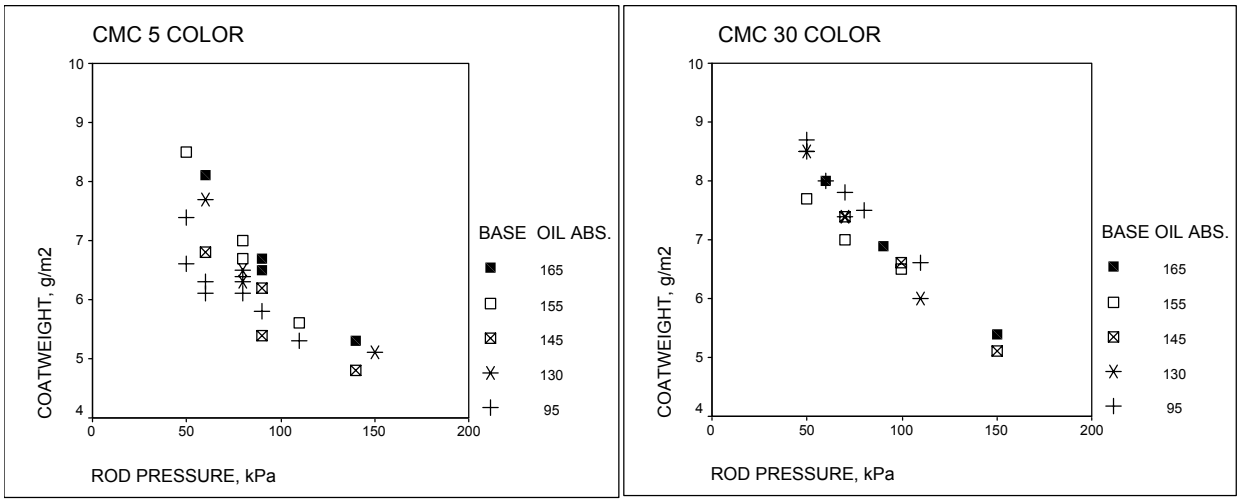

Figure 13. Coatweight as a function of rod pressure with different levels of surface openness measured as oil absorption rate for different mill base papers with two Latex-CMC colors with CMC of two different molecular weights: 23 000 g/mol, CMC 5 (left) and 83 000 /mol, CMC 30 (right).

5.3 Coating coverage

The base paper surface filler content seemed to have the largest effect on coated paper coverage and coverage increased linearly as a function of coatweight (Figure 14). The differences between the base papers were bigger with latex-CMC 5 coating color than latex-CMC 30 color due to the lower viscosity of the latex-CMC 5 coating color. The topsides of the base papers with higher filler content had a higher coating coverage, and the covered area was more uniform than with base paper bottom sides (Figure 15). The filler at the base paper topside surface prevented coating color penetration and the coating color underwent more dewatering at the base paper surface.

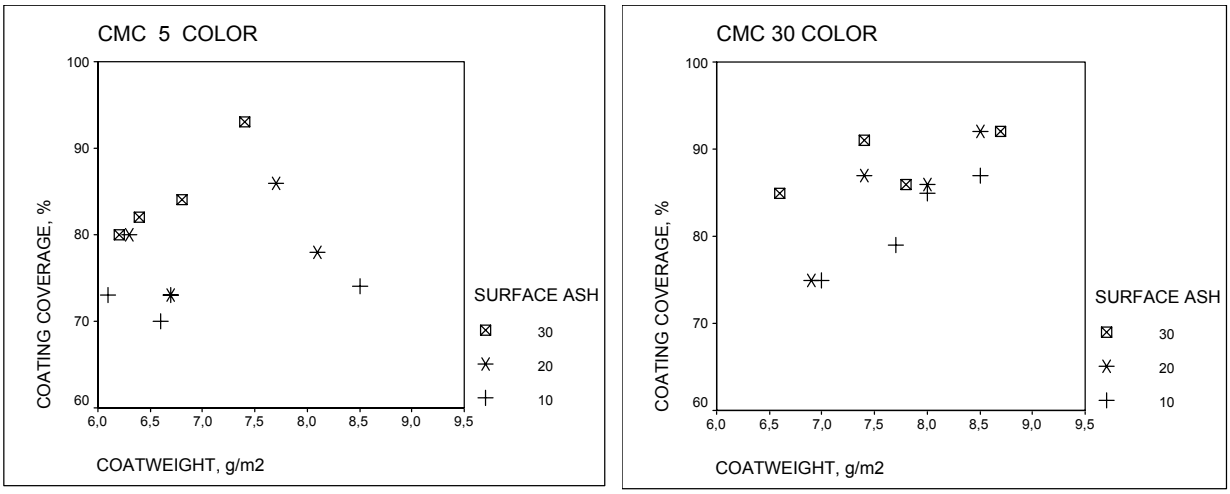

Figure 14. Coating coverage as a function of coatweight with base paper surface ash contents (10, 20 and 30%) with two different thickener modifications, CMC 5 (left) and CMC 30 (right).

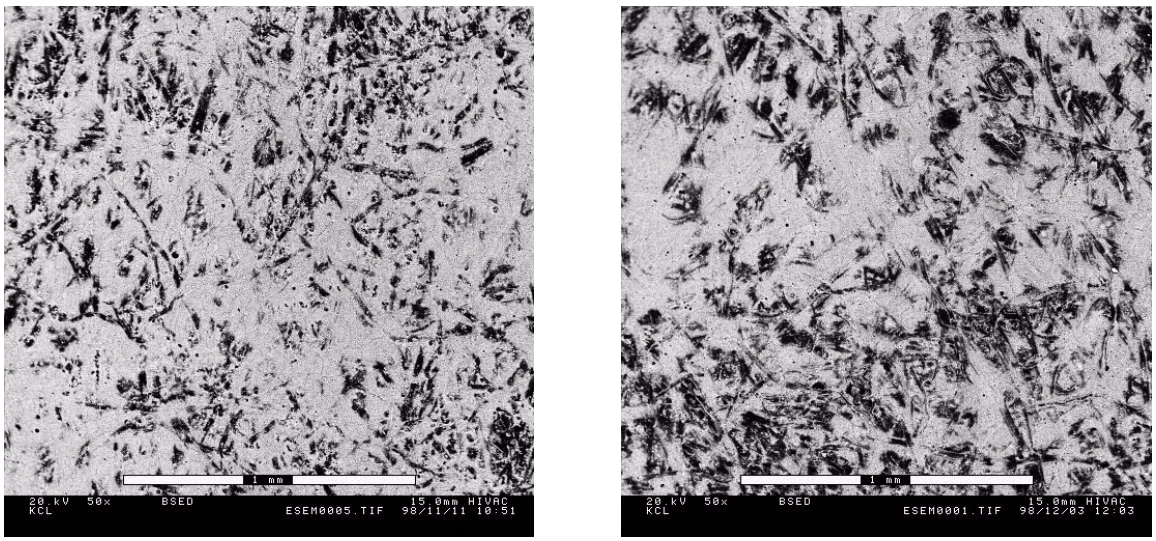

Figure 15. Surface coverage of base paper (1) with 30% filler giving 84% coverage (left) and 10% filler in the surface giving 73% coverage (right). The coatweight was approximately 6.8 g/m^2 with a latex-CMC 5 color.

5.4 Coating layer openness

The openness of the precoating layer was measured from the coated papers by both air permeability and oil absorption with the nozzle applicator. When coating only one side of the base paper, both methods gave very similar results for physical openness since the pore size and layer density restrict the measuring depth to the coating layer ($R^2 = 0.908$, Figure 17, left). Oil absorption rate was influenced by coating coverage and, at higher coatweights, also by the capillary structure of the coating layer. When the layer thickness was increased, the oil absorption rate of the coated paper decreased due to the better coverage, which means that the base sheet openness did not influence the values at high coating coverage (Figure 16). More filler on the surface of the base paper gave a well-covered base paper, but in this case the coating layer absorbed oil faster than the other samples (Figure 17 right).

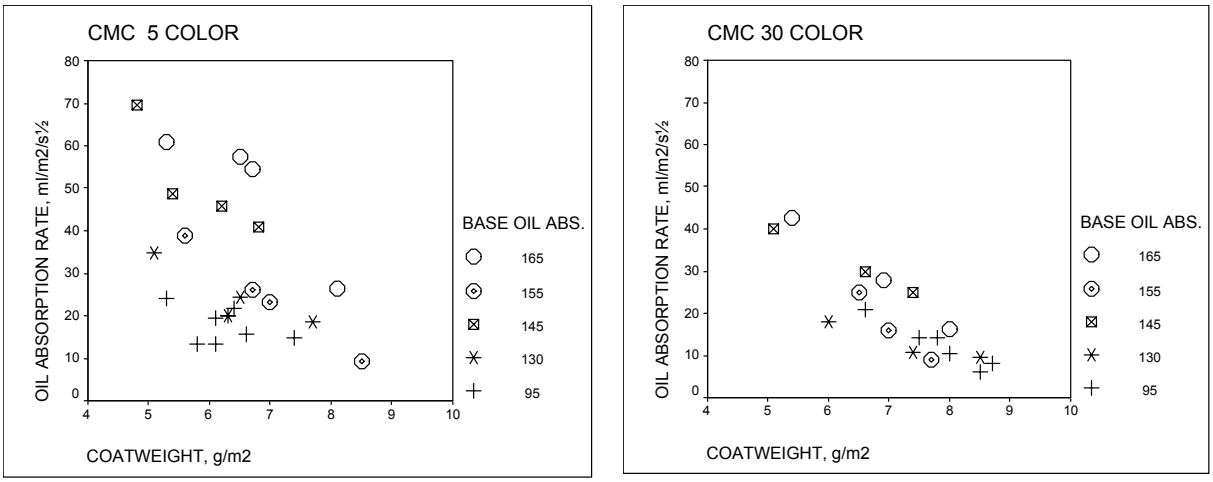

Figure 16. Coated paper oil absorption rate as a function of coatweight (g/m²) for different base papers differing in surface openness. CMC 5 color (left) and CMC 30 (right).

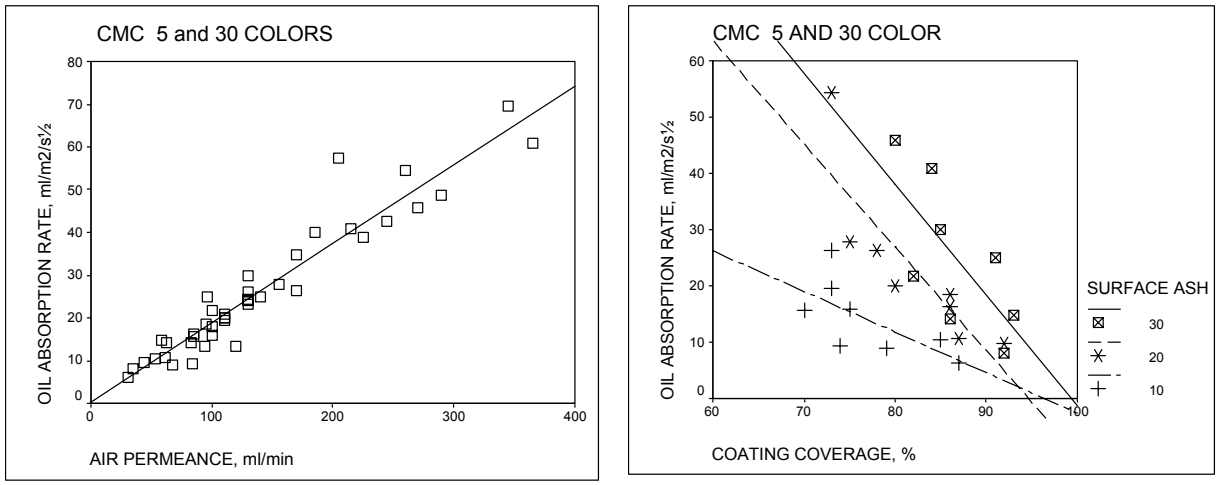

Figure 17. Coated paper oil absorption rate as a function of air permeability of the coated surfaces (high correlation, $R^2 = 0.908$, left) and as a function of coating coverage (%) with different base paper surface ash levels (right). Both CMC 5 and 30 colors.

5.5 Discussion

The coating layer formed on woodfree base paper in the MSP depended mainly on the amount of coating color film on the roll and the base paper surface openness. The base paper surface oil absorption rate correlated with coating layer formation, and the high base paper oil absorption level seemed to indicate a high coating uptake resulting in a high coatweight. Neither the base paper roughness nor the surface chemical properties in the area studied had any major influence on coating layer formation.

Low base paper surface openness and high filler content on the surface of the sheet retarded coating color penetration into the base paper structure. Less coating color penetration gave better coverage. Similar results have been reported with wood-containing base papers by Grön and Ahlroos [10, 13, 14]. With base papers containing less filler in the surface layer, the coverage can still be increased by using higher viscosity coating color. In this case, the bulk coating color penetration into the large voids of the base paper was reduced.

The openness of the coated paper was also measured as oil absorption rate. Oil absorption rate is influenced by the coating coverage and the capillary structure of the coating layer. As the coating layer thickness of the base papers was increased, the oil absorption rate of the coated paper decreased, which is explained by the higher coverage. More filler on the surface gave a well-covered base paper, but in this case the coating layer absorbed oil faster than with the other samples. One explanation can be drawn from the results obtained by Watanabe and Lepoutre [44], where the shrinkage of the coating layer caused compacting of the coating structure during water transport driven by the capillary forces in the drying sequence [44]. Therefore, coating layers that have been strongly dewatered in the nip show less coating structure shrinkage than coating structures with more water in the coating layer. Similar results have been reported: when coating color solids content was increased, coating layer shrinkage was decreased in drying [53] and coating layer openness was increased. In other words, a higher coating color solids content at the nip exit means that the second critical concentration (SCC) is reached earlier. The time available for shrinking and compacting is shorter than in the case where coating color is not dewatered into the base paper structure. SCC is the concentration at which the voids in the coating layer structure are filled by air and the particles are not able to move.

5.6 Summary

The coating layer formed on woodfree base paper when coated with an MSP unit depended mainly on the amount of film applied on the roll surface and the base paper surface openness. Neither the base paper roughness nor the surface chemical properties had any major influence on coating layer formation. More filler on the surface gave a well-covered base paper, but in this case the coating layer absorbed oil faster than with the other samples. A porous coating layer with good coverage was the result of coating color dewatering and filter cake formation in the MSP transfer nip.

6 EFFECT OF MSP COATING VARIABLES ON COVERAGE

In this coating study, the effect of coating process and coating color variables on coating coverage was studied to determine the sensitivity of the results to these variables. The study was designed using the MODDE multivariate program [124].

6.1 Coating coverage measured with the SEM-BSE method

The variables found to have a major impact on SEM-BSE coating coverage were base paper type, surface filler content, coatweight, solids content and pigment ratio. Also, two interaction terms were found to be significant: pigment ratio * coatweight and pigment ratio * solids content (Figure 18). The R^2 for the data was 0.93 and the model prediction (Q^2) was 0.84.

SEM-BSE coverage was found to increase as coatweight, filler content in the base paper surface, kaolin pigment content in the coating formula, and coating color solids content increased. More filler in the surface reduced the pore size and prevented the coating color bulk from penetrating into the surface, thus increasing the coating coverage. When base paper 1, which had a greater surface openness and contained a hydrophobic agent, was replaced with base paper 2, which had a lower surface openness and hydrophilic fibers, the coating coverage increased. It is suggested that the base paper surface chemical properties had no influence on coverage and that the effect was due to the structure of the base paper, as the coating color did not penetrate as far into the dense sheet as into the open sheet.

It was found that as the interaction pigment ratio * coatweight (Figure 18, left) increased, the coverage also increased. This was especially clearly seen for the pigment ratio * coatweight at low coatweights (~5 g/m^2), where the inclusion of a $CaCO_3$ /kaolin mixture in place of just $CaCO_3$ reduced the coverage by 6 to7 units. Round-shaped $CaCO_3$ particles have a tendency to penetrate further into the base paper, thus reducing the coverage, than pigments with a higher aspect ratio like kaolin. At coatweights over 8 g/m^2, the change in coverage was only 2 to 3 units, which is within the range of the measuring accuracy for the method.

As the interaction pigment ratio * solids (Figure 18, right) increased, the SEM-BSE coating coverage also increased. When the $CaCO_3$ content was high (70 : 30 $CaCO_3$: kaolin) and the solids changed from 56 to 60%, the coverage increased (5-6 units). The greater color viscosity at high solids content reduced the color flow into the sheet structure. For a low $CaCO_3$ content (30 : 70 $CaCO_3$: kaolin) in the coating color, the increase in solids content did not affect the coverage (difference 1 to 2 units, insignificant within the range of the measuring accuracy).

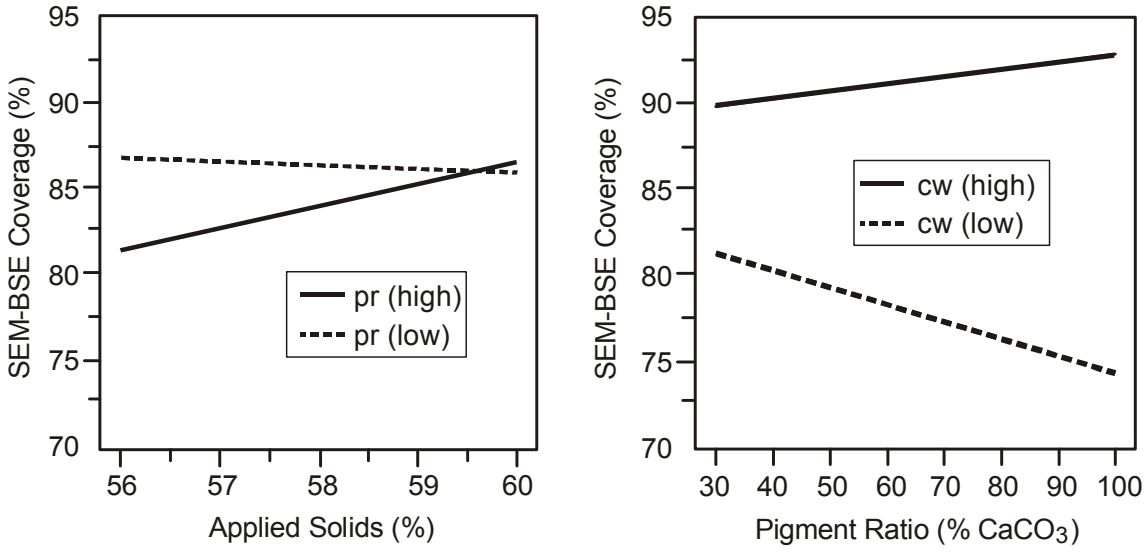

Figure 18. SEM-BSE coverage as a function of applied solids content (left) for two pigment ratios (low ratio 30 : 70 $CaCO_3$: kaolin and high 70 : 30) and as a function of pigment ratio ($CaCO_3$: kaolin, right) at two coatweights (low, 5 and high, 8 g/m^2 /side).

6.2 Coating coverage measured with the LIPS method

In assessing coating coverage with the Laser-Induced Plasma Spectroscopy (LIPS) method, the following variables were found to influence coverage: coatweight, surface filler content, pigment ratio, base paper type, roll hardness and the solids * coatweight interaction term. R^2 for the data was 0.90 and the model prediction (Q^2) was 0.79.

Factors such as an increased coatweight, reduced base paper surface openness, and higher color kaolin content increased LIPS coverage, as was also in the case with SEM-BSE coverage. LIPS coating coverage was also greater with a softer roll cover, with which the nip length increased and the maximum pressure acting on the coating was reduced. An increase in the value of the interaction term solids * coatweight (Figure 19, left) was found to reduce the LIPS coating coverage. At low coatweights of 4 g/m^2, the coverage improved by up to 6 units as the solids content increased. This was expected since the coating coverage usually increased as the solids content was increased. At a coatweight of 8 g/m^2, the LIPS coverage decreased slightly when the solids content was increased by approximately 4 units. This is believed to be due to the greater coating layer openness, which causes the laser ablation to penetrate deeper into the coating layer than with low solids contents. Because the extent of each ablation depends on the coating layer openness, an increase in the openness of the coating affected LIPS coverage results. The LIPS method for measuring precoating coverage is quick and requires very little sample preparation. However, the method needs further development to provide better understanding of the effect of coating layer openness on the results.

The different coating coverage methods correlated well each other, but LIPS coverage values were lower at low coatweights (Figure 19, right, $R^2 = 0.74$).

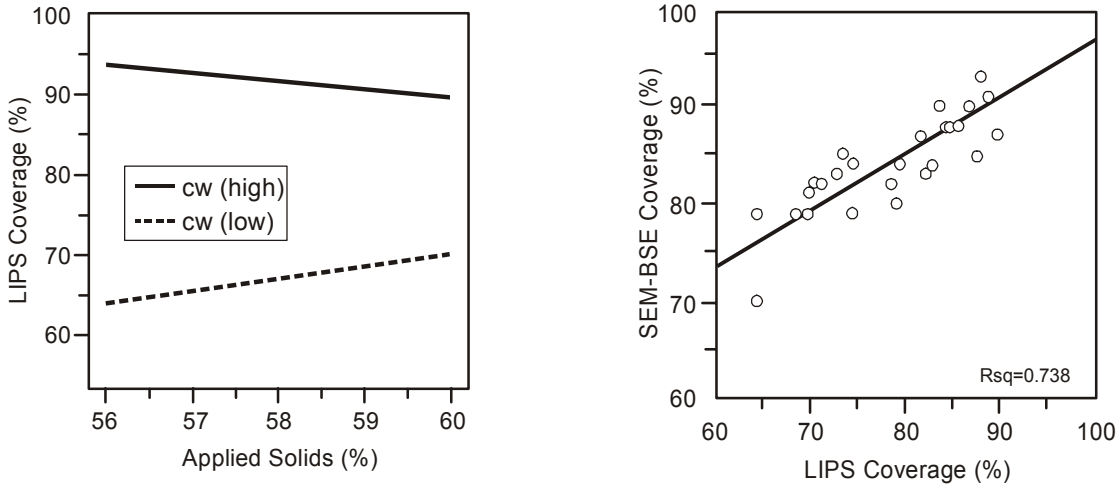

Figure 19. LIPS coverage as a function of coating color solids (left) at two coatweights (low coatweight, 5 g/m^2 and high, 8 g/m^2) and SEM-BSE coverage vs. LIPS coverage (right).

6.3 Discussion

SEM-BSE and LIPS methods gave similar coating coverage results for the precoated paper, but the LIPS coverage was lower at low coatweights. This indicates that with thin layers, the SEM-BSE method gives more reliable results than the LIPS method. The drawback of the LIPS method is that the extent of each ablation depends on the coating layer openness, which in turn affects the coverage results.

Both methods confirmed that improved coverage was obtained by using more filler in the surface of the base paper and higher levels of kaolin in the coating formulation. The impact of these variables became more pronounced at low coatweights. The machine speed and nip load did not affect precoating coverage. These results were not as expected, but they are in agreement with the recent results by Poranen [30, 31]. According to Poranen's results the maximum pressure and the area of the pressure pulse increased only slightly, but the nip width was not changed, when the speed was increased from 500 to 1500 m/min or the linear load was increased from 20 to 40 kN/m [30, 31]. Therefore, if the coating layer formation is affected by pressure-induced penetration of the bulk coating color and liquid phase into the base paper structure, as the first results (Chapter 5) indicated and the later results (Chapters 7 and 9) will confirm, it is logical that the delay time in the nip does not affect the coverage results.

Softer size press rolls and higher coating color solids content had only a small impact on precoating coverage. The results presented here were for a narrow range of values. In a recent study by Grön [41], where coating color solids content was increased from 60% to 69%, a

greater increase in coating coverage was obtained than in this coating study. The effect of base paper was believed to be due to structural differences in the base paper (as in the first coating study) and not to its surface chemistry. The effect of the latter was not established in this study, and was therefore studied further in Chapters 8 and 10 using both laboratory sheets and mill base papers. Because the effects of the MSP coating process conditions, the coating speed and the linear load in the transfer nip were insignificant, they were kept constant in the other coating studies. The hardness of the MSP transfer roll cover material had a small effect on coating coverage, and this was studied further in Chapter 10.

6.4 Summary

The SEM-BSE and LIPS methods gave similar coating coverage results for the precoated papers. The LIPS coverage was lower than the SEM-BSE coverage at low coatweights. This indicates that, with thin layers the SEM-BSE method gives more reliable results than the LIPS method. The drawback of the LIPS method is that the extent of each ablation depends on the coating layer openness, which in turn affects the coverage results. Both methods confirmed that improved coverage was obtained by using more filler in the surface of the base paper and higher levels of kaolin in the coating formulation. The impact of these variables became more pronounced at low coatweights. The machine speed and nip load had no significant effect on precoating coverage.

7 EFFECT OF BASE PAPER SURFACE CHEMICAL PROPERTIES ON COVERAGE

Earlier precoating studies involved coating mill base papers on the pilot scale. The difficulty of using mill base paper was that its quality varied from time to time even from the same mill, while base papers from different mills differed in many respects. This coating study was carried out with laboratory base sheets, which covered a wider quality range than the mill base papers used in the previous studies. The aim of this coating study was to confirm the results obtained for the effect of base paper properties on coating coverage with mill base papers in the first coating study. Base sheet quality was not very homogeneous, and the coatweight formed varied considerably because of the variations in base sheets caused by the sheet formation method.

7.1 Coating layer formation

The laboratory base sheets were coated at a constant rod pressure in the application, which means a constant amount of coating color film on the application roll. Different base sheets picked up different amounts of coating color. Base sheet quality was not very homogeneous and the coatweight formed varied considerably. Sheets had also basis weight and porosity variations in the cross-direction, and smaller-scale variations in porosity originating from the dynamic sheet former's drum holes. The shadow marking caused by the drum holes can be clearly seen in the image of coated porous paper from burnout treatment (Figure 23) and from the microscope images (Figures 31 and 32) taken from the coated porous base paper.

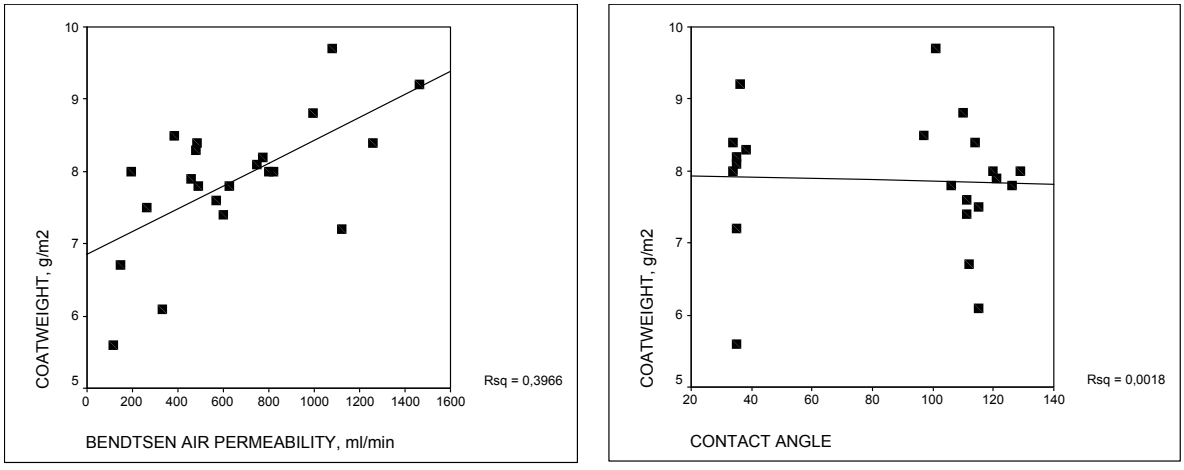

Figure 20. Correlation between coatweight and base paper air permeability (left) as well as base paper surface contact angle (right).

Regardless of the large variation in sheet quality, the coatweight transferred showed a statistically significant correlation with base paper air permeability (Figure 20, left) and with the average pore size of the base paper structure when coating was performed with a constant amount of film on the roll. Surface chemical properties had no effect on coating layer formation (Figure 20, right). The base papers were uncalendered and their roughness was

high. In this study, base paper Bendtsen roughness increased as base paper permeability decreased. Base paper roughness had no effect on coating layer formation.

7.2 Coating coverage and paper gloss

Coating coverage increased as base paper air permeability or pore size decreased, despite the slight simultaneous decrease in coatweight (Figure 21). Neither the Bendtsen roughness nor the contact angle of the base paper surface, measured with coating color liquid phase, had any effect on the coating coverage (Figure 22). Base paper roughness, or small-scale basis weight variation (beta formation), had no effect on the amount of coating color transferred. With the same amount of coating color film on the roll a higher amount of coating color was transferred to the porous base paper, but coating coverage was lower than with dense base papers. The final coating coverage was influenced by bulk coating color penetration into the porous base paper more than by the amount of color transferred alone.

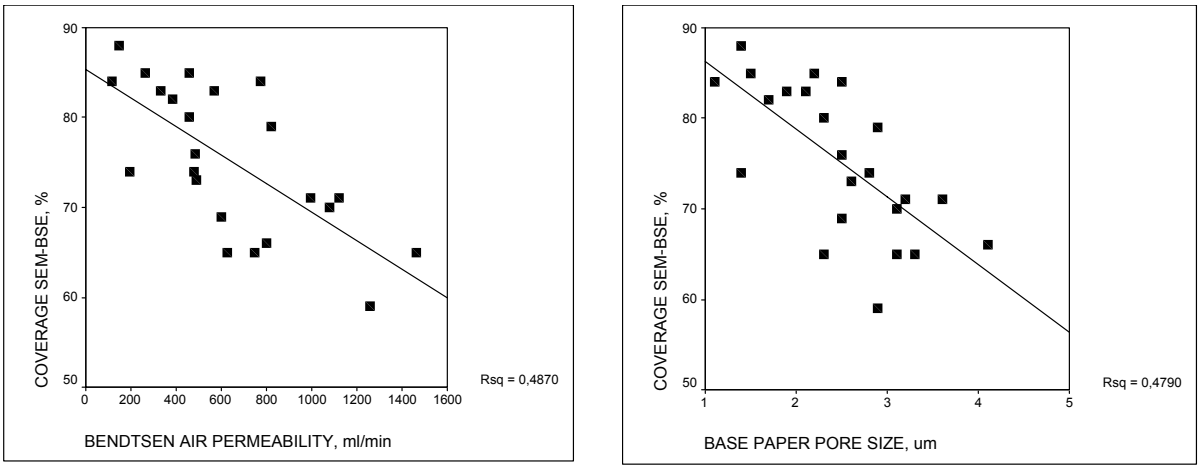

Figure 21. Coverage as a function of base paper air permeability (left) and average pore size (right).

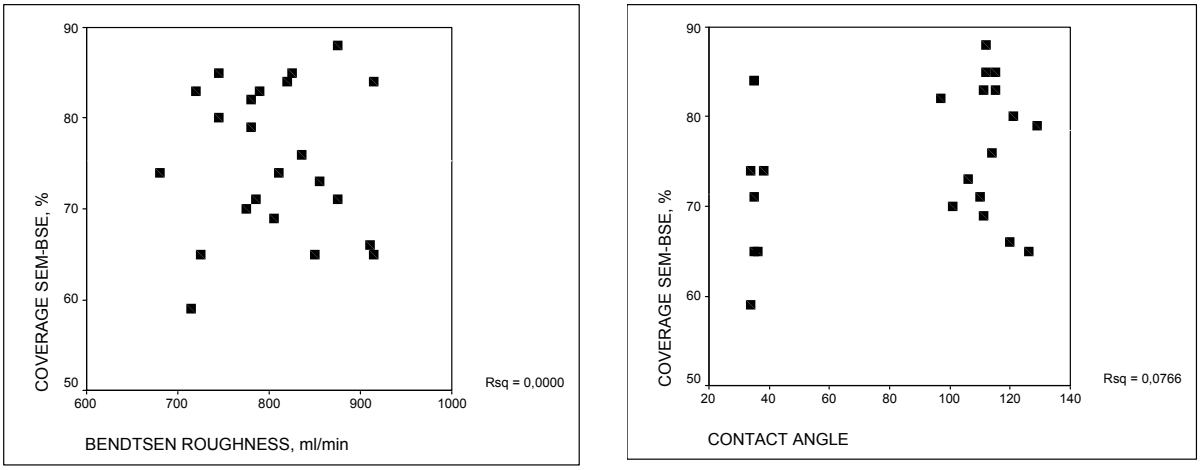

Figure 22. Coverage as a function of base paper roughness (left) and contact angle (right). No correlations.

The images taken from the coated samples after the burnout test showed clearly that porous base paper had greater non-uniformity on the large scale (Figure 23).

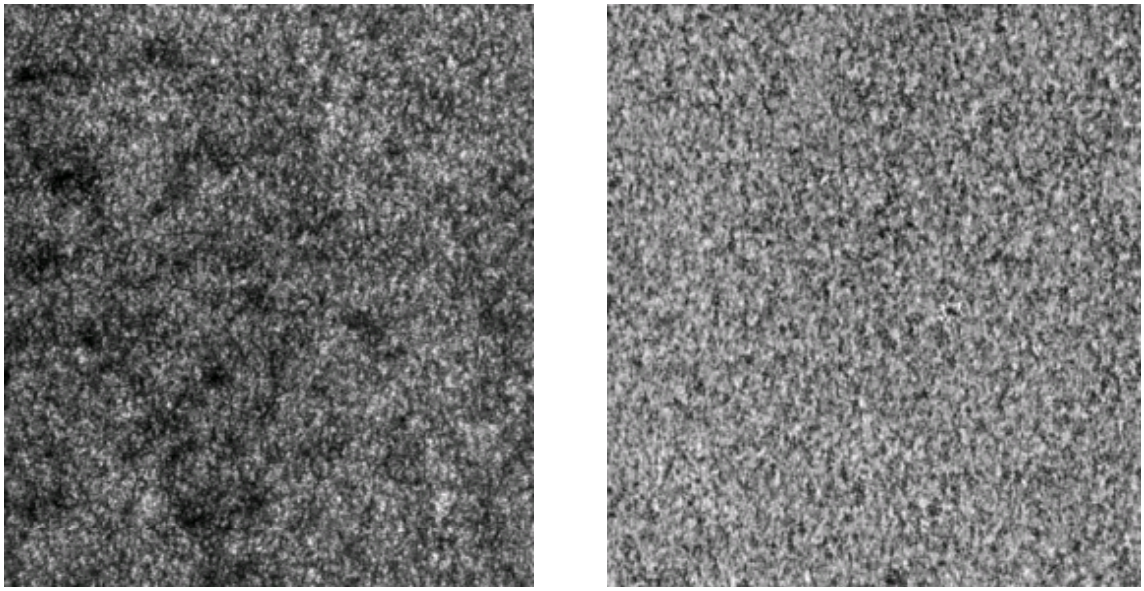

Figure 23. Burnout coverage images for base paper with high air permeability (800 ml/min, left), and low air permeability (150 ml/min right).

Coated paper gloss gave good correlations with both the average pore size and air permeability of the base paper (Figure 24). In this study, coated paper gloss was used as an indirect indication of how well coating color stayed on the base paper surface.

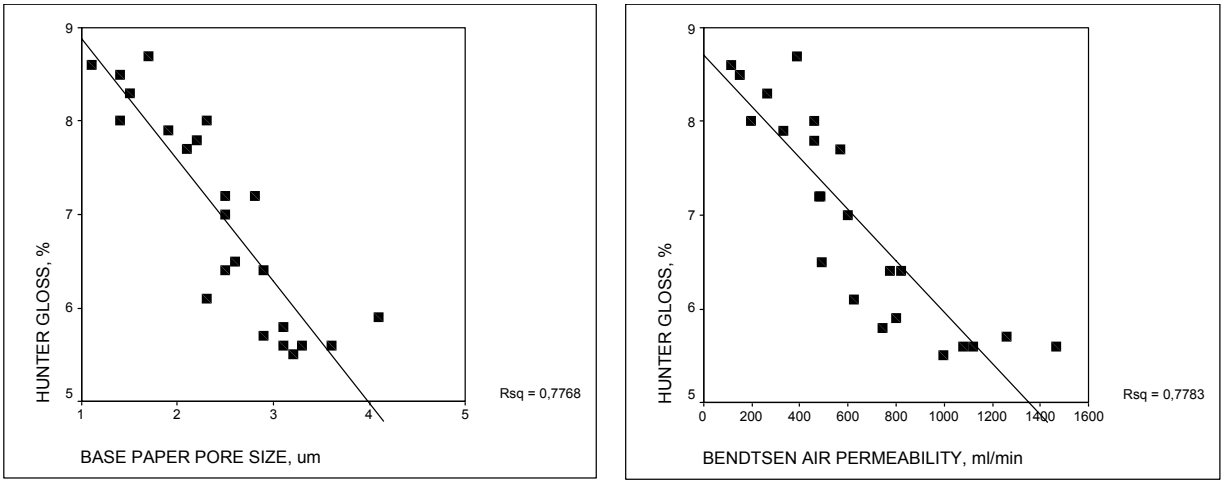

Figure 24. Coated paper gloss as a function of base paper pore size (left) and air permeability (right).

7.3 Coating color penetration and liquid phase (optical brightener) migration into the structure

Under the light microscope, the coating appeared as a black layer on the plastic film, cellophane or base paper (photos in Figures 25, 26, 27 and 28). With non-porous substrates such as plastic and cellophane, a very uniform coating layer was observed. Cross-section photographs of coated cellophane and plastic were also taken by light microscope equipped with a UV-filter. Optical brightener was seen in the coating layer (optical brightener appears bright in the coating layer) if the water transport mechanism was diffusion (cellophane, Figure 26) or else the base was non-porous and did not absorb liquid phase from the coating color (plastic, Figure 28). The results with cellophane were not as expected. The optical brightener used has an affinity for cellulose, so it was expected to move to the cellophane-coating interphase, while the water diffused into the cellophane, but it did not. The transport of optical brightener by diffusion was probably so slow that no optical brightener gradient in the coating layer was observable.

With woodfree base papers, if the base paper surface was dense with a permeability of 150 ml/min, the coating color stayed largely on the surface (Figure 29). The optical brightener is water soluble, and even when CMC was used as a carrier, optical brightener moved into the base paper surface and almost none was seen in the coating layer (Figures 30 and 32). With dense base paper, optical brightener was only observed in the walls of those fibers located at the base paper surface (Figure 30, mainly in the upper part of the fiber wall in the first layer of fibers).

Porous base papers with a permeability of 800 ml/min had a uniform coating layer on the surface, but in some places coating color penetrated deeper into the base paper (Figure 31). The optical brightener was also observed slightly deeper in the paper structure (Figure 32) due to the fact that the surface pores were broader and coating color went deeper into the structure. Optical brightener was seen through the whole fiber wall in the first and second fiber layers and not only in the upper part of the fiber wall as with the dense base paper. The physical structure of the base paper was the only factor affecting the coating color liquid phase movements in the paper. The migration of optical brightener was similar with hydrophilic and hydrophobic sheets of similar permeability.

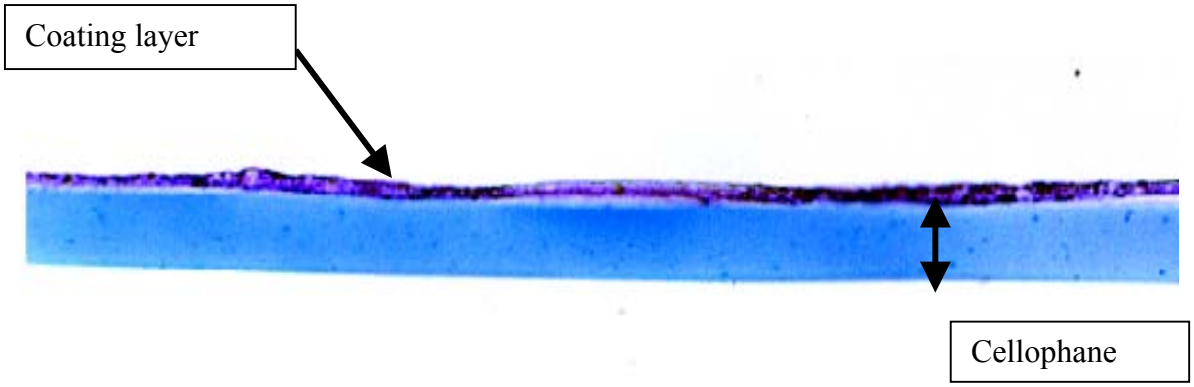

Figure 25. Light microscopy image of coating layer applied on a cellophane substrate.

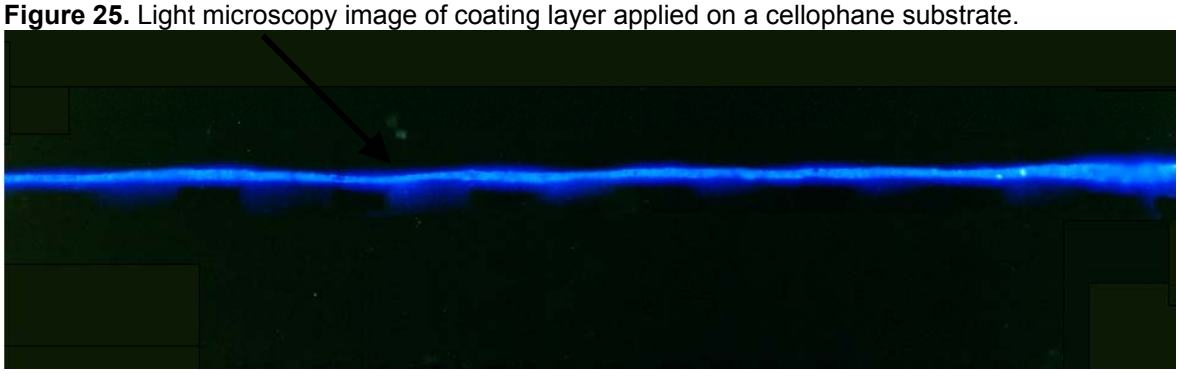

Figure 26. Light microscopy image in UV light of coating layer applied on a cellophane substrate.

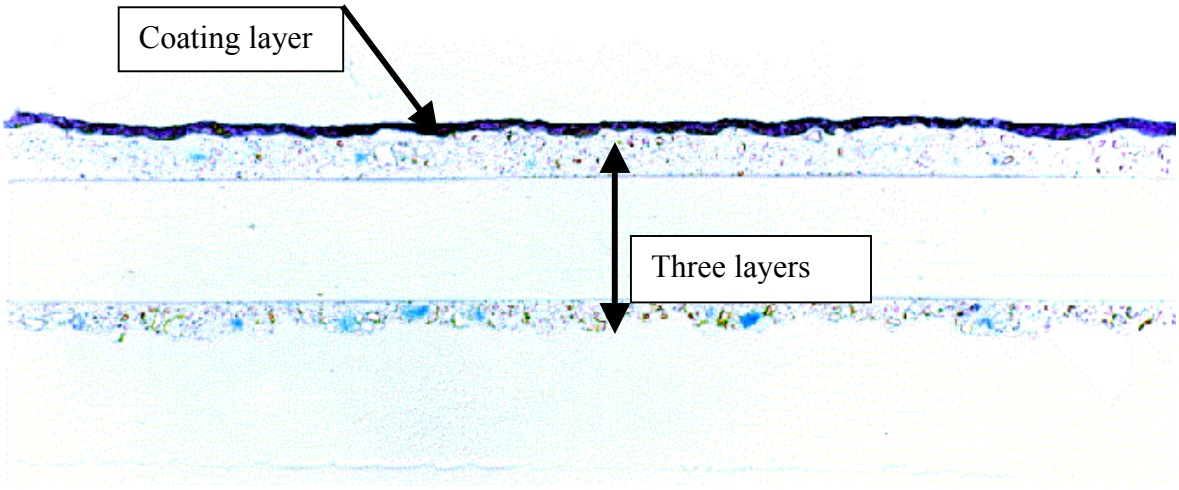

Figure 27. Light microscopy image of coating layer applied on a non-porous plastic substrate.

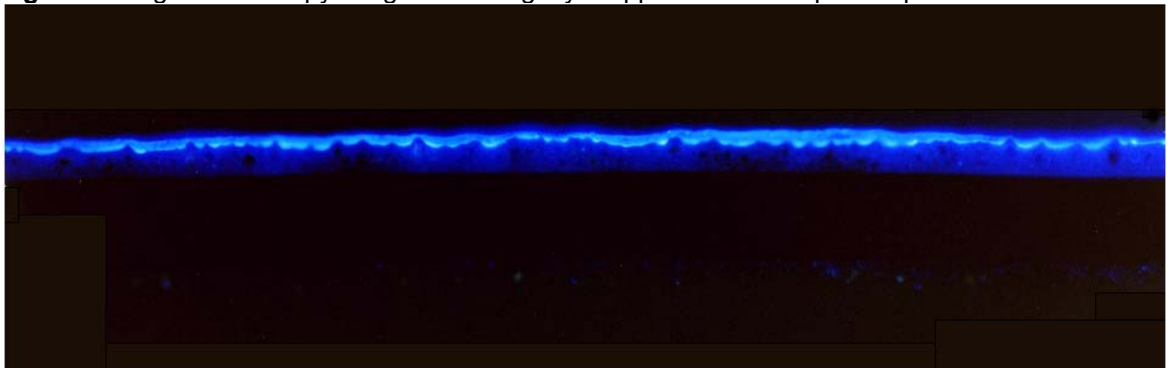

Figure 28. Light microscopy image in UV light of coating layer applied on a plastic substrate.

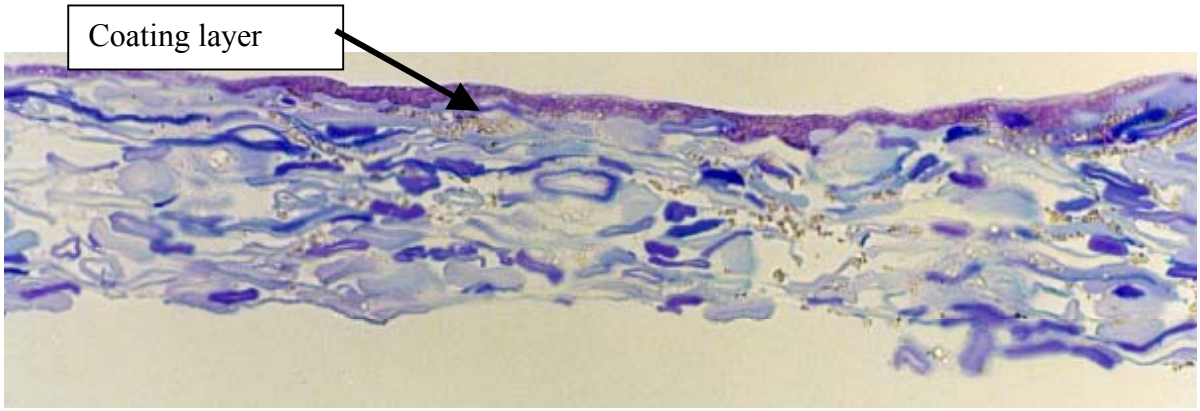

Figure 29. Light microscopy image of coating layer applied on a dense base sheet.

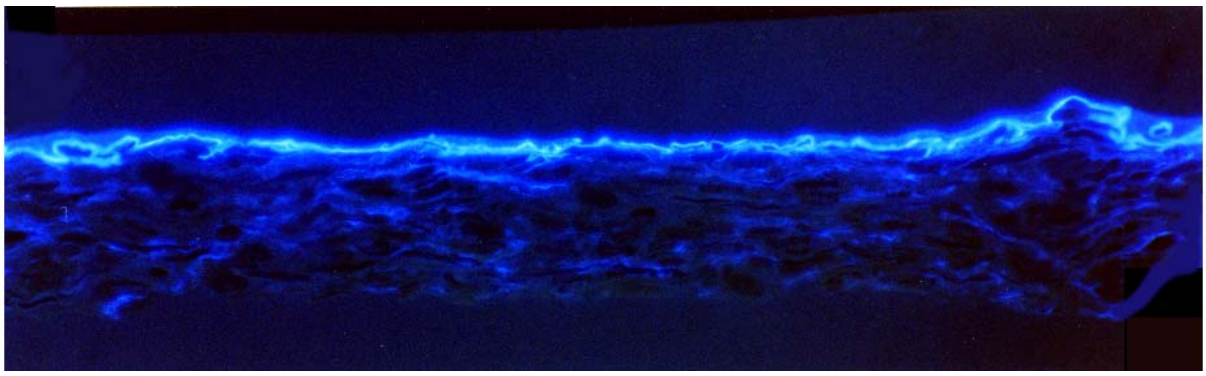

Figure 30. Light microscopy image in UV light of coating layer applied on a dense base sheet.

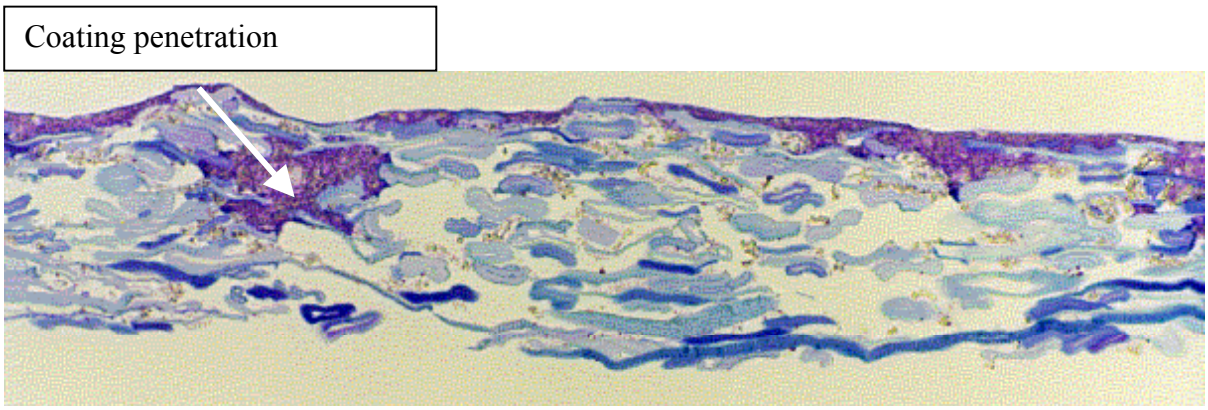

Figure 31. Light microscopy image of coating layer applied on a porous base sheet.

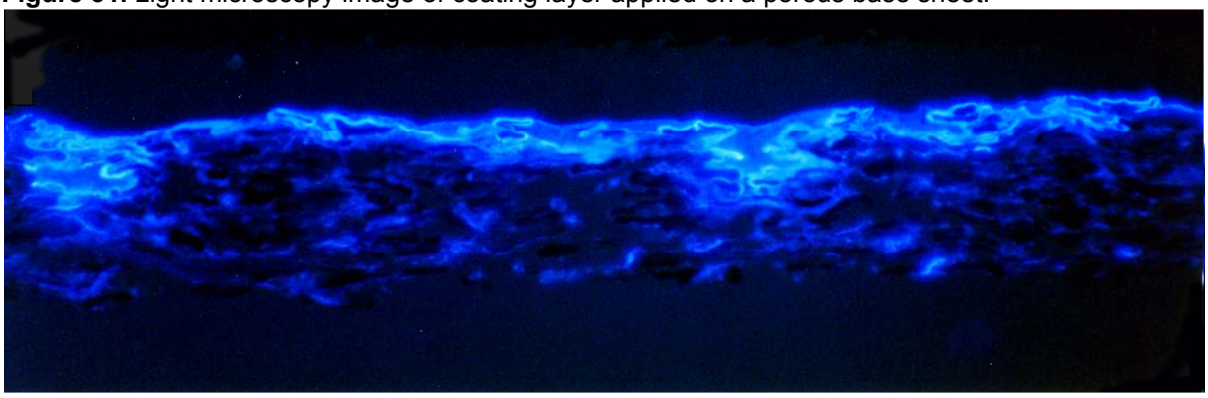

Figure 32. Light microscopy image in UV light of coating layer applied on a porous base sheet.

7.4 Discussion

In this study with porous woodfree base sheet, coating color transfer was determined by base paper permeability. A high permeability of the base paper resulted in a high coatweight (8 to 9 g/m^2) due to the penetration of coating color into the surface voids. Base paper roughness, or small-scale basis weight variation (beta formation), had no effect on the amount of coating. It is likely that the base paper roughness collapsed under the high pressure in the MSP transfer nip. This would be a logical explanation and is supported by other studies from blade coating. Cross-section images of commercially coated LWC papers [127] suggested that even in blade coating, which is a void-filling process, the base paper roughness with compressible base stocks partly collapsed under the blade. The nip pressure (400 kPa) and the delay time in the nip (1 to 4 ms) in metered size press coating are much higher than those in blade coating (120 kPa, 0.01 ms) and therefore the effect of base paper compressibility on base paper roughness in the nip might be even greater in metered size press coating.

The coating coverage obtained with high base paper permeability was lower than with dense base paper, even though the coatweight was higher at a given amount of film on the roll. Hydrophobic sizing of the fibers (hydrophilic/hydrophobic) had no effect on the coatweight formed or on the positioning of the coating in the base sheet. Therefore, dewatering by capillary absorption into the fibers plays no part in coating layer formation in MSP coating and the determining factor was the physical sheet structure.

Coating color liquid phase seemed to penetrate mainly into the pores between the fibers, because the contact time in the MSP transfer nip is very short compared to any laboratory measurements of water absorption. Rendering the base paper hydrophobic had no effect on transfer of the water phase. An earlier analysis by electron spectroscopy (ESCA) by Ström *et al.* [128] showed that AKD covered only part of the surface of the cellulose fibers and that the thickness of the AKD film was approximately 3 nm. Sizing was sufficient when 15% of the surface was covered by AKD [128].

Water moves into the dry fiber wall by diffusion. This will take place even if the fiber surface is hydrophobic. The results obtained in this study support the assumption that capillary absorption into the structure happens after the transfer nip, since the chemical properties of the base paper surface do not affect either coating layer formation or coating coverage. This agrees with a recent laboratory study, in which water transport into the paper and the dimensional changes occurring under dynamic conditions were studied with experimental methods and theoretical models [129]. When only a small amount of water was applied to the paper in a nip, capillary penetration was very fast and stopped soon after the application. For newsprint, the model predicted that a film of 4 g/m² of water would penetrate into the inter-fiber pores within a few milliseconds. After all the liquid had passed into the paper, the absorption of water from the pores into the dry fibers continued until the base paper pores were empty. This was called sorption into the fiber wall, and was much slower, lasting several seconds. According to the simulations, the water content at the fiber surface can be as high as 0.25-0.27 g/g fibers. The subsequent evening out of the moisture content throughout the paper structure (diffusion along fibers) was assumed to take a longer time (roughly 10 seconds). Good agreement was found between the experimental results and the model [129].

The results with cellophane were not as expected. The optical brightener used has an affinity for cellulose and it was expected to move to the cellophane-coating interphase, while the water diffused into the cellophane, but it did not. Although water is not a solvent for cellulose, it is a powerful swelling agent; it was found that 1.0 g of cellophane absorbed 1.65 g water in the fully swollen state [126]. The relative absorbance was slow. When measured with a method for measuring diffusion using a simple ATR device, absorbance increased after several tens of seconds up to hundreds of seconds [126]. The transport of optical brightener by diffusion was probably so slow that no optical brightener gradient was observable in the coating layer. The results of the movement of the optical brightener into the base paper coating layer interface agree with an earlier study of optical brightener and board [130]. Although optical brightener movement was expected to be different with hydrophilic and hydrophobic sheets, it was not.

The main mechanism for coating layer formation during transfer was pressure-induced penetration of coating color or coating color liquid phase into the voids between fibers. Coating color water phase moved into the walls of fibers located in the surface layers irrespective of the hydrophobic sizing of the fibers. Water sorption into the fibers was slower than capillary penetration, and it is reasonable to assume that the movement of coating color liquid phase takes place by diffusion and possibly by capillary absorption after the nip. The mechanism of water transport into the fiber wall remains unclear. Further studies and simulations under dynamic conditions are needed to prove how water moves into the fiber wall during coating.

7.5 Summary

The coating coverage obtained with high base paper permeability was lower than with a dense base paper, even when the coatweight was higher. The hydrophobic sizing of the fibers (hydrophilic/hydrophobic) had no effect on coating layer formation or the positioning of coating color in the base sheet. Therefore, dewatering by capillary absorption has no effect on coating layer formation in MSP coating. The determining factor was the physical sheet structure.

The main mechanism by which coating layer formation took place was pressure-induced penetration of coating color or coating color liquid phase into the voids between fibers. Coating color liquid phase moved into the walls of fibers located in the surface layers irrespective of the hydrophobic sizing of the fibers.

8 EFFECT OF BASE PAPER STRUCTURE POROSITY ON COVERAGE

The effect of the openness of the base paper surface appears to be clear in the case when woodfree base papers with high air permeability are coated with an MSP coating unit. To improve coating coverage, the porosity of the base paper structure and at the same time the surface openness were lowered by raising the mechanical pulp content of the furnish or intensifying the refining of the chemical pulp fibers. The aim here was to reduce the average pore size and the air permeability of the base paper. The addition of short-fibred mechanical pulp reduced the porosity of the base paper, but the addition of mechanical pulp to the woodfree base paper furnish is not the solution if the final product is required to have high brightness. Intensive refining of the chemical pulp fibers shortens and deforms the fibers, which densifies the sheet structure. This makes it possible to reduce the porosity of the base paper.

8.1 Effect of mechanical pulp addition on pore size and coverage

8.1.1 Base paper properties

Adding mechanical pulp (PGW or TMP) or de-inked pulp (DIP) reduced the sheet density, air permeability, oil absorption rate and average pore size, but increased sheet roughness, as shown in Table 7. Replacing the birch chemical pulp with eucalyptus pulp, made the sheet slightly smoother, reduced the oil absorption rate and improved formation. Oil absorption rate and average pore size correlated with each other ($R^2 = 0.7$). The lower air permeability could then be explained by the smaller average pore size ($R^2 = 0.97$).

Table 7. The properties of the laboratory sheets.

Base paper property	Reference	PGW	TMP	DIP	Eucalyptus
Density (kg/m^3)	676	599	541	625	656
Bendtsen roughness (ml/min)	725	920	1210	1015	685
Air permeability (ml/min)	1465	415	605	445	1450
Beta formation, standard deviation (g/m^2)	3.3	2.9	3.5	3.2	2,9
Average pore size, Coulter (μm)	3.3	1.7	2.1	2.0	3.1
Absorption coefficient, nozzle, oil (ml/m^2/s^{½})	158	125	144	117	187

8.1.2 Coated paper properties

A smaller base paper pore size resulted in a lower coatweight for a constant amount of coating color applied to the roll (Figure 33). However, despite the lower coat weight the coating coverage of these dense base papers was higher than with porous base papers (Figure 50), indicating that less coating color penetrated. Base paper roughness did not affect coating layer formation or the coverage results. These results confirm that base paper porosity and pore size can be reduced by adding mechanical pulp, which affects both coating layer formation and coverage. Because the average pore size of the woodfree base paper structure is large, the furnish composition of the base paper needs special attention if sufficient coverage is to be achieved at low coatweights.

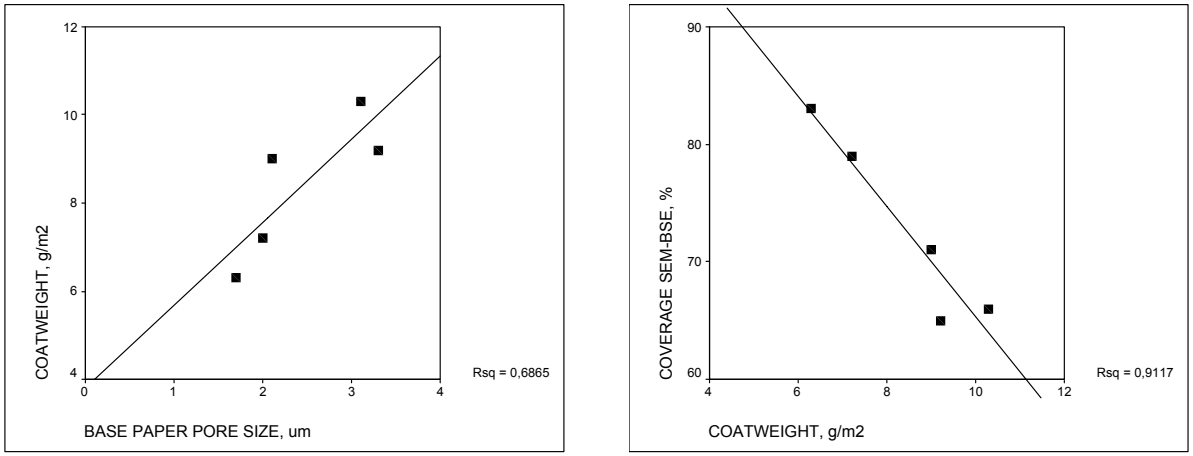

Figure 33. Coatweight as a function of average pore size (left) and coating coverage as a function of coatweight (right).

8.2 Effect of intensive chemical pulp refining on pore size and coverage

8.2.1 Base paper properties

The properties of the pilot base paper produced are presented in Table 8. The base paper permeability and formation were varied across a wide range (Figure 34). Differences in the mix between softwood and hardwood affected mainly the formation of the base paper. The degree of chemical pulp refining had the greatest effect on base paper air permeability. The chemical pulps refined to a CSF of 500 ml gave air permeabilities between 890 and 1100 ml/min, whereas those refined to low CSF values gave air permeabilities between 115 and 170 ml/min. All base papers carried markings from the pilot paper machine suction roll, which was more visible on porous than on dense base papers.

Table 8. Properties of the base paper.

Experimental Point	Roughness Bendtsen TS / BS ml/ min	Permeability Bendtsen ml/min	Average pore size, μm	Beta specific formation √g/m
1	354 / 434	149	1.1	0.49
2	300 / 378	169	1.4	0.44
3	359 / 358	359	2.2	0.69
4	231 / 271	234	2.3	0.49
5	237 / 312	198	1.6	0.52
6	218 / 251	562	2.7	0.50
7	248 / 261	891	3.6	0.73
8	182 / 178	1107	4.0	0.59
9	237 / 274	406	2.4	0.53

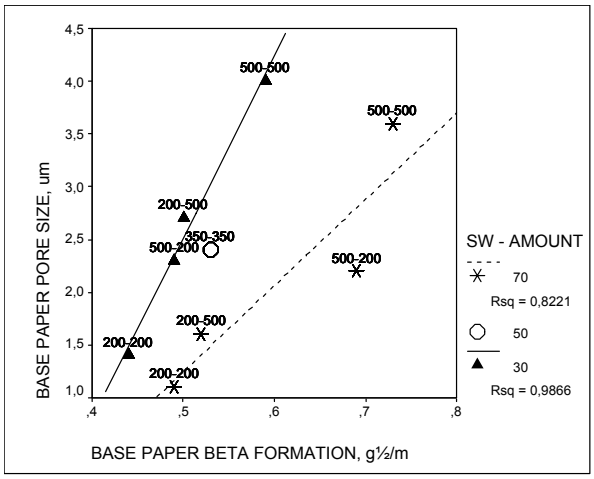

Figure 34. Average pore size of the base paper as a function of specific beta formation for different SW contents and refining levels (CSF 200-500 ml).

8.2.2 Coating layer formation

Four different amounts of coating color film were applied to the roll in this study. Small amounts of film gave high transfer ratios, and as a consequence the ratio deminished with higher coatweights, which increased as base paper porosity and surface openness increased (Figure 35). Neither base paper roughness nor small-scale basis weight variation (beta formation) influenced the coatweight (Figure 36). With a small amount of coating color film, almost all the coating color was transferred to the base paper and therefore no correlation was found between base paper properties and coatweight.

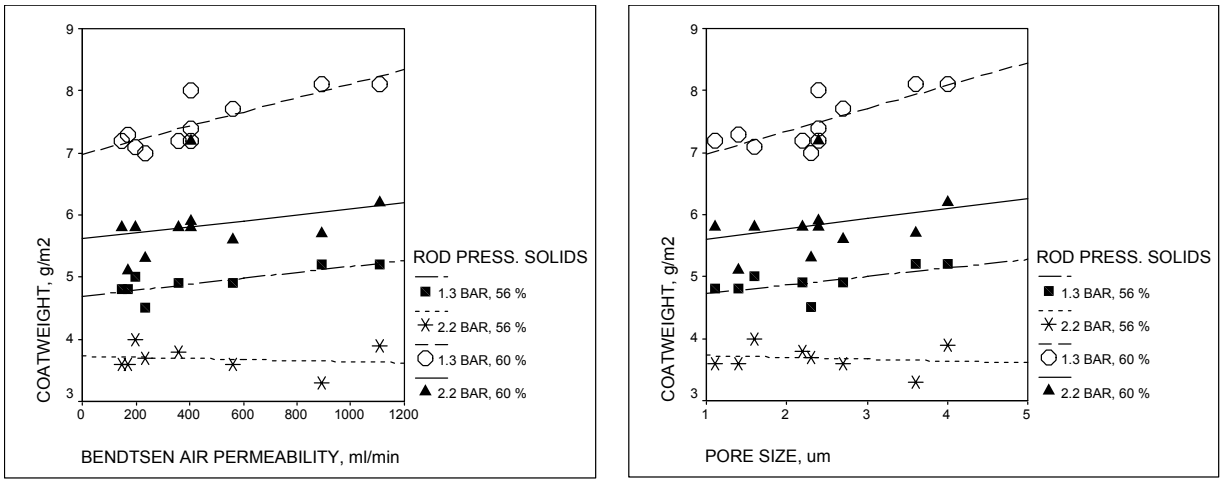

Figure 35. Coatweight as a function of base paper air permeability (left) and average pore size (Coulter, right) at different rod pressures and coating color solids contents.

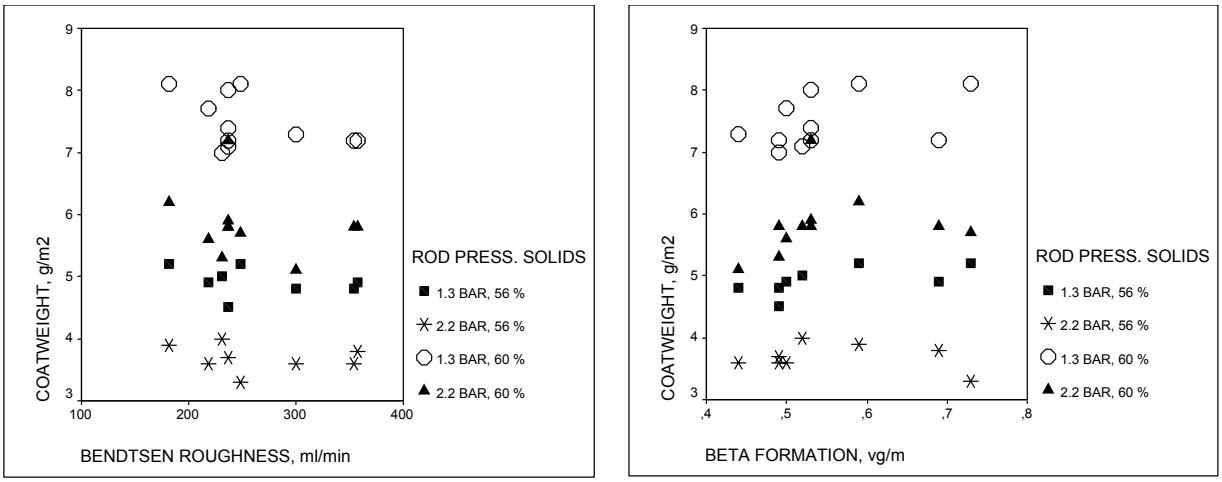

Figure 36. Coatweight as a function of base paper roughness (left) and the specific beta formation (right) at different rod pressures and coating color solids contents.

8.2.3 Coating coverage measured with the SEM-BSE method

With porous base papers, coating color penetrated into the base paper structure during color transfer. Base paper surface openness decreased and coating coverage increased when the chemical pulps were more refined, which is important at low coatweights (Figure 37, left). Reducing the openness of the base paper structure through chemical pulp refining improved the light scattering properties of the coated paper, despite the fact that the base paper exhibited poorer light scattering than the porous papers (Figure 37, right). This can be explained by the higher coating coverage.

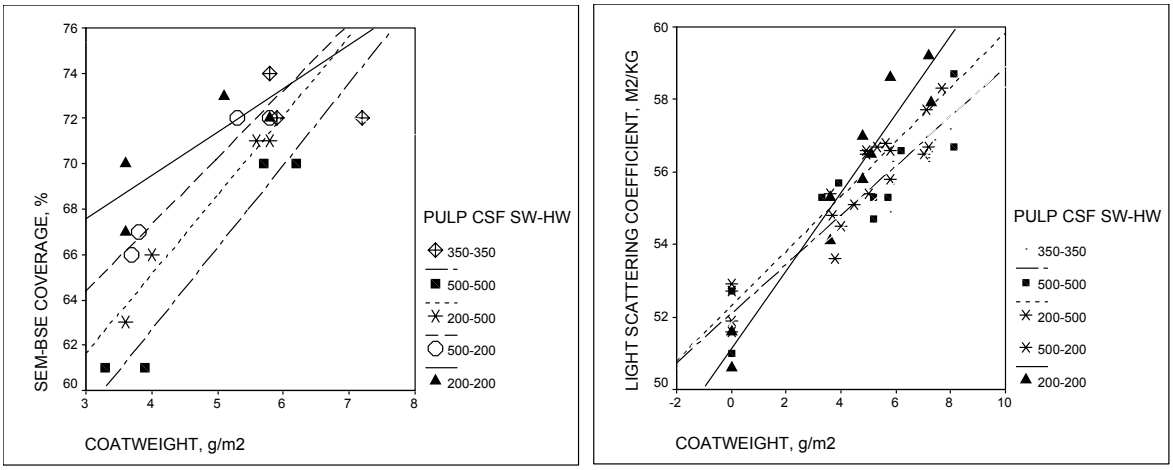

Figure 37. Coated paper coating coverage (left) and light scattering (right) as a function of coatweight with base papers containing chemical pulps with different CSF values.

The proportion of hardwood in the mixture affected base paper formation but not coating coverage. Dense base papers gave better small-scale uniformity than porous base papers (Figures 38 and 39).

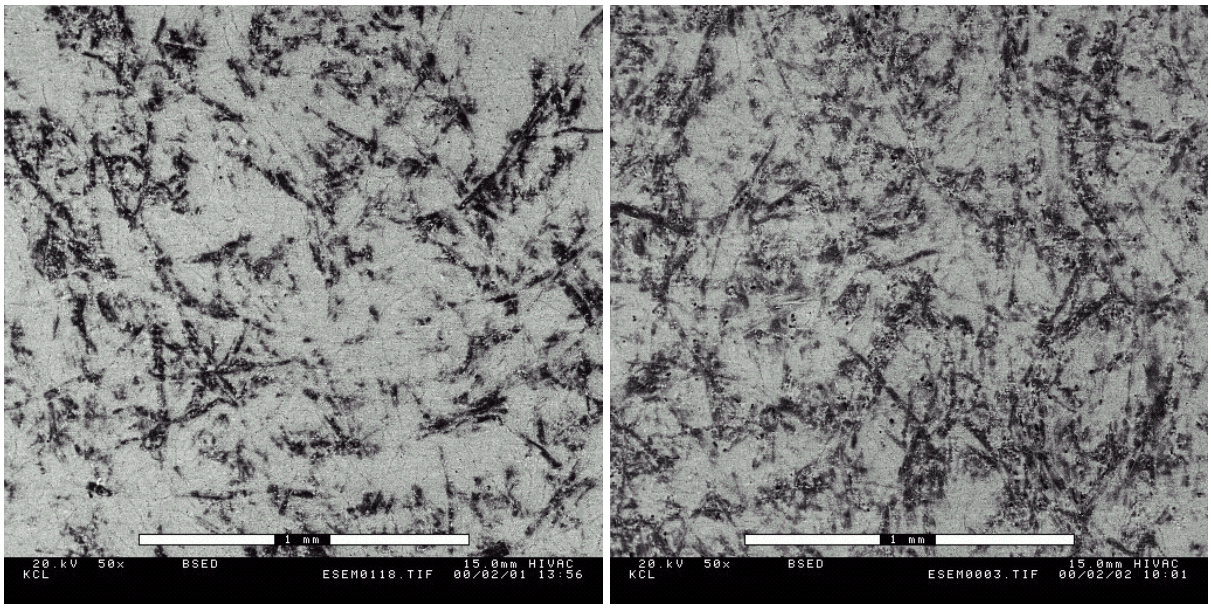

Figure 38. SEM image illustrating the coverage of coated papers. Dense base paper with a coatweight of 5.8 g/m² (left) and 3.6 g/m² (right).

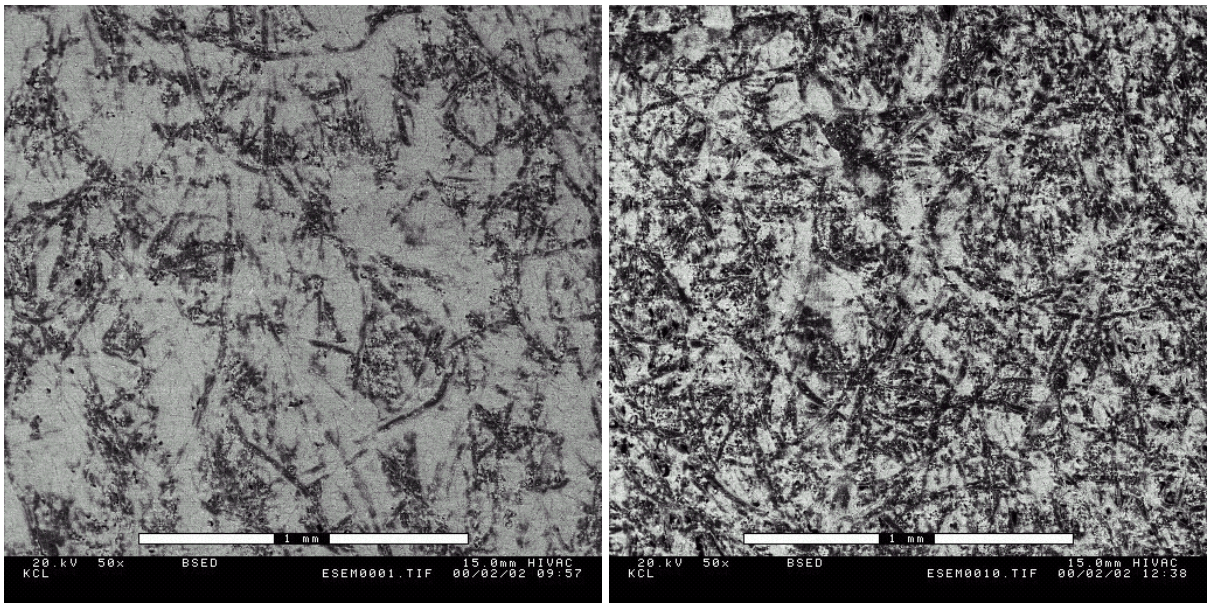

Figure 39. SEM image illustrating the coverage of coated papers. Porous base paper with a coatweight of 6.2 g/m² (left) and 3.9 g/m² (right).

8.2.4 Large-scale uniformity measured with the burnout method

Coating coverage uniformity on the large scale was examined visually from burnout-treated papers. Images showing large-scale coating coverage variations in the burnout test are presented in Figures 40 and 41 (dense and porous base papers). The coated topside of both the dense and porous base papers showed an uneven pattern caused by shadow marking from the pilot paper machine wire section. The marking from the suction roller caused large-scale variations in the coating layer. The large-scale non-uniformities in coating color penetration were clearly seen for the topside of the porous base paper, where the pattern was stronger for porous base paper than for dense base paper (Figure 41). This indicated that the fines content in the base paper surface had a strong impact on coating coverage.

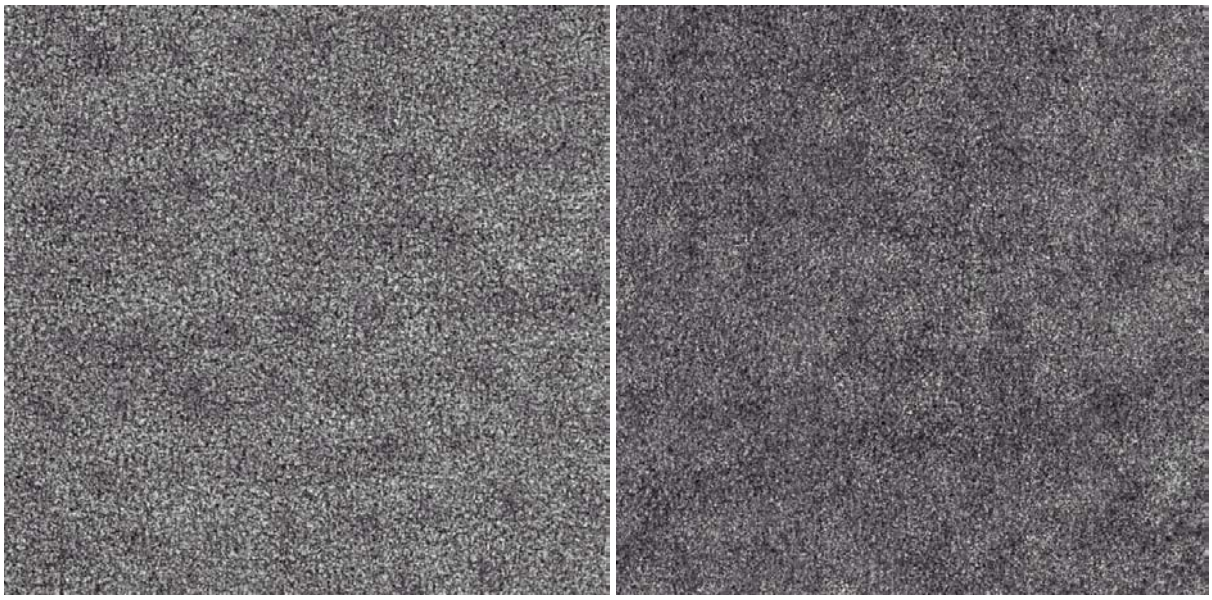

Figure 40. Burnout images of coated paper. Dense base paper with a coatweight of 5.8 g/m² on the topside (left) and with 5.5 g/m² on the bottom side (right).

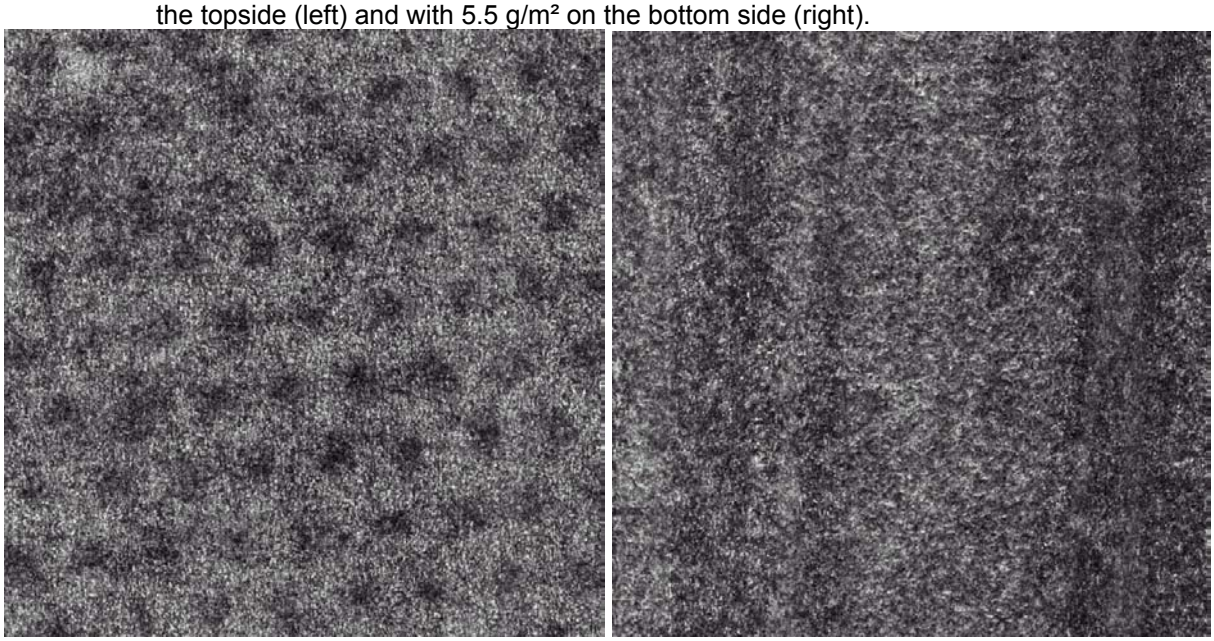

Figure 41. Burnout images of coated paper. Porous base paper with a coatweight of 6.2 g/m² on the topside (left) and with 6.1 g/m² on the bottom side (right).

8.2.5 Optical brightener migration into the paper structure

Penetration of the coating color liquid phase was investigated by studying the penetration of optical brightener into the base paper structure from cross-sectional images using a light microscope equipped with a UV source. The images showed that the penetration of liquid phase increased with increasing base paper openness. Coating color liquid phase and optical brightener penetrated less deeply into the dense base paper structure (Figure 42) than into the porous structure (Figure 43). At a coating color solids content of 56%, the penetration of coating color liquid phase was stronger for lower coatweights, and the fibers roughened more than at a solids content of 60% (Figures 44 and 45). Reducing the coating color solids did not increase the amount of liquid phase that penetrated into the paper; however, it reduced the coating suspension viscosity and thus resulted in a greater penetration depth. Fiber swelling increased despite the lower total amount of water applied at low solids content (~3 g/m²) than at high solids content (~4 g/m²). Theoretical calculations showed that the amount of water that penetrated into the structure at the immobilization point was lower when a lower coatweight was applied at lower solids content (~2.2 g/m^2) than for a higher coat weight at higher solids content (~2.8 g/m^2). It can be assumed that, due to the lower coating color viscosity, the color is pushed deeper into the base paper structure in the transfer nip, which caused deeper penetration and greater fiber swelling.

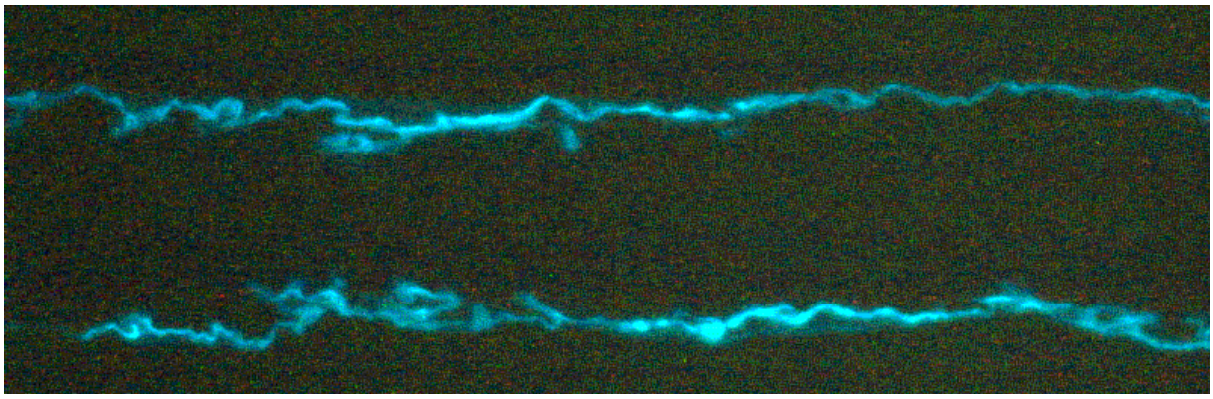

Figure 42. Cross-sectional image of a dense base paper coated with coating color at 60% solids content to 5.8 g/m² on the topside and 5.5 g/m² on the bottom side.

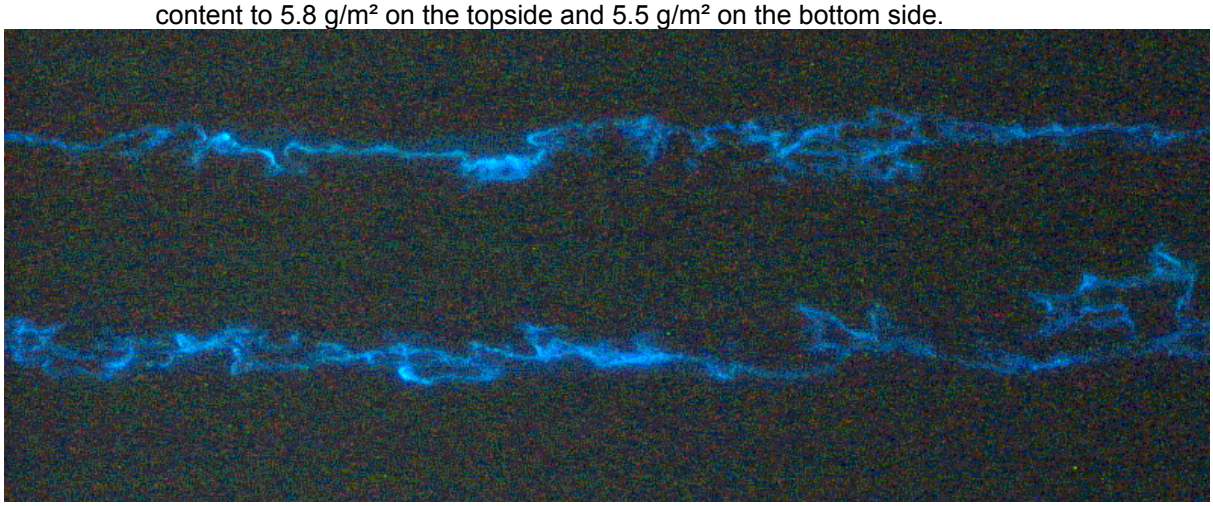

Figure 43. Cross-sectional image of a porous base paper coated with coating color at 60% solids content to 6.2 g/m² on the topside and 6.1 g/m² on the bottom side.

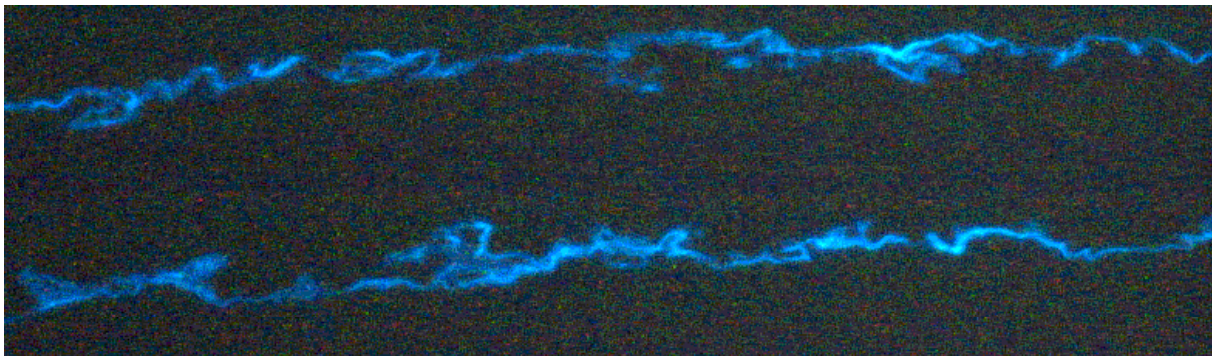

Figure 44. Cross-sectional image of a dense base paper coated with coating color at 56% solids content to 3.6 g/m² on the topside and 4.0 g/m² on the bottom side.

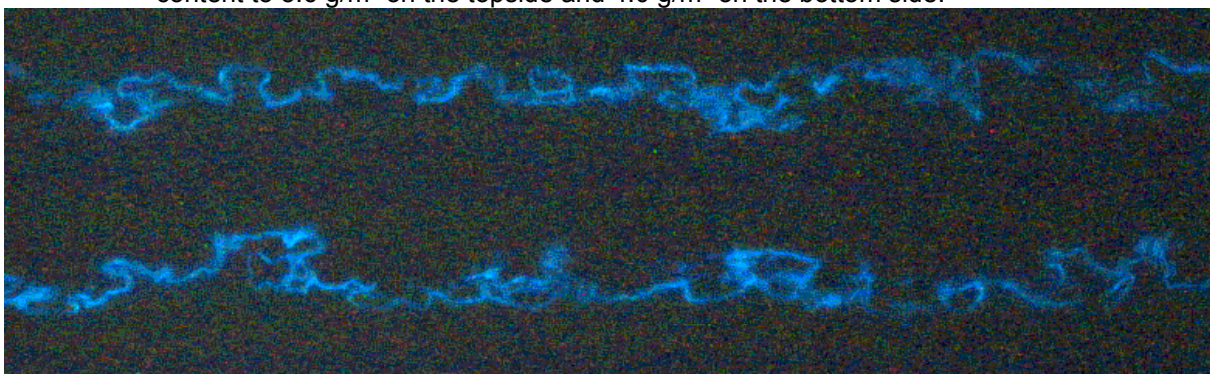

Figure 45. Cross-sectional image of a porous base paper coated with coating color at 56% solids content to 3.9 g/m² on the topside and 3.3 g/m² on the bottom side.

8.3 Discussion

The addition of short-fiber pulp and the intensive refining of softwood and hardwood pulps reduced both the permeability and the pore size of the base paper, which resulted in lower coatweights. Neither base paper roughness nor small-scale basis weight variation (beta formation) at same porosity level had any effect on coating color transfer. It could be that the base paper roughness collapsed under the high pressure in the MSP transfer nip, although it rebounded immediately at the nip exit, roughness, therefore, does not affect the formation of the coating layer.

Compression of the surface roughness would be a logical explanation and is supported by other studies from blade coating. Cross-sectional images of commercially coated LWC papers by Lepoutre and Silveira [127] suggested that, even in blade coating, which is a void-filling process, the base paper roughness with compressible base stocks collapsed to some extent under the blade. Zou *et al.* [131] have also shown that when the base paper was more compressible (e.g. 100 GW) coating thickness (measured) depended less on roughness than with a less compressible base paper (100% chemical pulp). These results indicated that the base paper was significantly compressed during application at low coatweights [131]. The nip pressure and the delay time in MSP coating are much higher than those in blade coating and therefore the effect of base paper compressibility on base paper roughness in the nip might be even greater in MSP coating. This is also in agreement with the results from studies of the effects of pre-calendering the base paper. According to these studies, both the openness and

the roughness of LWC base papers decreased slightly [14, 51, 132] bringing a slight improvement in coating coverage with pre-calendered base papers coated with an MSP [14]. Taking into account all these results, it is believed that better coating coverage is due more to the lower surface openness than to the lower roughness of pre-calendered paper.

Reducing the pore size improved the coating coverage of the paper, especially at low coatweights. Coating coverage was not significantly affected by base paper formation or roughness. Base paper pore size influenced coated paper coverage on both large and small scales. Dense base papers gave better small-scale uniformity than porous base papers. The coated topside had an uneven pattern caused by shadow marking from the wire section, the pattern being most pronounced in porous base papers. Dense base paper gave better light scattering properties than porous base paper because of the better coating coverage. Dense coated base papers gave better results even when the light scattering properties of the base paper were inferior to those of porous base papers. On the other hand, critical final product properties such as bulk and stiffness, as well as paper machine efficiency and wire section dewatering capacity, might limit the scope for reducing pore size through chemical pulp refining.

The results showed that both the liquid phase and the coating color bulk penetrated deeper into the base paper structure due to the pressure pulse when base paper openness was increased or coating color solids content was reduced. At lower solids content, the liquid phase made the base paper coating layer interface rougher than at high solids content despite the smaller amount of liquid phase transferred.

8.4 Summary

Reducing the pore size improved the coating coverage of the paper, especially at low coatweights. Coating coverage was not significantly affected by base paper formation or roughness. Base paper pore size influenced coated paper coverage on both large and small scales. Dense base papers gave better small-scale uniformity than porous base papers. The coating coverage was sensitive to shadow marking, which was clearly seen as large-scale coverage non-uniformity. The liquid phase of the color penetrated deeper into the base paper structure when base paper openness was increased or coating color solids content was reduced.

9 EFFECT OF PRESSURE PULSE ON COATING COVERAGE

According to the results reported in chapter 6, the softer polyurethane rolls gave slightly better coating coverage than the harder polyurethane rolls (with lower P&J). This was studied further with different mill base papers. The roll cover materials used were polyurethane with a hardness of 44 /42 P&J (**hard rolls**) and rubber with a hardness of 88/ 84 P&J (**soft rolls**).

9.1 Base paper properties

The base papers from different paper machines showed differences in formation, porosity and roughness. The most important base paper properties are given in Table 9. Typical of both base papers produced with fourdrinier forming sections is the two-sided filler distribution. The surface layers of the base paper showed a very low content on the bottom side and a high content on the topside. One of the base papers from the same paper machine was hydrophilic while the other was hydrophobic.

Table 9. Properties of the base papers.

Base paper		Structure Filler content the surface, %	Roughness		Beta form.	Absorption Nozzle appl.	Coulter pore	Air perm.	Surf.chem. Fibro
			Bendtsen	PPS10		oil		Bendtsen	liq. phase
No.	side		ml/min	µm	g/m^2	ml/m^2/s$^{1/2}$	size µm	ml/min	°
1	top	18	115	3.4	5.9	85	2.8	460	125
1	bottom	5	220	4.3		90			115
2	top	30	260	4.4	6.2	120	2.6	630	65
2	bottom	7	530	5.4		110			55
3	top	30	365	4.9	6.5	110	3.6	720	110
3	bottom	9	595	5.5		110			75
4	top	30	370	4.9	6.2	115	3.8	790	45
4	bottom	8	575	5.5		115			35

9.2 Coating coverage

With polyurethane rolls, the coating layer was formed more through penetration of the bulk coating color into the base paper structure. The average pore sizes of the first two base papers (both hydrophobic and hydrophilic papers, Table 9) were 2.6 – 3.0 μm (average 2.8 μm). The average pore sizes of the base papers (both hydrophobic and hydrophilic papers) from the other two papers were 3.6 – 3.8 μm (average 3.8 μm). The base papers with smaller average pore size gave 5-10% -points higher coverage than those with a larger average pore size at a constant coatweight of 6-8 g/m^2/side (Figure 46, left). The differences in coating coverage for different coating colors were small and not significant. Coating coverage was not affected by base paper surface chemical properties (contact angle) with either hard or soft rolls (Figure 46).

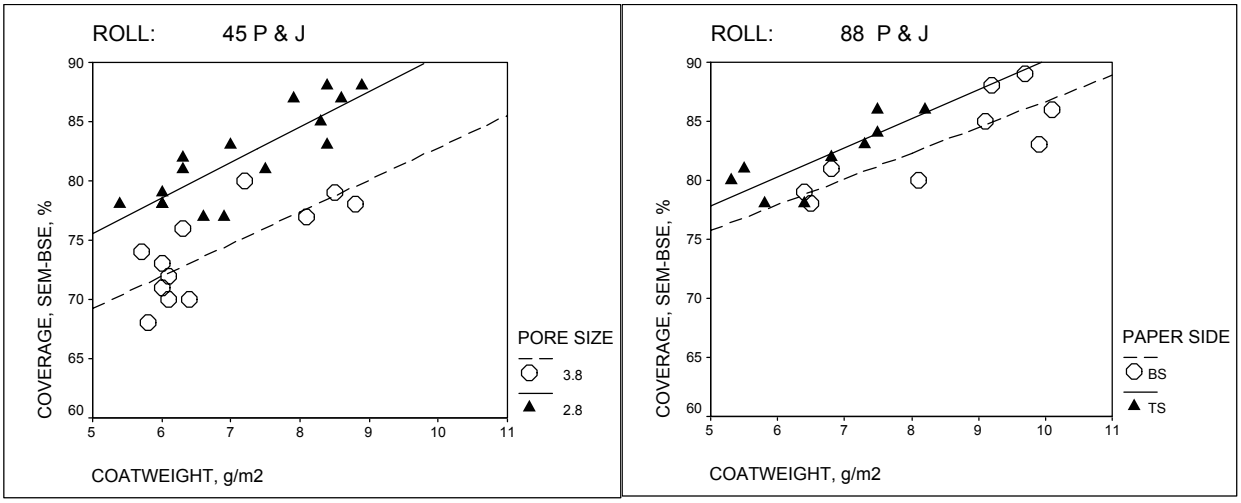

Figure 46. Coating coverage of the coated paper as a function of coatweight with polyurethane rolls (45 P & J) and different base papers with different pore sizes (3.8 and 2.8 μm, left) and as a function of coatweight with supported rubber rolls (88 P & J) and different base papers with different amounts of filler at the surface (TS 30%, BS 10%, right).

With supported rubber rolls, the coating layer formed through filter cake formation, especially on the topside of the dense base paper (produced with the fourdrinier machine). A high filler content at the surface resulted in greater coating color filtration. When both sides were coated at the same time, the side with most of the filler at the surface gave better coverage (Figure 46, right). The filler content of the base paper topside caused by the fourdrinier machine was 18-30% and that of bottom side 5-9%. The surface openness and roughness of the base paper topside were also lower than for the bottom side. Higher coating coverage was achieved with soft rubber rolls (Figure 46, right) than with hard polyurethane roll covers (Figure 46, left), especially at low coatweights.

Coating coverage was also evaluated using a parameter reflecting the size of the uncovered area (EDM). The uncovered areas on the topsides were in most cases smaller (EDM parameter values smaller) than on the bottom sides. With one bottom side sample, the smaller parameter value could be explained with higher coatweight. A visual impression of the images taken with SEM-BSE gave results similar to those with the EDM parameter.

Reducing the base paper pore size also improved the coating coverage and uniformity of the covered areas, especially at low coatweights (Figures 47-48). Higher coating coverage was achieved with dense base paper with a coatweight 5-6 g/m² than with porous base paper with 8-9 g/m² when coating with an MSP using polyurethane rolls (Figure 46).

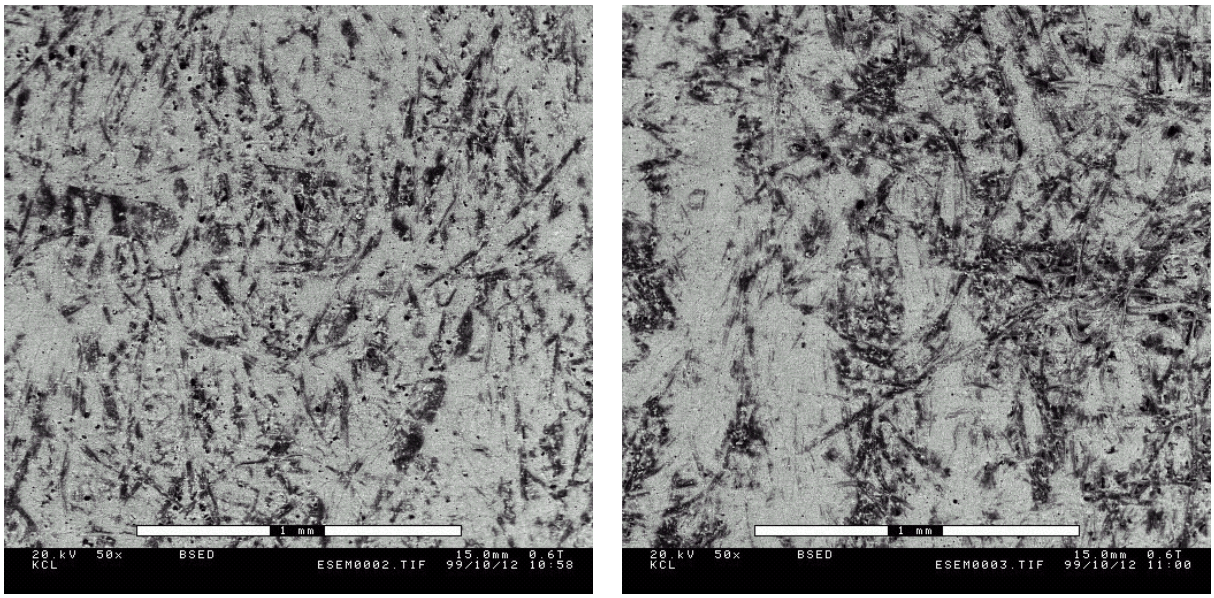

Figure 47. SEM–BSE image of MSP-coated porous base paper topside (left) with a pore size of 4.3 μm at 6.0 g/m² / coverage 71% / 1.9 (EDM = parameter for size of the uncovered area) and bottom side (right) at 6.4 g/m²/ coverage 70% / 2.4 (EDM). Polyurethane rolls (45 P&J).

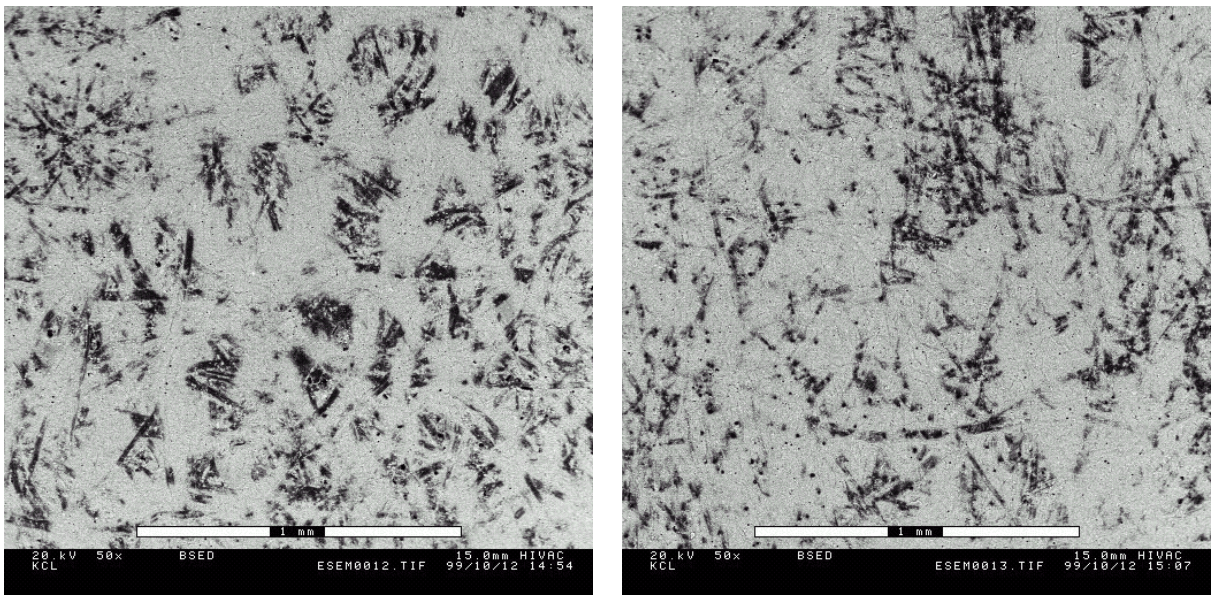

Figure 48. SEM-BSE image of MSP-coated dense base paper topside (left) with a pore size of 2.5 μm at 6.3 g/m² / coverage 81% / 1.9 (EDM = parameter for size of the uncovered area) and bottom side (right) at 6.3 g/m²/ coverage 83% / 1.7 (EDM). Polyurethane rolls (45 P&J).

The small-scale uniformity of coating coverage (measured with the EDM parameter) was better when coating with soft rubber rolls than polyurethane rolls with both dense and porous base papers (Figures 49-50). Base papers MSP coated using rubber rolls had slightly more small pores at the coated surface, which can be assumed to caused by air in the coating color

or by the loss of air from the base paper structure into the coating. The diameter of the holes was under 10 µm. Sufficient surface coverage was obtained even at low coatweight when coating was carried out with rubber rolls, and therefore coating coverage increased only slightly as coatweight increased.

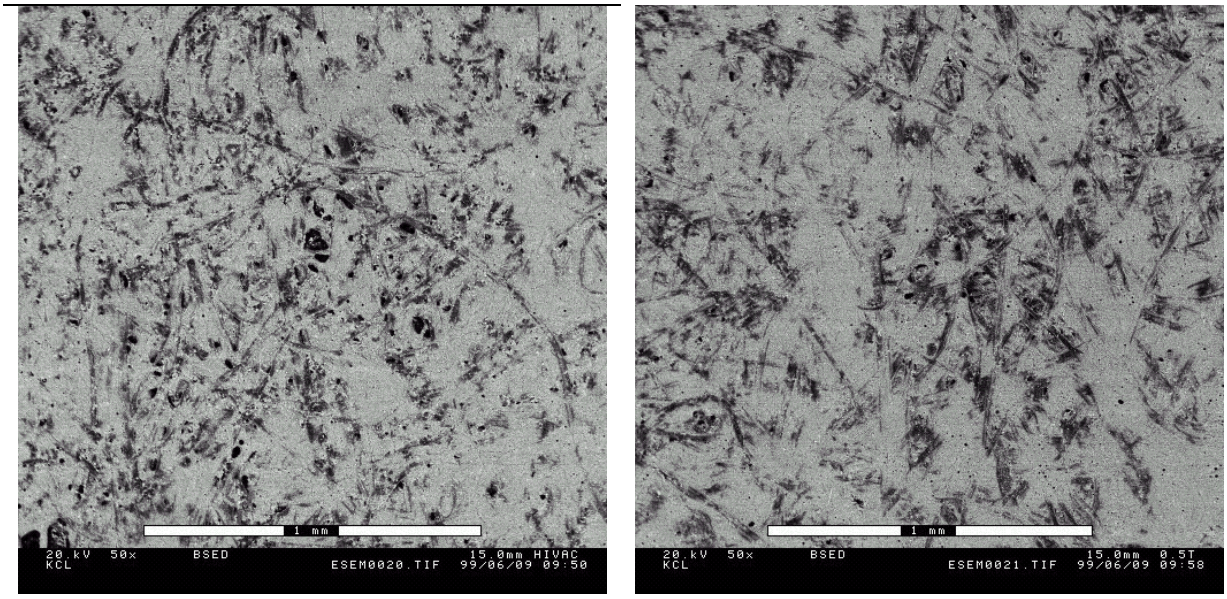

Figure 49. SEM-BSE image of MSP-coated porous base paper topside (left) with a pore size of 3.8 µm at 5.8 g/m² / coverage 78% / 1.7 (EDM = parameter for size of the uncovered area) and bottom side (right) at 6.5 g/m²/ coverage 78% / 2.2 (EDM). Rubber rolls (88 P&J).

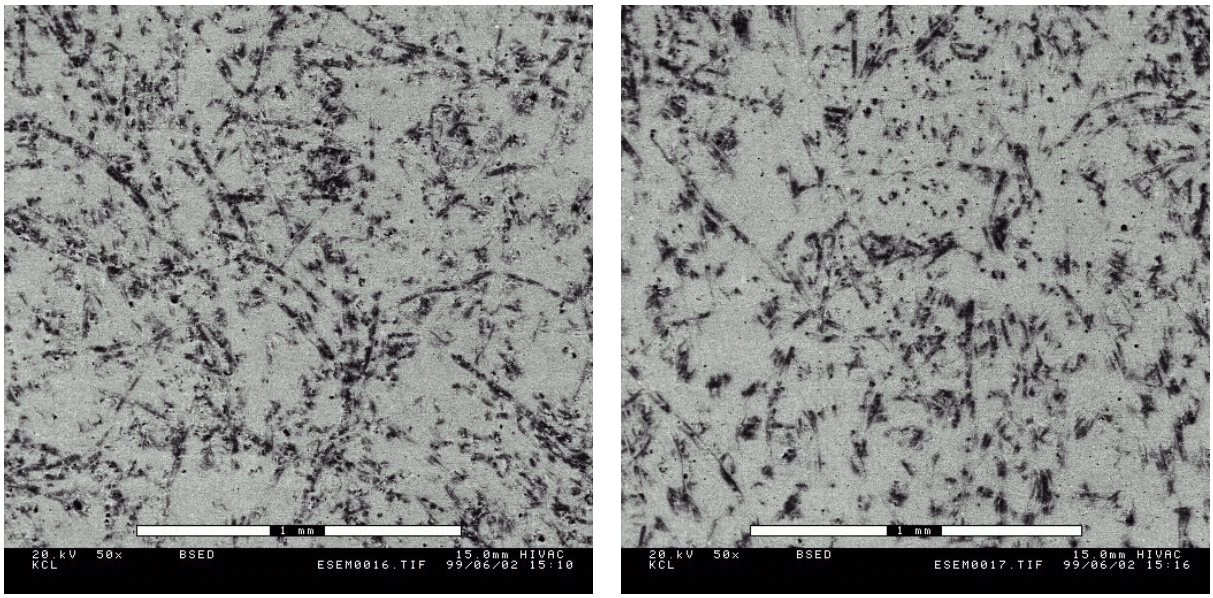

Figure 50. SEM–BSE image of MSP-coated dense base paper topside (left) with a pore size of 2.8 µm at 5.5 g/m² / coverage 81% / 1.6 (EDM = parameter for size of the uncovered area) and bottom side (right) at 6.8 g/m²/ coverage 81% / 1.8 (EDM). Rubber rolls (88 P&J).

9.3 Precoated paper openness

Coated paper surface openness was measured as oil absorption rate with the KCL' s nozzle application method. Base paper properties, coatweight, coating coverage and packing of the pigment all influence coated paper openness. Coated fourdrinier base paper topsides have higher oil absorption rates than the bottom sides. When coating was carried out with hard roll covers, coating layer was formed more by coating color penetration, resulting in a denser coated paper than with soft rubber roll covers. In the latter case, coating layer was formed on the dense base paper more by filter cake formation (Figure 51). With more open base paper bottom sides, coating layer was formed with both roll cover materials by coating color penetration. There was no statistical difference between the coating colors when different soluble binders were used. Coated paper openness measured as oil absorption rate was not affected by base paper surface chemical properties (e.g. contact angle).

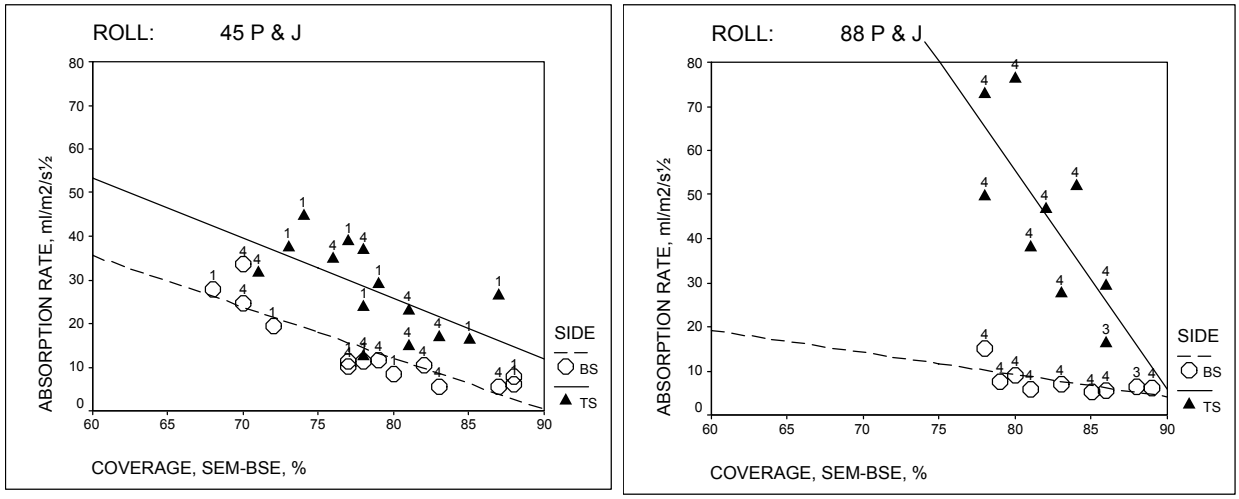

Figure 51. Oil absorption rate of the coated paper as a function of coating coverage for different base paper sides and polyurethane rolls (45 P&J, left). Oil absorption rate of the coated paper as a function of coating coverage with different base paper sides and supported rubber rolls (88 P&J, right). Coating colors marked above the points (latex-CMC coating colors, 1 = CMC 5, latex-CMC and latex-starch coating color, 3 = starch and 4 = CMC 150).

9.4 Summary

Smaller differences in coverage two-sidedness were observed when both paper sides were coated simultaneously and compared with the results from the earlier studies (Chapter 5). When the paper was coated using hard rolls, coating coverage depended largely on the pore size of the base paper. The coatweight was formed mainly through penetration, the result being a dense coating layer. With soft roll covers, coating layer formation occurred more through dewatering, in which case better coverage was obtained, albeit accompanied by a porous coating layer. Average pore size of the base paper structure, base paper surface openness and filler content at the surface are therefore the main variables affecting coating coverage and coating layer porosity. The effect of coating color dewatering on coated paper coverage was not statistically significant.

The topsides of the base papers produced on fourdrinier forming sections were dense with higher surface filler contents than the bottom sides, the result being a more uniform coating layer. The chemical properties of the base paper surface (hydrophobic / hydrophilic) had no effect on coating coverage or coating layer density. This was found with both hard and soft roll covers. These results are in agreement with the earlier coating studies with both mill and laboratory base papers (Chapters 5 and 7).

10 EFFECT OF PRECOATED PAPER PROPERTIES ON TOPCOATED PAPER QUALITY

The aim of the top coating was to determine the effect of precoated paper properties on the final double-coated paper quality. Precoated papers were top-coated to a constant coatweight.

10.1 Formation of the top coating layer

The differences in blade pressures on the topsides of the different precoated papers were minimal. Blade pressures were slightly higher for the precoated papers with higher oil absorption rate at a contact time of 10 ms or a lower coating coverage (Figure 82). Higher blade pressures were required when precoated papers were coated using a soft roll cover (Figure 52, rubber roll 88 P & J), which gave a more porous coating layer. The top coating color immobilized faster on the more porous coating layer than on the dense coating layer at the same coating coverage level. The surface chemistry of the base paper (hydrophobic or hydrophilic) did not influence the blade pressure required to reach a constant coatweight. The required blade pressure was governed by the precoated paper properties. The blade pressure needed to achieve constant coatweight on the bottom sides was similar to that needed for the topsides.

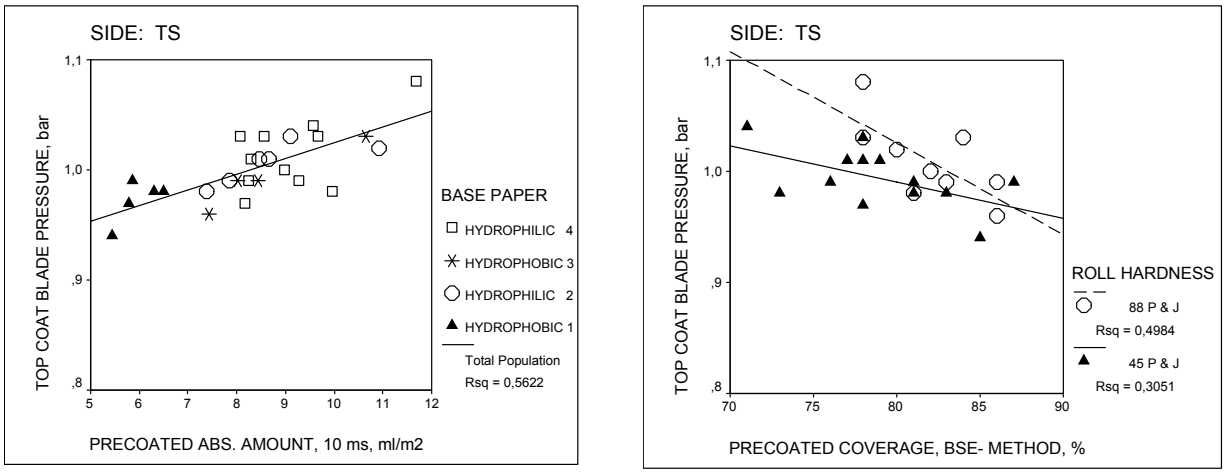

Figure 52. Top coating blade pressure as a function of precoating oil absorption (10 ms contact time), reflecting openness with different base paper surface chemical properties (left) and precoating coverage using different roll hardnesses (right).

10.2 Properties of the calendered double-coated paper

The bottom side of the double-coated paper was calendered first against the steel roll, which meant that the gloss values of the bottom sides were slightly higher than those of the topsides. A small difference in calendering temperature with roll surface temperatures of 120-130 °C did not influence gloss development (Figure 53). The gloss achieved with double-coated paper was influenced more by precoating coverage than by precoating coatweight. Precoating coverage was influenced by the parameters discussed in Chapter 9, such as base paper pore size and surface filler content, coatweight and the roll cover material used in the MSP coater. When the coverage was increased from 70% to 90%, the Hunter gloss of the calendered paper increased by 4 to 6%-points.

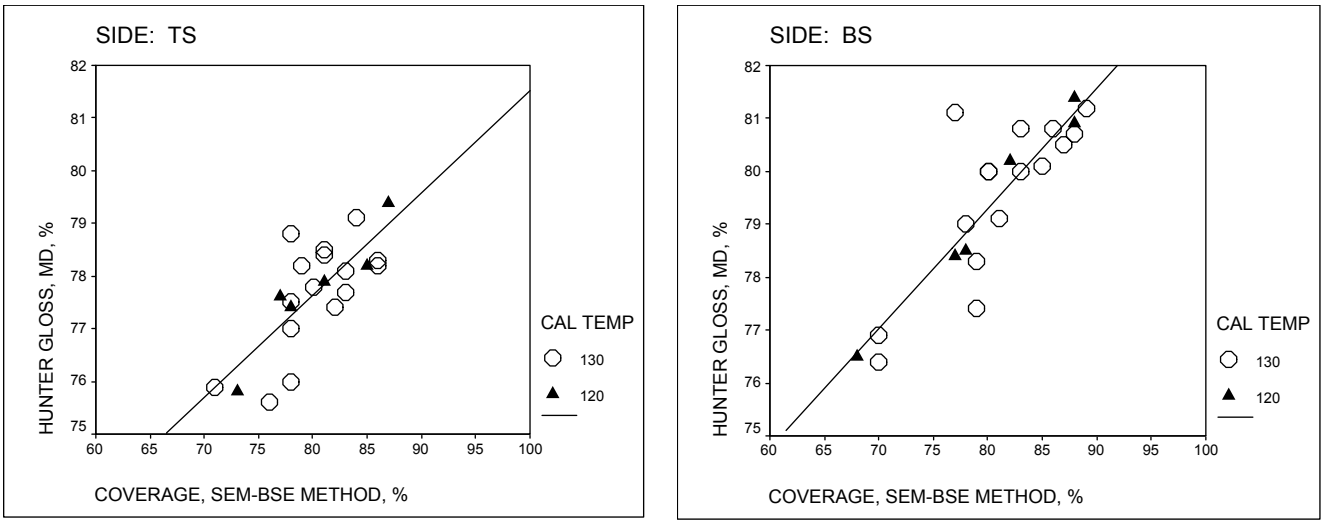

Figure 53. Gloss of the calendered double-coated paper as a function of precoating coverage for base paper topside (TS, left) and bottom side (BS, right).

10.3 Summary

All precoated papers were top-coated to a constant coatweight of 11 g/m^2/ side. Lowering the coating coverage and increasing the openness and roughness of the precoated paper surface increased the blade pressure required to achieve a constant coatweight. The base papers precoated using soft roll covers were more porous at the same coverage, which increased the blade pressures more than with the dense paper precoated using hard roll covers. The results were similar with both base paper sides, but more significant with the topsides. This was due to the fact that the topsides had a more porous precoating layer than the bottom sides.

In terms of the gloss acquired by the double-coated paper during calendering, precoating coverage was more important than coatweight.

11 CONCLUDING REMARKS

Sufficient coating coverage of the base paper for double-coated products is essential for optical properties (e.g. light scattering and gloss). The present study showed that dense base papers gave better precoated results even when the light scattering properties of the base paper were inferior to those with porous base papers. In terms of the gloss acquired by the double-coated paper during calendering, precoating coverage was more important than coatweight alone. This should be taken into consideration, especially with low basis weights and low coatweights.

The coating layer formation on woodfree base paper during MSP precoating depended mainly on the base paper surface openness. Reducing this openness by using a higher filler content, the addition of mechanical pulp or more intensive refining of the chemical pulps resulted in lower coatweights but better coating coverage. Base paper roughness, small-scale basis weight variation (beta formation) and the surface chemistry of the fibers (hydrophilic / hydrophobic) had no effect on precoating layer formation or coverage. Coating color liquid phase seemed to penetrate mainly into the voids between the fibers, because of the short contact time in the MSP transfer nip. The liquid phase of the color penetrated deeper into the base paper structure as base paper openness was increased or coating color solids content was reduced. At lower solids content the liquid phase made the base paper coating layer interface rougher than at high solids content. Rendering the base paper hydrophobic had no effect on transfer of the water phase.

Low base paper surface openness and high filler content on the surface of the sheet reduced coating color penetration into the base paper structure. SEM-BSE and LIPS coverage methods were found to give similar results for the precoated surfaces. The LIPS coverage results were lower than the SEM-BSE results at low coatweights. This indicated that the SEM-BSE method found thinner coating layers to be covered. Both methods confirmed that improved coverage was obtained by using more kaolin in the coating formula. The impact became more pronounced as coatweight decreased. Coating color solids content had a small impact on precoating coverage. With base papers with less filler on the surface, coverage could still be increased by using a higher coating color viscosity. Base paper pore size influenced coated paper coverage on both large and small scales. Dense base papers with high filler contents gave better small-scale uniformity than porous base papers. Coating coverage was sensitive to shadow marking, which was clearly seen as large-scale coverage non-uniformity. The machine speed and nip load did not affect precoating coverage.

Smaller differences in coverage two-sidedness were observed when both paper sides were coated simultaneously compared to the situation when only one side was coated. When the paper was coated using hard rolls, coating coverage depended largely on the pore size of the base paper. Coatweight was formed mainly through penetration, the result being a dense coating layer. With soft rolls, coating layer formation occurred more by dewatering, in which case better coverage was obtained, albeit accompanied by a porous coating layer. Average pore size of the base paper structure, base paper surface openness and filler content at the surface are therefore the main variables affecting coating coverage and coating layer openness. More filler on the surface gave a well-covered base paper, but in this case the

coating layer absorbed oil faster compared to the other samples. The openness of the coating layer was greater with soft rolls than hard rolls. The porous coating layer with good coverage was the result of coating color dewatering and filter cake formation in the MSP transfer nip.

The main mechanism by which coating layer formation took place was pressure-induced penetration of coating color or coating color liquid phase into the voids between fibers in the transfer nip. Water sorption into the fibers was slower than capillary penetration, and the movement of coating color liquid phase by diffusion and possibly by capillary absorption took place mainly after the nip. The mechanism of water transport into the fiber wall remains unclear. Further studies and simulations under dynamic conditions are needed to establish how water moves into the fiber wall during coating.

The first two hypothesis about coating layer formation proved to be right. The hypothesis concerning the effect of dwell-time and surface chemistry proved to be wrong. The main mechanism by which coating layer formation took place was always pressure-induced penetration of bulk coating color or coating color liquid phase into the voids between fibers in the transfer nip. Coating color water phase moved into the walls of fibers located in the surface layers irrespective of the surface chemical properties of the fibers. The dwell time with polyurethane rolls was about 4 ms (nip width about 60 mm at 1000 m/min), which was too short to allow significant sorption of the coating color liquid phase into the fiber walls. Sorption into the fiber walls was slower than capillary penetration, and the movement of coating color water phase took place mainly after the nip.

Understanding the mechanisms of coating color penetration and the transport of coating color liquid phase into the base paper will facilitate the development new products and permit improvements to be made to current paper grades coated with an MSP. In conclusion, the following combination would give good coating coverage in MSP coating:

1. Base paper structure engineered from short or flexible and conformable fibers with high fines and filler contents at the surface. This will give a base sheet surface with numerous small pores, which can be filled with the dewatered coating color liquid phase but not with the bulk coating color.
2. Coating color engineered for a strongly shear thinning behavior with a low or moderate water retention value and low elasticity (low film thickness on the roll and low misting and good leveling at high speeds).
3. An MSP coating process with a mild pressure pulse managed using a roll cover material that is soft under dynamic conditions and has good surface smoothness, especially at low coating speeds.

REFERENCES

1. *Sollinger, H-P.,* Der Speedsizer, das neue Leimpressenkonzept für das Leimen und Pigmentieren von Papier und Karton. Wochenblatt für Papierfabrikation 115 (1987): 23/24, p. 1063-1068.

2. *Rantanen, R.,* Pigmentieren mit der Filmleimpresse. Wochenblatt für Papierfabrikation 120 (1992): 6, p. 193-197.

3. *Turunen, R.,* Experience of film press pigmenting and coating. Pulp & Paper Canada 97 (1996): 5, p. 39-42.

4. *Trefz, M.,* Theoretical aspects and practical experiences for film coated offset grades. Tappi Journal 79 (1996): 1, p. 223-230.

5. *Trefz, M.,* Oberflächenveredelung mit dem Speedcoater. Das Papier 69 (1995): 6, p. 355-364.

6. *Michell, A.,* Kirkniemi makes the grade with Film Coated Offset. Pulp & Paper International 36 (1994): 5, p. 34-35.

7. *McGraig, G. and Harala, E.,* Manufacturing of No. 5 Light Weight Coated using on-line film press coating and soft nip calendaring- Experience from MacMillan Bloedel PM 5. Annual meeting, Technical Section, CPPA, January 28-29, 1997, Montreal, Canada, p. 57-61.

8. *Johansson, B.,* "Neue Dimensionen" - die weltweit erste OptiConsept LWC-Einheit online in Betrieb. Wochenblatt für Papierfabrikation 128 (2000): 23/24, p. 1654-1659.

9. *Varsa, P., Anttila, T. and Toppila, M.*, The quality of high deinked pulp content magazine paper produced with various coating methods. TAPPI Coating Conference, May 2-5, 1997, Philadelphia, PE, USA, p. 281-290.

10. *Grön, J. and Ahlroos, J.*, Effect of base paper filler content and pre-calendering on coating color mist and coverage in MSP coating. Journal Pulp and Paper Science 27(2001): 2, p. 66- 73.

11. *Ahlroos, J., Alexandersson, M. and Grön, J.,* Influence of base paper filler content and precalendering on metered film press coating - paper and print quality. Tappi Journal 82 (1999): 5, p. 94-100.

12. *Grön, J. and Rautiainen, P.,* Coating solutions for wood-containing and woodfree paper grades. TAPPI Coating Conference, May 2-5, 1999, Toronto, ON, Canada, p. 457-467.

13. *Grön, J.,* Significance of paper machine calendering on coating coverage. Paperi ja Puu - Paper and Timber 82 (2000): 4, p. 245-249.

14. *Ahlroos, J. and Grön, J.*, A comparison of SGW and TMP as fiber raw material for film coated LWC. TAPPI Coating Conference, May 3-5, 1999, Toronto, ON, Canada, p. 481-500.

15. *Drage, G., Vaughan, C., Henderson, K., Parsons, J. and Hiorns, T.,* The influence of freesheet and groundwood basepaper formation on coated and printed paper properties. TAPPI Coating Conference, May 3-5, 1999, Toronto, ON, Canada, p. 469-479.

16. *Suontausta, O.,* The influence of some coating and calendaring variables on the smoothness and gloss of LWC paper. Proceedings from International Symposium on Paper Coating Coverage, February 16-17, 1999, Helsinki, Finland.

17. *Zou, X., Vidal, D. and Allem, R.,* Film press for pigment coating: Coated paper quality and basestock effects. TAPPI Metered Size Press Forum IV, May 1-4, 2002, Orlando, Florida, USA, p. 159-170.

18. *Reglat, O. and Tanguy, P. A.,* Experimental study of the flow in the metering nip of a metering size press. AIChE Journal 43 (1997): 11, p. 2911-2920.

19. *Reglat, O. and Tanguy, P. A.,* Rheological investigations of $CaCO_3$ slurries in the metering nip of a metering size press. Tappi Journal 81 (1998): 5, p. 195-205.

20. *Grön, J. and Rantanen, R*., Surface sizing and film coating, in Handbook of Papermaking Science and Technology, Pigment Coating and Surface Sizing (Lehtinen, E., Ed.), Fapet Oy, Helsinki, Finland, 2000, p. 487-541.

21. *Wikström, M. and Grön, J.,* Formation of patterns on paper coated with a metering size press. Journal of Pulp and Paper Science 29 (2003): 1, p. 11-16.

22. *Roper III, J., Salminen, P., Urscheler, R. and Bousfield, D.,* Studies of orange peel formation in high-speed filmcoating. TAPPI Coating/Papermakers Conference, May 4-6, 1998, New Orleans, LA, USA, p. 763-776.

23. *Toivokka, M., Kokko, A., Salminen, P., Urscher, R. and Bousfield, D. W.,* Leveling of surface defects in thin films of pigmented coatings. Nordic Pulp and Paper Research Journal 16 (2001): 3, p. 246-250.

24. *Stränger, K.,* The filmpress - a versatile coating system. Paper Technology 38 (1997): 2, p. 29-35.

25. *Glittenberg, D. and Hemmes, J-L.,* Improved runnability of film press coatings. Paper Technology 39 (1998): 3, p. 35-41.

26. *Alonso, S., Regat, O., Bertrand, F. and Tanguy, P. A.,* Process viscosity in a film coater. Paperi ja Puu - Paper and Timber 82 (2000): 1, p. 34-40.

27. *Poranen, J., Kataja, M., Niemistö, A. and Grön, J.,* A novel technique for measuring pressure in the metering nip of a MSP process. TAPPI Coating Conference and Trade Fair, May 1-4, 2000, Washington DC, USA, p. 367-380.

28. *Poranen, J., Kataja, M., Niemistö, A. and Grön, J.,* A method for measuring and controlling the pressure in the metering nip of a metering size press coating process. Nordic Pulp and Paper Research Journal 15 (2000): 5, p. 486-493.

29. *Poranen, J., Grön, J., Kataja, M. and Niemistö, A.,* An experimental study of a metering nip in a metering size press. TAPPI Advanced Coating Fundamentals Symposium, May 4-5, 2001, San Diego, California, USA, p. 159-170.

30. *Poranen, J., Kataja, M., Grön, J. and Niemistö, A.,* Experimental study of nip dynamics in metered size coating. TAPPI Coating Conference and Graphic Arts Conference and Trade Fair, May 5-8, 2002, Orlando, Florida, USA, p. 543-564.

31. *Poranen, J.,* Experimental techniques for studying nip dynamics in Metered Size Press coating. PhD thesis, Department of Physics, University of Jyväskylä, Research report no. 7/2001, Jyväskylä, Finland, 2001, 94 pages.

32. *Alonso, S. and Tanguy, P.,* Hydrodynamic instabilities in the metering nip of a film coater. Tappi Journal 84 (2000): 5, p. 67.

33. *Grön, J., Sunde, H. and Nikula, E.,* Runnability Aspects in High Speed Film Transfer Coating. Tappi Journal 81 (1998): 2, p. 157-165.

34. *Grön, J., Molarius-Mäyränen, S. and Ånäs, P-H.,* Improving the process runnability and FCO quality by optimizing the coating color composition. TAPPI Coating Conference, May 2-5, 1999, Toronto, ON, Canada, p. 23-39.

35. *Grön, J.,* Coating color structure and rheology. PhD thesis, Department of Chemical Engineering, Åbo Akademi University, Åbo, Finland, 1998, 203 pages.

36. *Korhonen, H.,* Päällystemäärän muodostuminen ja päällystyspastojen reologiaan liittyvät ilmiöt filmipäällystyksessä (in Finnish). Licentiate of Technology thesis, Department of Forest Products Technology, Helsinki University of Technology, Espoo, Finland, 1999, 77 pages.

37. *Hintermaier, J. C. and White, R. E.,* The splitting of a water film between rotating rolls. Tappi 48 (1965): 11, p. 617-625.

38. *Walker, W. C. and Fetsko, J. M.,* A concept of ink transfer in printing. American ink maker 33 (1955): 12, p. 38-42, 44, 69, 71.

39. *Rantanen, R.,* Smooth coating with Sym-Sizer. PaperAge 112 (1996): 2, p. 26-27.

40. *Grön, J., Nikula, E. and Sunde, H.,* Influence of coating composition on web release in high speed film transfer coating. Tappi Journal 81 (1998): 1, p. 216-225.

41. *Grön, J. and Fors, S.,* Metered size press coating with high solids content formulations at high machine speeds. TAPPI Metered Size Press Forum IV, May 1-4, 2002, Orlando, Florida, USA, p. 115-126.

42. *Windle, W., Beazley, K. M. and Climspon, M.,* Liquid migration from coating colors. Tappi 53 (1970): 12, p. 2232-2236.

43. *Letzelter P.,* Dewatering of coating colors: A filtration or thickening mechanism? TAPPI Advanced Coating Fundamentals Symposium, May 9-10, 1997, Philadelphia, PA, USA, p. 103-131.

44. *Watanabe, J. and Lepoutre, P.,* A mechanism for the consolidation of the structure of clay-latex coatings. Journal of Applied Polymer Science 27 (1982): 11, p. 4207-4219.

45. *Böhmer, E*., The relationship between coating weight and other variables during blade coating. Norsk Skogindustri 23 (1969): 11, p. 308-324.

46. *Lohmander, S., Martinez, M., Larson, L. and Rigdahl, M.,* Dewatering of coating dispersions - model experiments and analysis. TAPPI Advanced Coating Fundamentals Symposium, April 29-May 1, 1999, Toronto, Canada, p. 43-58.

47. *Letzelter, P. and Eklund D.,* Coating color dewatering in blade coaters, Part I: Mathematical model and the influence of color parameters. Tappi Journal 76 (1993): 5, p. 63-68.

48. *Letzelter, P. and Eklund D.,* Coating color dewatering in blade coaters, Part II: The influence of machine configuration. Tappi Journal 76 (1993): 6, p. 93-98.

49. *Letzelter, P.,* Studier över avvattningen av en bestrykningssmet i en bladbestrykare, (in Swedish). Licentiate of Technology thesis, Department of Chemical Engineering, Åbo Akademi University, Åbo, Finland, 1993, p. 27-50.

50. *Letzelter, P and Eklund, D.,* Dewatering of coating colors in the film press. TAPPI Coating Conference, May 19-22, 1996, Nashville, TN, USA, p. 269-281.

51. *Salminen, P.,* Studies of water transport in paper during short contact times. PhD thesis, Department of Chemical Engineering, Åbo Akademi University, Åbo, Finland, 1988, 94 pages.

52. *Eriksson, U. and Rigdahl, M.,* Dewatering of Coating Colours Containing CMC or Starch. Journal of Pulp and Paper Science 20 (1994): 11, p. J333-J337.

53. *Baumeister, M.,* Quality optimization by control of coating structure. TAPPI Coating Conference, April 27-30, 1980, Miami Beach, Florida, USA, p. 11-22.

54. *Baumeister, M.,* Significance and implications of the concept of immobilization solids in relation with coating structure. TAPPI Coating Conference, May 17-21, 1987, Huston, TX, USA, p. 84-85.

55. *Odell, M.,* Customizing roll and blade forming to control paper structure. Valmet Paper Machine Days, Jyväskylä, Finland, 1996.

56. *Häggblom-Ahnger, U., Pakarinen, P., Odell, M. and Eklund, D.,* Conventional and stratified forming of office paper grades. Tappi Journal 81 (1998): 4, p. 149-158.

57. *Häggblom-Ahnger, U.,* Three-ply office paper. PhD thesis, Department of Chemical Engineering, Åbo Akademi University, Åbo, Finland, 1998, 59 pages.

58. *Kinnunen, J. S., Lloyd, M. D. and Konttinen, A.,* A new world of papermaking - the layered SC-paper. Paperi ja Puu - Paper and Timber 80 (1998): 3, p. 167-171.

59. *Szikla, Z. and Paulapuro, H.,* Z-directional distribution of fines and filler material in the paper web under pressing conditions. Paperi ja Puu - Paper and Timber 78 (1986): 9, p. 654-664.

60. *Szikla, Z.* On the basic mechanisms of wet pressing. PhD thesis, Department of Forest Products Technology, Helsinki University of Technology, Espoo, Finland, 1992, 88 pages.

61. *Szikla, Z., Paulapuro, H.,* Changes in z-direction density distribution of paper in wet pressing. Journal of Pulp and Paper Science 15 (1989): 1, p. J11-17.

62. *Wicks, L.,* The influence of pressing on sheet two-sidedness. Practical aspects of Pressing and Drying Short Course, March 27-31, 1995, New Orleans, LA, USA, p. 55-60.

63. *Grön, J.,* Development of metered size press coating for high-speed operations. TAPPI Metered Size Press Forum III, April 29 -30, 2000, Washington, DC, USA, p. 293-307.

64. *Trefz, M. and Seiz, R.,* Investigation on film transfer in metered size presses as related to base paper coating color properties. TAPPI Metered Size Press Forum II, April 30-May 2, 1998, New Orleans, LA, USA, p. 85-105.

65. *Huang, T. and Lepoutre, P.,* Effect of basestock surface structure and chemistry on coating holdout and coated paper properties. Tappi Journal 81 (1998): 8, p. 145-152.

66. *Huang, T. and Lepoutre, P.,* Coating - paper interactions - the effect of basestock roughness, absorbency and formation on coated paper properties. Paperi ja Puu - Paper and Timber 77 (1995): 8, p. 484-490.

67. *Salminen, P. and Eklund, D.,* Einfluss der Hydrophobierung und der Struktur von Papier auf das Eindragen von Wasser. Wochenblatt für Papierfabrikation 120 (1992): 14, p. 572-574.

68. *Pekarovicova, A., Venditti, R.A., Cao, H., Lou, Y.M. and Jean, Y.C.,* Positron annihilation lifetime spectroscopical study of kraft pulps after individual bleaching stages and beating. Cellulose Chemistry and Technology 33 (1999): 5-6, p. 483-493.

69. *Wang, X., Maloney, T.C. and Paulapuro, H.,* Internal fibrillation in never-dired and once-dried chemical pulps. 56th Appita Annual Conference, March 18-20, 2002, Rotorua, New Zealand, p. 469-473.

70. *Stone, J.E., Scallan, A.M. and Aberson, G.M.A.,* Pulp and Paper Magazine Canada 67 (1966): 5, p. 263- 268.

71. *Stone, J.E. and Scallan, A.M.,* The effect of component removal upon the porous structure of the cell wall of wood. II Swelling in water and the fiber saturation point. Tappi 50 (1967): 10, p. 496-501.

72. *Stone, J.E., Scallan, A.M. and Abrahamson, B.,* Influence of beating on cell wall swelling and internal fibrillation. Svensk Papperstidning 71 (1968): 19, p. 687-694.

73. *Stone, J.E. and Scallan, A.M.,* A structural model for the cell of water-swollen wood pulp fibres based on their accessibility to macromolecules. Cellulose Chemistry and Technology 2 (1968): 2, p. 343-358.

74. *Kartovaara, I.,* Gradienttikalanterointi: gradienttien syntymisen ja kalanterointituloksen arvostelun perusteet (in Finnish). Licentiate of Technology thesis, Department of Forest Products Technology, Helsinki University of Technology, Espoo, Finland, 1989, p. 36.

75. *Maloney, T.,* On the pore structure and dewatering properties of the pulp fiber cell wall. PhD thesis, Department of Forest Products Technology, Helsinki University of Technology, Espoo, Finland, 2000, 52 pages.

76. *Weise, U.* Characterization and mechanisms of changes in wood pulp fibres caused by water removal. PhD thesis, Department of Forest Products Technology, Helsinki University of Technology, Espoo, Finland, 1997, 104 pages.

77. *Moore, R.R.,* Influence of roll covers in film transfer size presses and coaters. Tappi Jounal 82 (1999): 5, p. 111-114.

78. *Beltzung, M., Stübegger, T. and Moore, R.R..,* Effect of roll cover in the film transfer presses. TAPPI Metered Size Press Forum III, April 29 -30, 1998, Washington, DC, USA, p. 23-28.

79. *Zang, Y. H., Aspler, J. S., Boluk, M. Y. and De Grace, J. H.,* Direct measurement of tensile stress ("tack") in thin ink films. Journal of Rheology 35 (1991): 3, p. 345-361.

80. *Aspler, J. S., Maine, C., De Grace, J. H., Zang, Y. H. and Taylor, S.,* Printing tack, Part I: Influence of paper structure on ink "tack" measured in a printing nip, 22nd International Conference of Printing Research Institutes, IARIGAI, September 5-8, 1993, Munich, Germany, 19 pages.

81. *Taylor, J. and Zettlemoyer, A.,* Hypothesis on the mechanism of ink splitting during printing, Tappi 41 (1958): 12, p. 749-757.

82. *Ninnes, B., Bousfield, D. and Triantafillopoulos, N.,* Fluid dynamics model of the film-fed rolling nip with a porous web. TAPPI Coating/Papermakers Conference, May 4-6, 1998, New Orleans, LA, USA, p. 515-530.

83. *Salminen, P., Roper III, J., Urscheler, R. and Chase, D.,* Optimizing the coating formulation to reduce misting in high-speed MSP coating. TAPPI Metered Size Press Forum I, May 16-18, 1996, Nashville, TN, USA, p. 51-55.

84. *Hiorns, A.G., Oak, G.A.R., Coggon, L. and Engley, M.S.*, The runnability of high speed metered size presses when coating mechanical paper with high solids colours. TAPPI Metered Size Press Forum I, May 16-18, 1996, Nashville, TN, USA, p. 161-170.

85. *Drage, P.G. and Hiorns, A.G.,* The use of pigments to produce high quality MSP coatings. TAPPI Metered Size Press Forum I, May 16-18, 1996, Nashville, TN, USA, p. 135-152.

86. *Roper III, J., Urscheler, R., Bousfield, D. and Salminen, P.,* Observations and proposed mechanisms of misting on high-speed metered size press coaters. TAPPI Coating Conference, May 2-5, 1997, Philadelpia, PE, USA, p. 1-14.

87. *Gane, P.A.C., Burri, P., Spielmann, D., Drechsel, J. and Reimers, O.,* Formulation optimization for improved runnability of high speed pigmented coatings on the metered size press. TAPPI Coating Conference, May 2-5, 1997, Philadelpia, PE, USA, p. 15-22.

88. *Voss, M., Ramthun, J., Tadjbach, J., Lamprecht, J. Ch. and Tietz, M.,* Die Filmpresse- Strömungsmechanik und Rheologie von Steichfarben. Wochenblatt für Papierfabrikation 130 (2002): 11/12, p. 782-791.

89. *Hedman, A., Wikström, M. and Rigdahl, M.,* Assessment of the causes of a print defect in a film-coated LWC-paper. Nordic Pulp and Paper Research Journal 16 (2001): 4, p. 266-283.

90. *Grön, J. and Harmaala, A.,* Compact paper surface treatment by integrated process solutions, Proceedings of the Asian Paper NAT Conference, Singapore, 2000, p. 120-126.

91. *Myers, R.,* Application of adhesives. Tappi 46 (1963): 12, p. 745-750.

92. *Silvy, J., Caret, C., Belamaalem, B. and Mahrous, M.,* The three-dimensional structure of paper: Methods of analysis and implications on his physical properties. International Paper Physics Conference, September 11-14, 1995, Niagara on the Lake, ON, Canada, p. 91-95.

93. *Nordström, J. and Grön, J.,* Thin-film transfer in printing and coating. Pan-Pacific and Inernational Printing and Graphic Arts Conference, October 6-8, 1998, Quebec City, Quebec, Canada, p. 139-143.

94. *Dullien, F.A.L.,* Handbook of Porous media: Fluid Transport and Pore Structure, Academic Press, San Diego, USA, 1979, p. 171.

95. *Lyne, M.B.,* Wetting and the penetration of aqueous liquids, in Handbook of Physical and Mechanical Testing of Paper and Paperboard (Mark, R.E., Ed.), Marcel Dekker Inc., New York, USA, 1984, vol. 2, p. 103-121.

96. *Leskelä, M. and Simula, S.,* Transport phenomena, in Handbook of Papermaking Science and Technology, Paper Physics (Niskanen, K., Ed.), Fapet Oy, Helsinki, 1998, p. 285-315.

97. *Lindsay, D. J.,* The anisotropic permeability of paper. Tappi Journal 73 (1990): 5, p. 223-229.

98. *Kadoya, T. and Usuda, M.,* The penetration of nonaqueous liquids, in Handbook of Physical and Mechanical Testing of Paper and Paperboard (Mark, R.E., Ed.), Marcel Dekker Inc., New York, USA, 1984, vol. 2, p. 123-141.

99. *Lepoutre, P.,* Liquid absorption and coating porosity, Paper Technology and Industry 19 (1978): 11, p. 298-300, 304.

100. *Tanford, C.,* Expermental determination of diffusion coefficients, in Handbook of Physical Chemistry of Macromolecules, John Wiley & Sons Inc, New York, USA, 1967, p. 353-356.

101. *Corte, H.,* The porosity of paper, in Handbook of Paper Science (Rance, H., F., Ed.), Elsevier Scientific Publishing Company, Amsterdam, The Netherlands, 1982, vol. 2, p. 1-70.

102. *Topgraad, D. and Söderman, O.,* Diffusion of water absorbed in cellulose fibers studied with H-NMR. Langmuir 17 (2001): 9, p. 2694-2702.

103. *Engström, G.,* Coating coverage – definition and measuring techniques. International Symposium on Paper Coating Coverage, February 16-17, 1999, Helsinki, Finland.

104. *Eklund, H. and Laamanen, J.,* Paperin päällysteen karakterisointi SEM-IPS kuva-anlysaattorilla (in Finnish). 13 FINEM-koulutuspäivät, Helsinki, Finland, 1987.

105. *Kartovaara. I.,* Coatweight distribution and coating coverage in blade coating. Paperi ja Puu - Papper och Trä 71 (1989): 9, p. 1033-1042.

106. *Gane, P., and Hooper, J.,* An evaluation of interactions between coating color and basepaper by coating profile analysis. Fundamentals of Papermaking, in Trans. 9th Fundamental Reasearch Symposium, Ed. Baker and Punton, Mech. Eng. Publ., London, UK, vol. 2, 1989, p. 871-893.

107. *Gane, P., Hooper, J. and Baumeister, M*., A determination of the influence of furnish content on formation and basesheet profile stability during coating. TAPPI Coating Conference, May 19-22, 1991, Montreal, Quebec, Canada, p. 157-168.

108. *Person, R.A. and Williams, C.L.,* Determining paper-coating thickness with electron microscopy and image analysis. Tappi Journal 75 (1992): 10, p. 122-126.

109. *Allem, R.,* Characterization of Paper Coatings by Scanning Electron Microscopy and Image Analysis. Journal of Pulp and Paper Science 24 (1998): 10, p. 329-336.

110. *Allem, R. and Uesaka, T.,*Characterization of paper microstructure: A new tool for assessing the effects of base sheet structure on paper properties. TAPPI Advanced Coating Fundamentals Symposium, April 29- May 1, 1999, Toronto, ON, Canada, p. 111- 120.

111. *Engström, G., Johansson, P-Å., Rigdahl, M. and Norrdahl, P.,* Factors in blade coating process which influence the coating mass distribution. Fundamentals of Papermaking, in Trans. 9th Fundamental Reasearch Symposium, Ed. Baker and Punton, Mech. Eng. Publ., London, UK, vol. 2, 1989, p. 921-950.

112. *Tomimasu, H., Suzuki, K. and Toshimasa, O.,* The effect of basestock structure on coating weight distribution. Tappi Journal 73 (1990): 4, p. 179-187.

113. *Dobson, R. L.,* Burnout, a coatweight determination test re-invented. TAPPI Coating Conference, April 21-23, 1975, Chicago, IN, USA, p. 123-131.

114. *Engström, G., Morin, V. and Bi, S. L.,* Analysis of porosity distribution in coating layers. Tappi Journal 80 (1997): 5, p. 203-209.

115. *Engström, G. and Lafaye. J. F.,* Precalendering and its effect on paper-coating interaction. Tappi Journal 75 (1992): 8, p. 117-122.

116. *Häkkänen, H.,* Development of a method based on laser-induced plasma spectrometry for rapid spatial analysis of material distributions in paper coatings. PhD Thesis, Department of Chemistry, University of Jyväskylä, Finland, 1998, 60 pages.

117. *Häkkänen, H. and Korppi-Tommola, J. E. I.,* Analysis of coating structure by Laser-Induced Plasma Spectrometry, TAPPI Advanced Coating Fundamentals Symposium, April 29- May 1, 1999, Toronto, ON, Canada, p. 191-198.

118. *Erkkilä, A-L., Pakarinen, P. and Odell, M.,* The effect of forming mechanisms on layered fiber structure in roll and blade forming. TAPPI 99, Preparing for the Next Millennium, Vol. 2, March 1-4, 1999, Atlanta, Georgia, USA, p. 389-400.

119. Reference manual for the Coulter® porometer, Coulter Electronics Limited, 1986.

120. *Komppa, A.,* Measurement of formation. Paperi ja Puu - Paper and Timber 70 (1998): 3, p. 243-250.

121. *Komppa, A. and Komppa, O.,* Measurement of paper formation, 50th Appita Annual General Conference, 1996, Auckland, New Zealand, p. 803-808.

122. *Bristow, A.,* Liquid absorption into paper during short time intervals. Svensk Papperstidning, 70 (1967): 19, p. 623- 629.

123. *Lehtinen, E.,* Kosketuskulmien ja pintaenergian mittaus paperista (in Finnish). Licentiate of Technology thesis, Department of Forest Products Technology, Helsinki University of Technology, Espoo, Finland, 1994, p. 63-75.

124. MODDE 4.0. Graphical software for design of experments. User's guide to MODDE. Manual 1997.

125. *Anczurowski, E., Jones, A.Y. and Rutland, D.F.,* Simulation of fourdrinier paper machine forming in the laboratory. Pulp and Paper Canada 84 (1983): 12, p. T283-T286.

126. *Laity, P.R. and Hay, J. N.,* Measurement of water diffusion through cellophane using attenuated total reflectance-fourier transform infrared spectroscopy. Cellulose 7 (2000): 4, p. 387-397.

127. *Lepoutre, P. and de Silveira, G.,* Examination of cross-sections of blade- and roll-coated LWC paper. Journal of Pulp and Paper Science 17 (1991): 5, p. J184-J186.

128. *Ström, G., Carlsson, G. and Kiar, M.,* Bestimmung der Alkylketendimer - Verteilung in Probeblättern mittels Elektronenspektroskopie (ESCA), Wochenblatt für Papierfabrikation 120 (1992): 15, p. 606-611.

129. *Ketoja, J. A., Kananen, J., Niskanen, K. J. and Tattari, H*., Sorption and web expansion mechanisms. 12th Fundamental Research Symposium, The Science of Papermaking, Oxford, UK (2001), p. 1357-1370.

130. *Korpela, A.,* Fluoresoivien vaalenteiden sitoutuminen kartongin päällysteisiin (in Finnish). Licentiate of Technology thesis, Department of Forest Products Technology, Helsinki University of Technology, Espoo, Finland, 1992, p. 92-95.

131. *Zou, X., Allem, R. and Uesaka, T.,* Relationship between coating uniformity and basestock structures. Part I: Lightweight coated papers. Paper Technology 42 (2001): 6, p. 27-37.

132. *Enomae, T., Huang, T. and Lepoutre, P.,* Softcalendering: Effect of temperature, pressure and speed on sheet properties. Nordic Pulp and Paper Research Journal 12 (1997): 1, p. 13-18.

APPENDICES

I Forsström, U., Dickson, R. J. and Grön, J., Strichdeckung und Struktur von holzfreien Papieren, die in der Filmpresse vorgestrichen wurden (in German). Wochenblatt für Papierfabrikation 128 (2000): 14/15, 985-992.

II Dickson, R.J., Forsström, U. and Grön, J., Coating coverage of metered size press precoated paper. Nordic Pulp and Paper Research Journal 17 (2002): 4, 374-379.

III Forsström, U., Saharinen, E., Dickson, R. J. and Fagerholm, K., Coating Layer Formation and Liquid Phase Penetration in Metered Size Press Coating. Journal of Pulp and Paper Science 29 (2003): 5, 159-166.

IV Forsström, U., Fagerholm, K. and Saharinen, E., The role of base paper porosity in MSP coating. Accepted for publication in Paperi ja Puu - Paper and Timber (2003).

V Forsström, U. and Grön, J., Interactions Between Base Paper and Coating Color with Double-Coated Paper, Wochenblatt für Papierfabrikation 130 (2002): 18, 1208-1214.